Aus dem Institut für Experimentelle und Klinische Pharmakologie und Toxikologie
der Albert-Ludwigs-Universität Freiburg

The *E. coli* Cytotoxic Necrotizing Factor 1 induces negative regulation of Rac1 and RhoA by different mechanisms

INAUGURALDISSERTATION

zur Erlangung des Doktorgrades
der Fakultät für Biologie
der Albert-Ludwigs-Universität Freiburg im Breisgau

vorgelegt von

Heike Shelagh Bielek

geboren in Frankfurt
Freiburg im Breisgau, Juni 2012

Die Untersuchungen zur vorliegenden Arbeit wurden von April 2008 bis September 2011 am Institut für Experimentelle und Klinische Pharmakologie und Toxikologie der Albert- Ludwigs-Universität Freiburg i. Br. unter der Leitung von Frau Prof. Dr. Gudula Schmidt durchgeführt.
Die Arbeit wurde der Fakultät für Biologie der Albert-Ludwigs-Universität Freiburg vorgelegt.

Dekan: Prof. Dr. Gunther Neuhaus

Vorsitzender des Promotionsausschusses: Prof. Dr. Samuel Rossel

Betreuerin: Prof. Dr. Gudula Schmidt

Erstgutachter: Prof. Dr. Dr. Klaus Aktories

Zweitgutachter: Dr. Tilman Brummer

Drittprüfer: Dr. Andreas Eizinger

Danksagung

An erster Stelle danke ich Frau Prof. Dr. Gudula Schmidt für das interessante Dissertationsthema, für alle motivierenden Worte und den stetigen Enthusiasmus zur Lösung der RhoA Regulation.

Herrn Prof. Dr. Dr. Klaus Aktories danke ich für die Aufnahme am Institut und die hervorragenden Arbeitsbedingungen.

Herrn Prof. Dr. Norbert Klugbauer und Dr. Kirstin Sandrock danke ich für die Zusammenarbeit für das Rac1 Projekt.

Zeynep Knust, Sarah Lang und Selda Genisyürek danke ich für die anregenden Diskussionen. Danke an die technischen Assistenten, Jürgen Dumbach für die (widerwilligen doch nett gemeinten) Hilfestellungen im Labor und Gerhard Wetterer für alle Computer-technischen Probleme. Dr. Panagiotis Papatheodorou alias Dimi danke ich für seine tolle Persönlichkeit und sein reges wissenschaftliches Interesse.

Weiterhin möchte ich mich ganz besonders bei Anke Augspach und Tina Tzivelekidis für alle wissenschaftlichen und nicht-wissenschaftlichen Gespräche bedanken. Ihr habt mir den Laboralltag sehr versüßt! Ein spezieller Dank geht auch an Dr. Gregor Guttenberg für die intensive, gemeinsame Zeit.

Zu guter Letzt gilt ein ganz großer Dank meiner Familie, die mich immer unterstützt haben.

1 INTRODUCTION 1

1.1 Rho GTPases and the actin cytoskeleton 1
1.1.1 The actin cytoskeleton 1
1.1.2 Rho family of small GTPases 2
1.1.3 RhoA, Rac1 and Cdc42 3
1.1.4 Rho GTPase structure 4
1.1.5 Rho GTPase cycle 7
1.1.6 Rho GTPase crosstalk 8

1.2 Bacterial toxins modifying Rho GTPases 9
1.2.1 Inactivating toxins 10
1.2.3 Activating toxins 11

1.3 Cytotoxic Necrotizing Factors 12
1.3.1 Structure of CNFs 12
1.3.3 Uptake and enzymatic function of CNF 14

1.4 Rho GTPase modifications 15
1.4.1 Ubiquitination and degradation 16
1.4.2 Nuclear import 17
1.4.3 Rho GTPases and cancer 18

1.5 Objectives 20

2 Materials and Methods 21

2.1 Materials 21
2.1.1 Companies 21
2.1.2 Inhibitors 21
2.1.3 Kits 22
2.1.4 Other materials 22
2.1.5 Culture media and supplements 22
2.1.6 Cell lines 23
2.1.7 Antibodies for Western blotting and Immunoprecipitation 23
2.1.8 Primers and vectors 24
2.1.9 Buffers and solutions 25

2.2 Methods 27
2.2.1 Polymerase chain reaction 27
2.2.2 Site-directed mutagenesis 28
2.2.3 Primer design 28
2.2.4 DNA purification 28
2.2.5 Agarose gel electrophoresis and gel extraction 29
2.2.6 Restriction enzyme digestion 29
2.2.7 Ligation 29
2.2.8 Transformation of bacteria by heat shock 30
2.2.9 Preparation of glycerol stocks 30
2.2.10 Expression and purification of GST-constructs in E. coli 30
2.2.11 Cell culture 31
2.2.12 Toxin treatment 31

2.2.13 Transfection of mammalian cells 31
2.2.14 Preparation of cell lysate 32
2.2.15 Subcellular fractionation of nuclei and cytosol 32
2.2.16 Membrane isolation 32
2.2.17 BCA protein quantification assay 33
2.2.18 Effector pull-down assay 33
2.2.19 Immunoprecipitation (IP) and Co-IP 34
2.2.20 SDS polyacrylamide gel electrophoresis 34
2.2.21 Western blotting 35
2.2.22 Preparation of probes for mass spectrometry 35
2.2.23 Dual-Luciferase® reporter assay 36
2.2.24 Immunostaining and microscopy 36

3 Results 37

3.1 Effects on Rho GTPases by CNF1 and CNFY 37
3.1.1 Activation of Rac1, RhoA and Cdc42 by CNF1 and CNFY 37
3.1.2 Transient stress fiber and lamellipodia formation 39

3.3 Time-dependent inactivation of Rac1 after CNF1 40
3.3.2 CNF1 induces Rac1 degradation via the 26S proteasome 41
3.3.3 Rac1 interaction with Karyopherin α2 after CNF1 deamidation 42
3.3.4 CNF1 induces Rac1 translocation to the nucleus via its C-terminal polybasic region 43
3.3.5 Rac1Q61E interacts with a variety of nuclear proteins 45

3.4 Time-dependent inactivation of RhoA after CNF1 49
3.4.1 CNF1-deamidated RhoA is not degraded by the 26S proteasome 50
3.4.2 Protein expression is not altered by CNF1 51
3.4.3 Inactivation of RhoA by CNF1 is a dominant effect over CNFY-pre-activation 52
3.4.4 CNF1 decreases CNFY-induced RhoA signaling in Dual-Luciferase® reporter assay 54
3.4.5 CNF1 induces inactivation of RhoAQ63E and RhoAG14V but not of RhoAQ63L 55
3.4.6 CNF1-induced RhoA regulation is independent of Cdc42 signaling 57
3.4.7 RhoGDIα is not involved in the CNF1-induced inactivation of RhoA 59
3.4.8 Lack of Isoprenyl group blocks CNF1-induced RhoA regulation 63
3.4.9 RhoAS188E is not inactivated by CNF1 compared to RhoAS188A 64
3.4.10 Membrane distribution correlates with the RhoA activity pattern 65
3.4.11 Cell line responsiveness to RhoA inactivation by CNF1 67
3.4.12 Membrane distribution of RhoA correlates with cell line specificity 69

3.5 Biological relevance of RhoA inactivation by CNF1 71
3.5.1 CNFY-induced RhoA signaling pathway leads to apoptosis in LNCaP cells 71
3.5.2 CNFY-dependent apoptosis in LNCaP cells is blocked by CNF1 73

4 Discussion _____ 75

4.1 Activation of Rho GTPases Rac1 and RhoA by CNF1 is transient _____ 75

4.2 Deamidated Rac1 is subjected to degradation _____ 76

4.3 Deamidated Rac1 is translocated to the nucleus by C-terminal interaction with KPNA2 _____ 77

4.4 Interaction partners of nuclear Rac1 _____ 78

4.5 CNF1-deamidated RhoA is not degraded or differentially expressed _____ 80

4.6 CNF1-induced inactivation dominates over generally activated RhoA _____ 81

4.7 RhoA negative regulation is independent from Cdc42 or RhoGDI _____ 82

4.7.1 Cdc42 is not involved in the CNF1-induced inactivation of RhoA _____ 82

4.7.2 RhoGDI is dispensable for the CNF1 effect _____ 83

4.8 The isoprenylation and membrane binding of RhoA is essential for the CNF1-promoted inactivation mechanism _____ 84

4.9 CNF1 induces transient membrane binding of RhoA _____ 86

4.10 Model of RhoA and Rac1 inactivation by CNF1 _____ 88

4.11 Physiological effects of CNFY and CNF1 in LNCaP cancer cells _____ 90

5 Outlook _____ 93

6 Summary _____ 95

7 Reference List _____ 97

8 List of Abbreviations _____ 108

9 Publications _____ 111

1 INTRODUCTION

Bacterial pathogens developed several strategies to overcome defense systems of eukaryotic hosts. Within the infection process they attach to and cross through epithelial layers, escape from the innate and adaptive immune response and find a physiological niche to survive. Many bacterial pathogens accomplish this by modulating the actin cytoskeleton since it plays pivotal roles in host-pathogen interactions such as in the control of epithelial barrier functions and in processes of the immune response.

1.1 Rho GTPases and the actin cytoskeleton

1.1.1 The actin cytoskeleton

The actin cytoskeleton is involved in many cellular events such as intracellular vesicle transport, phagocytosis and cytokinesis, cell migration, immune signaling, the control of cytokine and reactive oxygen production and in epithelial barrier regulation (Dominguez, R. and Holmes, K. C., 2011; Insall, R. H. and Machesky, L. M., 2009). Fundamental to these functions is the assembly and disassembly of actin filaments. Actin is an ATP-binding protein that exists in a highly dynamic equilibrium of monomeric globular actin (G-actin) and polymerized filaments (F-actin). Diverse proteins regulate the process of assembly and disassembly, such as the actin-related protein (Arp) 2/3 complex, cofilin, profilin and many others (Dominguez, R. and Holmes, K. C., 2011). The Arp2/3 complex is a seven-subunit protein that catalyzes nucleation of actin. Two of its subunits, the actin-related proteins Arp2 and Arp3 closely resemble the structure of monomeric actin and thereby serve as nucleation sites for new actin filaments. Arp2/3 is activated by Wiskott–Aldrich syndrome protein (WASP) and WASP-family verprolin homologue (WAVE) (Millard, T. H. *et al.*, 2004). Polarized elongation is promoted by profilin, which binds ATP-bound G-actin and attaches the monomer to the plus end of the filament. Filament length is controlled by depolymerization at the minus end, where cofilin (a member of the actin-depolymerizing factor (ADF) family) removes assembled GDP-bound F-actin (Mazur, A. J. *et al.*, 2010).

The most abundant morphological features of the actin cytoskeleton in cultured cells are the formation of lamellipodia, filopodia and stress fibers. Lamellipodial actin is arranged in a branched network of actin filaments localized beneath the membrane, promoting broad protrusions, while filopodia are long thin protrusions that are composed of parallel F-actin. Stress fibers consist of thick acto-myosin bundles located within the cell. Their contraction is mediated by myosin II, which moves antiparallel actin filaments past each other and thereby provides the force that rearranges the actin cytoskeleton (Burridge, K. and Doughman, R., 2006; Ridley, A. J., 2006; Krugmann, S. *et al.*, 2001). Most actin functions are regulated by small GTPases of the Rho family.

1.1.2 Rho family of small GTPases

Small GTPases are monomeric proteins with a molecular mass ranging from 20 to 40 kDa. The Ras superfamily of small GTPases is divided into seven families: Ras, Rho, Rab, Rap, Arf, Ran and Rheb. Members of the Ras superfamily regulate many features of cell behavior. Primarily, cell proliferation and differentiation is controlled by Ras proteins, whereas the most profound effects on the actin cytoskeleton are controlled by the Rho family (Takai, Y. *et al.*, 2001). The Rho family comprises approximately 20 members that are further divided into the Rho-like, Rac-like, Cdc42-like, Rnd, RhoBTB and RhoT subfamilies (see Figure 1). Since Rho GTPases are key regulators of the actin cytoskeleton, they are important for cell migration, cytokinesis, phagocytosis, cell adhesion and many other actin-related cellular functions. Moreover, Rho proteins are also involved in other aspects of cellular functions such as vesicle trafficking, differentiation, oncogenesis and gene transcription (Heasman, S. J. and Ridley, A. J., 2008; Takai, Y. *et al.*, 2001; Matozaki, T. *et al.*, 2000).

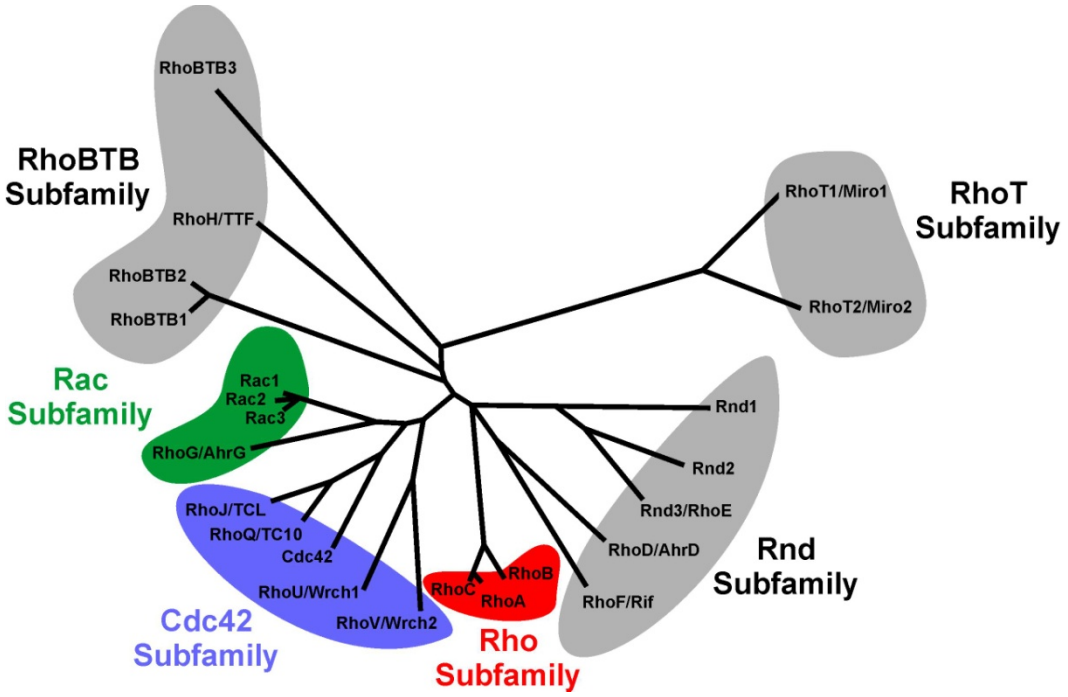


Figure 1: Dendrogram of the Rho family of small GTPases. Members of the same subfamily are grouped by shaded areas. Best-characterized subfamilies are highlighted in green (Rac), blue (Cdc42) and red (Rho). Adapted from (Bustelo, X. R. *et al.*, 2007)

1.1.3 RhoA, Rac1 and Cdc42

The best-characterized members of the Rho GTPase family are RhoA, Rac1 and Cdc42, which are strongly linked to changes in the filamentous actin system. RhoA regulates stress fiber formation and contraction, whereas Rac1 and Cdc42 induce the formation of lamellipodia and filopodia, respectively. Stress fibers and focal adhesions confer contractility on a cell and are mainly mediated by the RhoA/Rho kinase (ROCK)-signaling pathway. The serine/threonine kinase ROCK inactivates the myosin light chain phosphatase (MLC-P) and thereby indirectly leads to the increase of myosin light chain II (MLC) phosphorylation. In addition, ROCK achieves this by direct phosphorylation of MLC. Thereby, the phosphorylated MLC is stabilized and causes the formation of actin bundles. ROCK is also capable of activating LIM kinase, which in turn phosphorylates cofilin. Cofilin, is thereby inhibited in its actin-depolymerizing function (Lappalainen, P. and Drubin, D. G., 1997). Both, Rac1 and Cdc42 bind to a common set of effectors, e.g. p21-activated kinase (PAK1). The serine/threonine kinase PAK1 activates the LIM kinase and thereby stabilizes actin filaments

due to cofilin inhibition. Rac1 leads to formation of lamellipodia via the Rac/WAVE protein pathway. Similarly, Cdc42 contributes to actin reorganization and filopodia formation by means of the WASP pathway. RhoA, Rac1 and Cdc42 signaling that link to actin rearrangement are shown in Figure 2 (Matozaki, T. *et al.*, 2000).

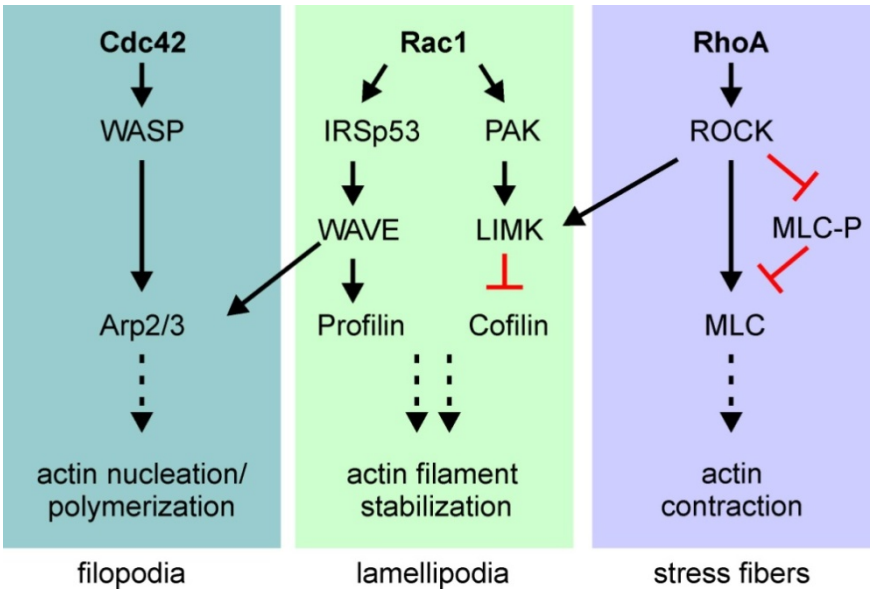


Figure 2: Signaling pathways from RhoA, Rac1 and Cdc42. Cdc42 leads to the formation of filopodia, Rac1 to lamellipodia and RhoA to the formation of stress fibers. Modified from (Spiering, D. and Hodgson, L., 2011; Matozaki, T. *et al.*, 2000)

1.1.4 Rho GTPase structure

Rho GTPases share a common G-domain fold, which consists of a six-stranded β-sheet surrounded by α-helices. A structural feature that distinguishes the Rho proteins from other small GTPases is the so-called Rho insert domain located between the fifth β strand and the fourth α helix in the protein (Vetter, I. R. and Wittinghofer, A., 2001; Zong, H. *et al.*, 2001). Like the classic monomeric Ras GTPases, Rho proteins act as molecular switches, existing in an inactive GDP- or active GTP-bound state. These two states are regulated profoundly by switch I and switch II regions within the G-domain (encompassing amino acids 29–42 and 62–68 for RhoA), which change their conformation upon GDP or GTP binding (Figure 3) (Ihara, K. *et al.*, 1998). The variable C-terminus of small GTPases is posttranslationally geranylgeranylated or farnesylated at the so-called CaaX-Box (C: cysteine, a: aliphatic, X: any

amino acid). First, the cysteine is isoprenylated, then the tripeptide aaX is cleaved off and the protein is carboxymethylated at the cysteine. This lipid anchor allows them to attach to cellular membranes (Roberts, P. J. *et al.*, 2008). In the inactive GDP-loaded state, the isoprenyl-anchor is inserted into the hydrophobic pocket of Rho GTPase guanine nucleotide dissociation inhibitors (RhoGDIs), which sequester the Rho GTPase in the cytosol (DerMardirossian, C. and Bokoch, G. M., 2005). Other structural determinants at the C-terminus include the polybasic region (PBR) and the destruction box (D-Box). The D-Box (RXXL) is essential for ubiquitination and degradation of Rac (RAVL) and RhoA (RAAL) by the 26S proteasome, while Cdc42 (LAAL) is not a substrate (Pop, M. *et al.*, 2004). The PBR is comprised of a series of lysines and arginines and often immediately precedes the C-terminal CaaX sequence. In many GTPases the PBR contains a nuclear localization sequence (NLS) (K(K/R)X(K/R)). The NLS is an indicator of nucleocytoplasmic shuttling that e.g. also discriminates between the different Rac isoforms as seen in Figure 3C, allowing only Rac1 to operate in the nucleus (Lanning, C. C. *et al.*, 2004).

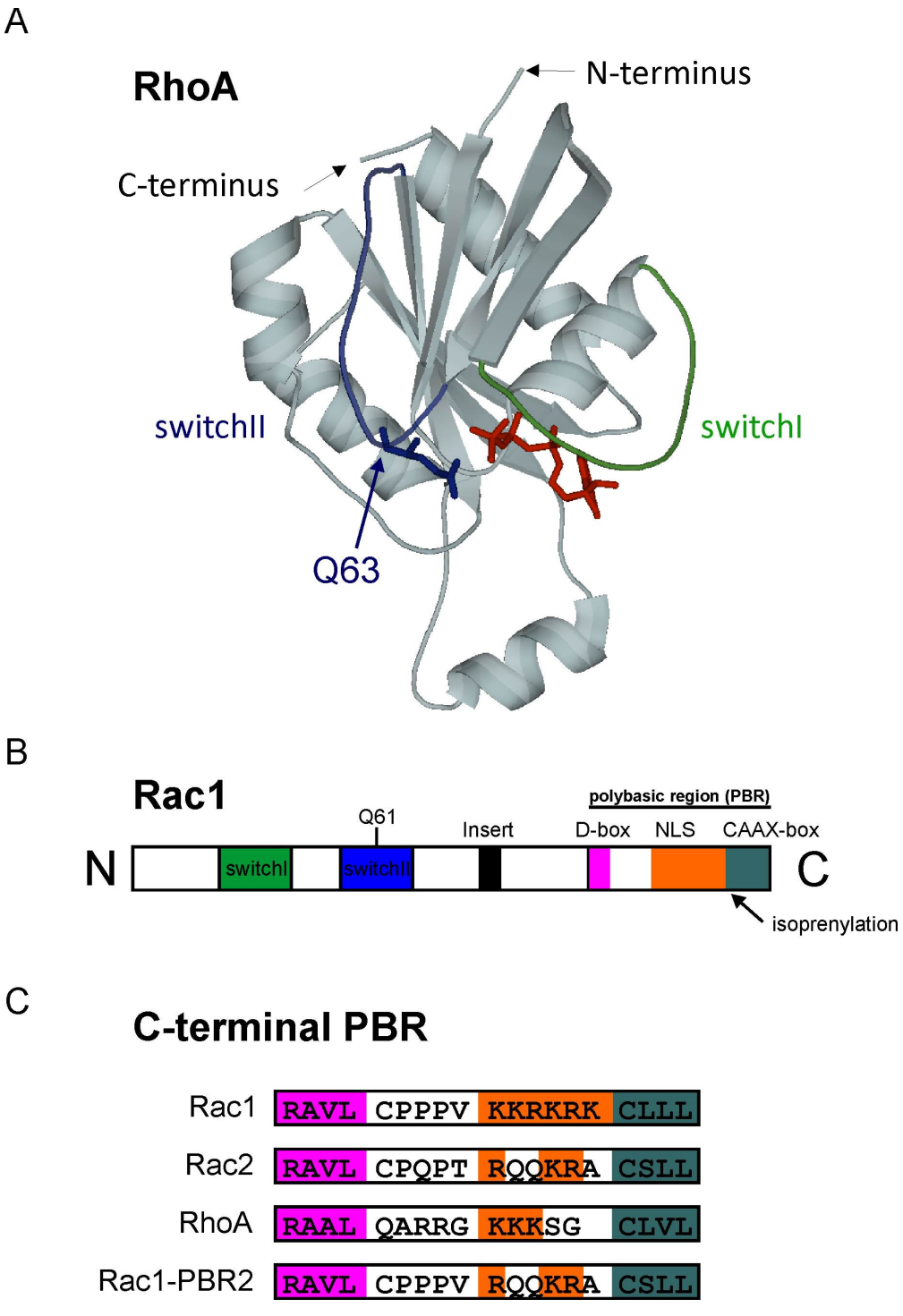


Figure 3: Crystal structure and scheme of RhoA and Rac isoforms. A] A cartoon representation of human RhoA in the constitutive active form with GTP analogue is shown. GTP is colored in red. Switch I and switch II are marked as indicated. The glutamine 63 (Q63), which is essential for the hydrolysis of GTP, is located in the switch II region. The structure was modified from (Ihara, K. *et al.*, 1998) using PyMOL™ v0.99. B] The scheme of the complete Rac1 protein with functional domains is displayed. C] The sequence of the C-terminal polybasic region (PBR) of Rac1, Rac2, RhoA and the chimera Rac1-PBR2 are aligned. Only Rac1 contains a functional NLS. Pink: D-box sequence (RXXL). Orange: canonical nuclear localization sequence (NLS) (K(K/R)X(K/R)). Grey: CaaX-box.

1.1.5 Rho GTPase cycle

Rho GTPase activation and inactivation are tightly regulated by a number of proteins. For Rho GTPases to become active, they are released from RhoGDIs (DerMardirossian, C. and Bokoch, G. M., 2005). Via their isoprenylated C-terminus they attach to membranes and interact with membrane-associated guanine nucleotide exchange factors (GEFs). GEFs catalyze the exchange of GDP to GTP. Once GDP is released, GTP is bound immediately due to its 10-fold higher cellular concentration as compared to GDP (van, Triest M. and Bos, J. L., 2004). Through GTP-loading, the highly flexible switch regions change their conformations to the active form. Membrane localization and conformational changes determine the interaction with their effectors, which bind to the surface of Rho GTPases formed by the switch regions. Signal termination is induced by hydrolysis of GTP to promote effector dissociation. Similar to the GDP exchange, the slow intrinsic hydrolytic activity is accelerated by GTPase-activating proteins (GAPs). The GDP-loaded Rho proteins are captured back by RhoGDIs in the cytosol (Takai, Y. *et al.*, 2001) (Figure 4).

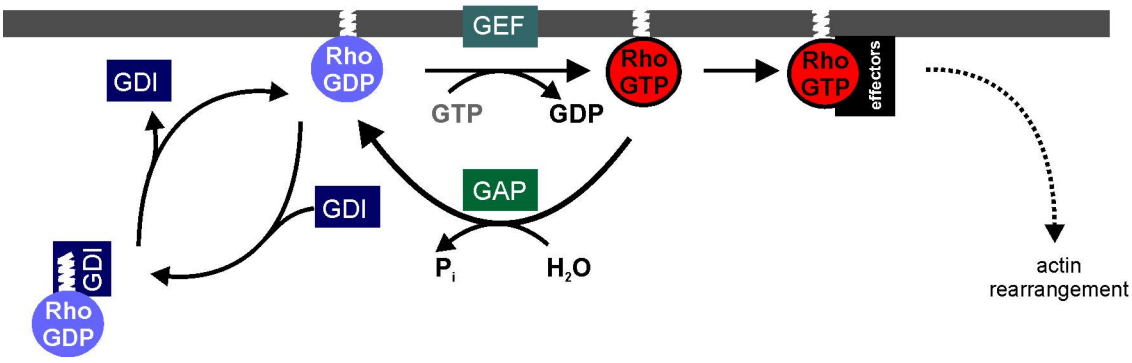


Figure 4: Rho GTPase cycle. The inactive GDP-bound Rho is in complex with guanine nucleotide dissociation inhibitor (GDI) in the cytosol. Upon RhoGDI release, Rho is activated by GDP/GTP exchange, catalyzed by guanine nucleotide exchange factors (GEFs) and interacts with effectors at the membrane. GTPase-activating proteins (GAPs) catalyze the inactivation by GTP hydrolysis. RhoGDI sequesters the GDP-bound Rho GTPase in cytosol.

1.1.6 Rho GTPase crosstalk

Currently, one of the exciting aspects in the field of Rho GTPase regulation concerns the multiple interaction pathways between Rho family proteins. Reported crosstalk range from positive to negative feedback loops. Moreover, signaling pathways of Rho GTPases are capable to work in concert to accelerate a physiological effect. The complexity becomes even more obvious, when all regulatory levels are taken into account, including signaling via GEFs, GAPs, GDIs or downstream effectors.

It was reported that Cdc42 activates Rac1, which in turn activates RhoA (Ridley, A. J. *et al.*, 1992). More recently, the dogma was turned toward an antagonistic relationship, where activation of Rac1 leads to the inactivation of RhoA. For example, Rac1-mediated PAK1 activation promotes loss of stress fibers and focal adhesions via inhibition of the MLC-kinase (Sanders, L. C. *et al.*, 1999). Furthermore, NET1 (neuroepithelioma transforming gene 1) a specific exchange factor for RhoA is phosphorylated and blocked by PAK1, leading to decreased RhoA activity (Alberts, A. S. *et al.*, 2005). Moreover, PAK1 phosphorylation of RhoGDI enhances Rac1 release from this complex to further increase Rac1 activity (DerMardirossian, C. *et al.*, 2004).

The molar amount of RhoGDI is roughly equal to the total levels of RhoA, Rac1 and Cdc42 (DerMardirossian, C. and Bokoch, G. M., 2005). Therefore, an alteration of RhoGDI binding affinity to one GTPase disturbs the balance of inactive pools and influences the activation levels of the remaining other GTPases. Bourmeyster *et al.* elucidated the aspect of phosphorylation concerning the interaction between RhoA and GDI. They have provided evidence that the kinases, modulating the phosphorylation state of RhoGDIs, are important regulatory elements, where low phosphorylation of RhoGDI coincides with an increased RhoA activity. But also phosphorylation of the Rho GTPase itself has been observed to affect binding affinity for RhoGDI (Bourmeyster, N. and Vignais, P. V., 1996). The involvement of protein kinase C (PKC)-dependent phosphorylation of RhoGDI was shown to correlate with RhoA activation (Dovas, A. *et al.*, 2010). Protein kinase A (PKA) mediates phosphorylation of RhoA on Ser188 at the C-terminus, thereby enhances binding affinity to RhoGDI and blocks interaction with membrane-associated exchange factors and effectors (Rolli-Derkinderen, M. *et al.*, 2005).

1.2 Bacterial toxins modifying Rho GTPases

Many pathogenic microorganisms produce effectors/toxins that disturb the function of the actin cytoskeleton to promote their survival in the host. Several toxins like *Clostridium botulinum* C2 toxin act directly on actin (Schleberger, C. *et al.*, 2006). However, the majority of bacterial toxins/effectors target the family of Rho GTPases. It has been shown that all phases of Rho GTPase cycling can be affected. Some toxins catalyze a covalent modification, while others act in a modulatory fashion. Thereby, they lead to dramatic changes of the actin cytoskeleton and downstream signaling events. Basically, bacterial toxins that act directly on Rho GTPases can be classified into two groups: the Rho GTPase inactivating or activating toxins. The model in Figure 5 visualizes the mode of action of different toxins.

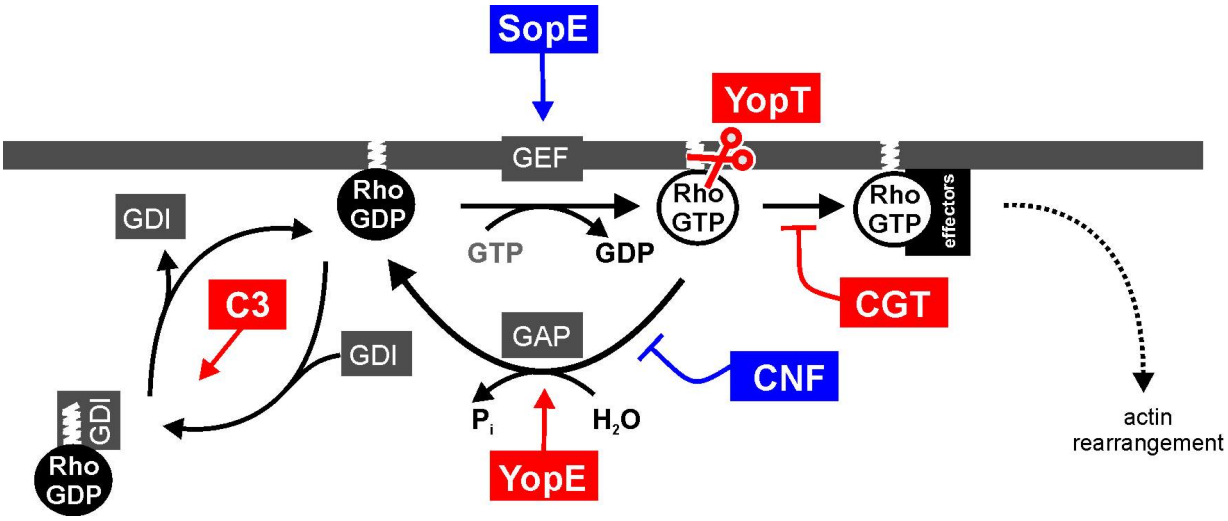


Figure 5: Overview of bacterial toxins/effectors acting on the Rho GTPase cycle. Bacterial toxins/effectors interfere with the Rho GTPase cycle at multiple steps by inactivation (red boxes) or activation (blue boxes). The most efficient inactivating toxins are the CGTs like toxin A/B, which glucosylate Thr37/35 (Rho, Rac and Cdc42) and thereby block interaction with GDIs, GEFs, GAPs and effectors. Consequently, downstream signaling e.g. to the actin cytoskeleton is inhibited. ADP-ribosylation of RhoA at Asn41 by C3 exoenzymes leads to increased GDI affinity and inhibition of GEF interaction. The cysteine protease YopT cleaves off the isoprenylated C-terminus, causing release of Rho proteins from membranes. YopE mimics GAP activity to enhance GTP hydrolysis. Activating toxins like SopE function as GEFs to facilitate GDP/GTP exchange and activate Rho GTPases. Deamidation and transglutamination of Gln63/61 (Rho, Rac and Cdc42) by CNFs and DNT constitutively activate Rho proteins (1). Abbreviations: GDI, guanine nucleotide dissociation inhibitor; GEF, guanine nucleotide exchange factor; GAP, GTPase-activating protein; CGT, clostridial glucosylating toxin; CNF, cytotoxic necrotizing factor; YopT/E, *Yersinia* outer protein E/T; SopE, *Salmonella* outer protein E. Modified from (Aktories, K., 2011)

1.2.1 Inactivating toxins

Glucosylation, ADP-ribosylation, AMPylation/adenylylation and proteolytic cleavage can inactivate Rho GTPases. The very potent large clostridial glucosylating cytotoxins (CGTs), e.g. toxin A/B from *Clostridium difficile*, catalyze the transfer of the glucose moiety to a conserved threonine residue in the switch I region (Thr37 in RhoA, and Thr35 in Rac/Cdc42), which is involved in the coordination of the Mg^{2+} ion and the binding of the nucleotide. This glucosylation blocks binding to regulators of the GTPase cycle: GEFs, GDIs, GAPs but most importantly to Rho effectors. Thus, CGTs cause cell rounding by blockage of Rho GTPase downstream signaling (Aktories, K. *et al.*, 2011). Similarly, *Vibrio* VopS modifies the same threonine residue by adding an adenosine 5'-monophosphate (AMP). The resulting AMPylation/adenylylation prevents the interaction of Rho GTPases with downstream effectors, thereby inhibiting actin assembly and rounding of cells (Yarbrough, M. L. *et al.*, 2009). The same cellular effects are seen by intoxication with *Yersinia* effector YopT but the mechanism is completely different. As a cysteine protease, YopT cleaves off the isoprenylated C-terminus, which is essential for membrane insertion and RhoGDI interaction. Thereby, Rho GTPases detach from the membrane and are incapable of interacting with membrane-bound GEFs (Fueller, F. and Schmidt, G., 2008). Consequently, YopT intoxication leads to actin disruption and cell rounding (Sorg, I. *et al.*, 2001; Aepfelbacher, M. *et al.*, 2005). The exoenzyme C3 from *Clostridium botulinum*, a member of the C3-like toxin family, also belongs to the class of inactivating toxins. It is an ADP-ribosyltransferase that modifies Rho (A, B, C) at Asn41. This modification enhances the affinity to RhoGDI and leads to Rho inactivation and subsequent disappearance of RhoA-induced stress fiber formation (Genth, H. *et al.*, 2003; Aktories, K. *et al.*, 2004). Reversible inhibition is achieved through the mimicry of GAP-like activity e.g. *Salmonella* effector YopE promotes GTP hydrolysis and enrichment of the GDP-bound inactive state of Rho proteins (Aili, M. *et al.*, 2006; Andor, A. *et al.*, 2001; von Pawel-Rammingen, U. *et al.*, 2000). Thus, inactivation of Rho proteins is a widespread strategy of bacteria to disrupt the actin cytoskeleton. However, there are few toxins that can activate Rho GTPases.

1.2.3 Activating toxins

SopE from *Salmonella* species ranks among the Rho-activating bacterial effectors with a modulatory action. By imitating host GEF activity SopE enhances GTP exchange, leading to increased activation of Rho proteins (Friebel, A. and Hardt, W. D., 2000). Only a small family of toxins achieves activation via covalent modification. In contrast to the inhibitory functions of C3-like toxins, ADP-ribosylation of Gln61/63 by TccC5 toxin from *Photorhabdus luminescens* activates Rho, Rac and Cdc42 (Lang, A. E. *et al.*, 2010). Activation is also achieved through deamidation and transglutamination of the same glutamine residue by the dermonecrotic toxin (DNT) from *Bordetella* species and the cytotoxic necrotizing factors (CNFs) from *E. coli* and *Y. pseudotuberculosis* (Hoffmann, C. and Schmidt, G., 2004). The carboxamide nitrogen of this glutamine stabilizes the transition state during GTP hydrolysis and is thus essential for the intrinsic and GAP-stimulated GTPase activity of small GTPases. Therefore, modification of this residue by ADP-ribosylation, deamidation or transglutamination blocks GTP hydrolysis and triggers RhoA GTPase activation.

1.3 Cytotoxic Necrotizing Factors

1.3.1 Structure of CNFs

The CNF family comprises four members: CNF1, 2, 3 and Y. CNF1 shares more than 80% sequence identity with CNF2, 70% with CNF3 and 60% with CNFY. CNF1 (2, 3) originates from uropathogenic *E.coli* strains, while CNFY was isolated from *Yersinia pseudotuberculosis (Stoll, T. et al., 2009; Orden, J. A. et al., 2007; Boquet, P., 2001; Hoffmann, C. et al., 2004; Denko, N. et al., 1997).* All CNFs are single chain autotransporter-toxins of approximately 115 kDa. The N-terminus exhibits the receptor-binding domain (RBD). The N-terminal domain mediates uptake via endocytosis into mammalian cells, while the catalytic center is located at the very C-terminus. Both domains are connected by a translocation domain. Structural analysis revealed that the catalytic triad consists of Cys866, His881 and a stabilizing Val833 as shown in Figure 6A. The catalytic center is similar but not identical to the catalytic triads of transglutaminases and of certain cysteine proteases, which encompass a cysteine, a histidine and an aspartate (Schmidt, G. *et al.*, 1998; Hoffmann, C. *et al.*, 2007). The CNF family members show different substrate specificity. While CNF1 (2 and 3) modify RhoA, Rac1 and Cdc42 in intact cells, CNFY is specific for RhoA. The flexible loop regions in the substrate-binding pocket of the toxins have been shown to account for the different substrate specificity (Figure 6B). Especially the surface loops 2, 3 and 8 seem to play a superior role in CNF1 and CNFY substrate recognition (Schmidt, G. *et al.*, 1998; Hoffmann, C. *et al.*, 2007).

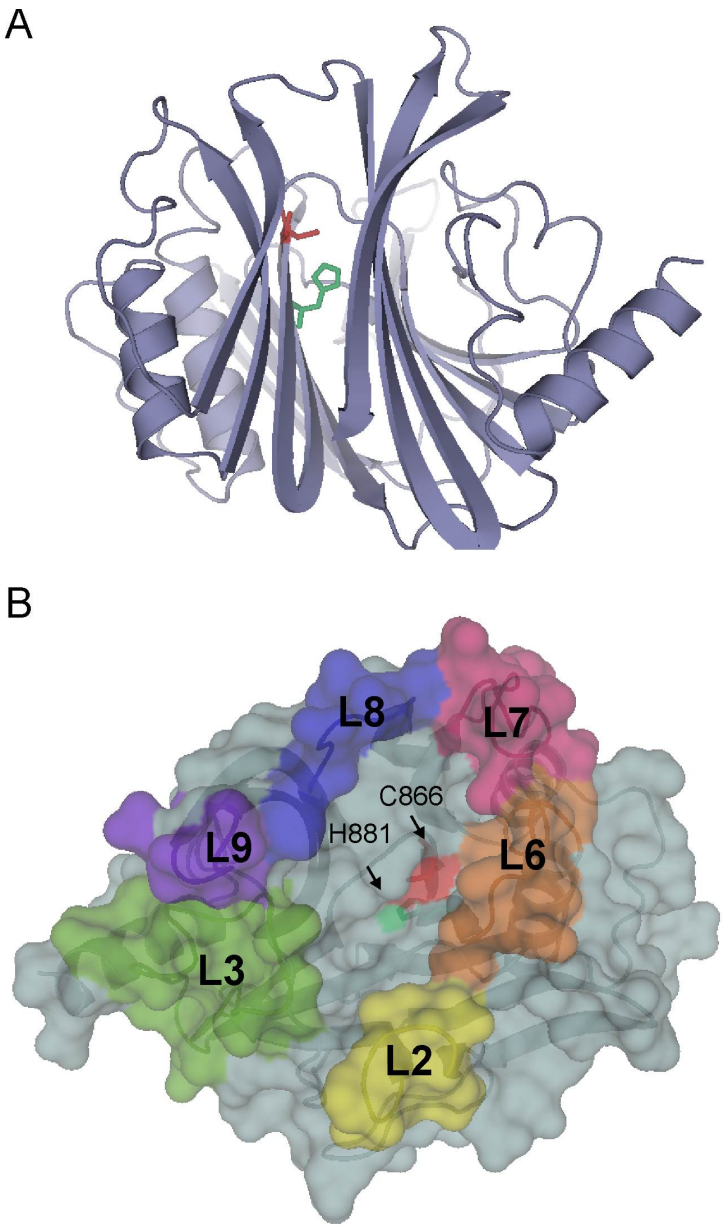


Figure 6: Crystal structure of CNF1. A] Ribbon representation of the catalytic domain of CNF1 (amino acids 720-1014) with view from the 13 ß-sheets (rear of the substrate-binding site). The catalytic residues Cys866 (red) and His881 (green) are highlighted. B] Surface-ribbon presentation of the substrate binding site of CNF1 with highlighted flexible loop regions (L) and the catalytic cysteine/histidine. The numbering of loop elements is according to chain succession. Both structures were created from (Buetow, L. *et al.*, 2001) using PyMOL™ v0.99.

1.3.3 Uptake and enzymatic function of CNF

The p67 non-integrin laminin receptor was identified and suggested to be the receptor for CNF1 (Chung, J. W. *et al.*, 2003), while the receptor for CNFY has not been identified yet. However, it was suggested that two different receptors for the uptake of CNF1 and CNFY exist leading to receptor-mediated endocytosis (Contamin, S. *et al.*, 2000) (Hoffmann, C. *et al.*, 2007). According to this model, the CNF containing endosome is acidified, leading to a conformational change of the toxin and insertion of the translocation domain into the vesicular membrane. Proteolytic cleavage releases the C-terminus with its catalytic function into the host cytosol. Once CNF has reached the cytosol, it modifies Rho GTPases by deamidation of glutamine 63 (RhoA) or glutamine 61 (Rac1 /Cdc42), respectively, and thereby leads to constitutive activation of the Rho GTPase (Figure 7).

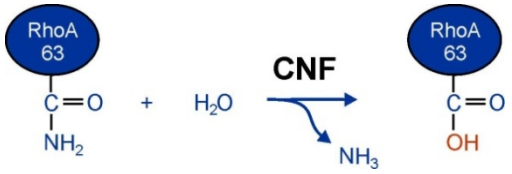


Figure 7: CNF deamidase reaction. RhoA is deamidated at glutamine 63 to glutamate.

In vitro, CNF is also able to cause this effect by transglutamination, but *in vivo* it primarily acts as a deamidase. Vice versa, the related DNT from *Bordetella* targets the same residue of RhoA by transglutamination/ deamidation, but predominantly favors the transglutamination reaction with primary amines as substrates *in vivo* (Hoffmann, C. and Schmidt, G., 2004). Constitutive activation of Rho GTPases leads to massive alterations of the actin cytoskeleton. As a consequence, CNF1 induces striking morphological effects on cultured cells such as flattening of cells, formation of stress fibers (RhoA effect), lamellipodia (Rac1 effect), filopodia (Cdc42 effect) while CNFY specifically leads to RhoA dependent structures. Both toxins promote multinucleation (Boquet, P., 2001; Fiorentini, C. *et al.*, 1997).

1.4 Rho GTPase modifications

As described above, many modifications of Rho proteins by bacterial toxins or endogenous signaling pathways can regulate their activation status. A summary of most known modifications is presented in Figure 8.

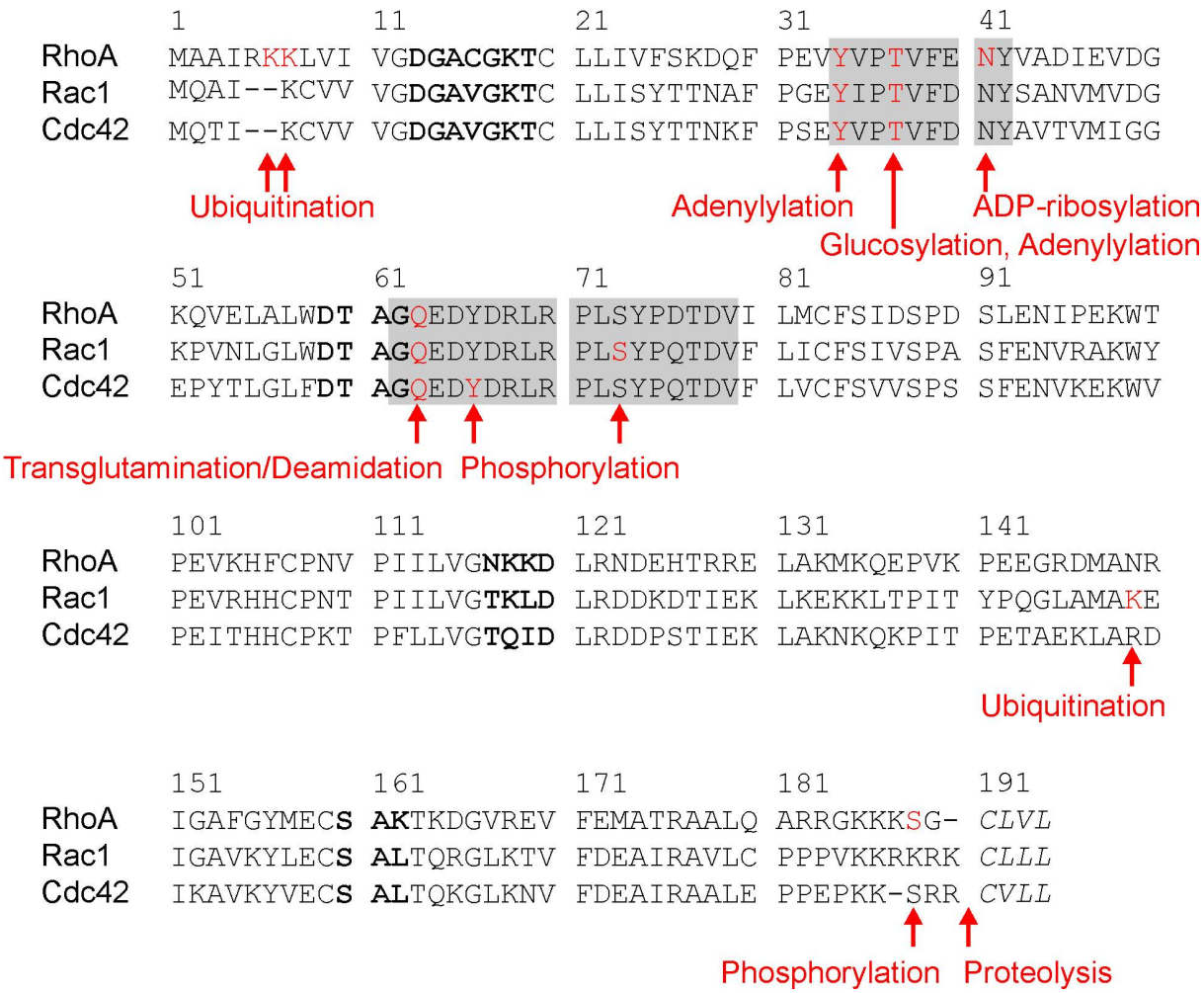


Figure 8: Alignment of RhoA, Rac1 and Cdc42 with indicated sites of modification. The switch I and switch II region are highlighted in grey. Residues in bold correspond to the different G-boxes (involved in the binding of the nucleotide). The conserved C-terminal CaaX-box (C, cysteine; a, aliphatic amino acid; X, any amino acid) motif is shown in italics. Known residues modified by posttranslational modifications and the type of modification are indicated in red. Adapted from (Visvikis, O. *et al.*, 2010; Fueller, F. and Schmidt, G., 2008)

1.4.1 Ubiquitination and degradation

Rho proteins are regulated by posttranslational modification but also through the control of protein synthesis, especially at the level of transcription, and by proteolytic degradation. In eukaryotes, proteins are typically degraded by their targeting to a soluble proteolytic complex called the proteasome, which is abundant in the cytosol and nuclear compartments (von, Mikecz A., 2006; Craiu, A. *et al.*, 1997). Proteasomal substrates include damaged or denatured proteins that need to be removed, but also numerous regulatory proteins whose removal is part of basal housekeeping functions to rapidly and irreversibly inactivate a protein by destroying it. Degradation of many proteins involves their initial modification by conjugation of ubiquitin (Ub). The 26S proteasomes are multi-subunit proteolytic machines that preferentially degrade proteins tagged with poly-ubiquitin chains. The covalent attachment of ubiquitin occurs at the amino group of a lysine residue of the substrate and the C-terminal carboxylate group of ubiquitin. Conjugation is accomplished in three sequential reactions, which are catalyzed by an ubiquitin-activating enzyme (E1), an ubiquitin-conjugating enzyme (E2) and an ubiquitin-protein ligase (E3). After the formation of the ubiquitin-substrate isopeptide bond, a second ubiquitin can be conjugated to a specific lysine residue, typically Lys48, of the first ubiquitin. Repetition of this reaction leads to assembly of a poly-ubiquitin chain on the proteolytic substrate that targets the protein for degradation by the 26S proteasome (Pickart, C. M., 1997). A model of ubiquitination and degradation is shown in Figure 9. Intracellular proteolysis plays a crucial role in the cell cycle, signal transduction, gene expression, development, maintenance of proper protein folding, antigen processing and other cellular processes (von, Mikecz A., 2006).

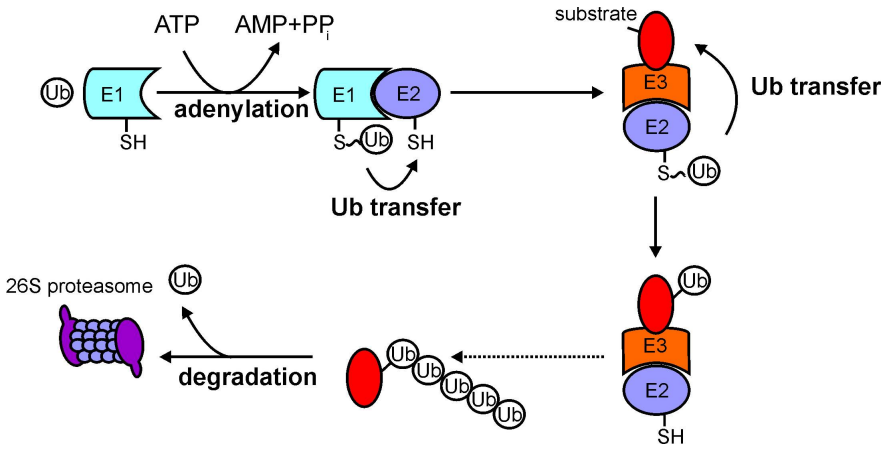


Figure 9: Ubiquitylation and degradation of proteins. Ubiquitination is a cascade that involves of E1 ubiquitin-activating, E2 ubiquitin-conjugating and E3 ubiquitin ligase enzymes. E1 adenylates ubiquitin (Ub) and forms an E1-Ub intermediate via a thioester bond. Ubiquitin is transferred from E1 to E2, and then to the substrate in complex with E3. This can be repeated several times. Poly-ubiquitinated proteins are targeted to the 26S proteasome, where ubiquitin is released during substrate protein degradation. PPi, inorganic pyrophosphate. Modified after (Maupin-Furlow, J., 2012)

1.4.2 Nuclear import

Preliminary data indicate that Rho proteins have been localized to the nucleus (Michaelson, D. *et al.*, 2008). Nuclear transport is a fundamental physiological process occurring in eukaryotic cells to regulate gene expression. Thus, an extracellular signal must be transduced across the plasma membrane and subsequently across the nuclear envelope to propagate the signal from the cytosol to the nucleus. Many signaling responses, therefore, rapidly effect the nuclear localization of transcription factors or alternatively of kinases that, once translocated, phosphorylate and activate transcription factors in the nucleus.

Molecular trafficking between the nucleus and the cytoplasm occurs through nuclear pore complexes (NPC). To enter the nucleus, proteins larger than 40 kDa usually require polybasic nuclear localization signals (NLS). Transport cargoes with a NLS sequence are potential substrates for the nuclear import receptor Karyopherin α2 (KPNA2). Together with importin β, the KPNA2-bound cargo protein forms a ternary complex, which interacts with the nuclear pore complex and translocates to the nucleus (Lange, A. *et al.*, 2007). Inside the nucleus, the trimeric complex is dissociated by binding of Ran-GTP. The nucleotide state of Ran is determined by interaction with its GEF (RCC1) and GAP (RanGAP1), which is distributed

asymmetrically in the cell. Ran-GTP is preferentially found in the nucleus, whereas Ran-GDP is enriched in the cytoplasm. The asymmetric distribution of Ran enables a directed nuclear transport by acting as a molecular switch that is responsible for the binding and release of the cargo. Once released in the nucleus, the protein can carry out its nuclear function mainly involving the regulation of gene transcription (Chook, Y. M. and Blobel, G., 2001).

1.4.3 Rho GTPases and cancer

It is well established that the effector pathways controlled by Ras are key determinants in the regulation of both normal cell proliferation and oncogenic transformation. Direct mutation in Ras (glutamine 61) results in reduced GTP-hydrolyzing activity and, consequently, leads to a permanent activation of the molecule and to tumor onset (Downward, J., 2003). It is worth noting that this glutamine mutation in Ras corresponds to the glutamine (61/63) on Rho proteins modified by CNF1. However, unlike the mutational activation of Ras in human cancers, there are no known examples of activating mutations for Rho GTPases. But there are numerous examples of overexpression in malignant tissue relative to normal tissue, and it is believed that the elevated Rho expression results in enhanced signaling. Rho signaling pathways crosstalk with different oncogenic signaling cascades and contribute to various aspects of tumorigenesis, including survival, growth, and progression of tumor cells (Sahai, E. and Marshall, C. J., 2002). Rho GTPases, found to be aberrantly expressed in human cancers, include RhoA, RhoB, RhoC, Rac1, Rac2, Rac3, RhoG, Cdc42 and Rnd3/RhoE. For example, Rac1 is over-expressed in testicular-, gastric-, squamous cell- and breast cancer. Increased RhoA expression was observed in various human tumors including liver, skin- and colon cancer and also correlated with progression of ovarian, bladder, testicular, gastric and breast cancer. RhoA has been implicated in virtually all stages of cancer progression: for example, constitutively active RhoA was shown to stimulate transformation *in vitro* (Parri, M. and Chiarugi, P., 2010). Studies also implicate that, as a consequence of elevated expression, RhoA is localized to the plasma membrane where it is activated and promotes tumor cell invasion by signaling towards ROCK and actomyosin (Ellenbroek, S. I. and Collard, J. G., 2007). A recent study described that activation of Rho-GTPases in prostate cancer cells lead to apoptotic responses controlled by actin

reorganization (Papadopoulou, N. *et al.*, 2008). Furthermore, it was postulated that RhoA activation by phorbolester treatment with subsequent stress fiber formation induced apoptosis in LNCaP cells (Xiao, L. *et al.*, 2009), a cell line, which was established from a lymph node metastasis of a human prostatic adenocarcinoma (Horoszewicz, J. S. *et al.*, 1983).

Thus, given the significant contributions that elevated Ras and Rho signaling make to tumor growth and progression, targeting these signaling pathways has become a major endeavor in the fight against cancer by targeting directly the activity of Ras and Rho GTPases.

1.5 Objectives

Since the discovery of CNF1 almost three decades ago (Caprioli, A. *et al.*, 1983), many studies have been done to clarify to the activating function of CNF1 towards Rho GTPases. In accordance to these findings, CNF1 has been listed as an activating Rho GTPase toxin. Recently, new findings indicate that in intact cells the assumed constitutive activation of Rho GTPases (especially Rac1 and RhoA) by CNF1 is only a transient effect. Therefore, the main objective of this work was to study the pathways of the so-called CNF1-induced "inactivation" of deamidated Rac1 and RhoA. Moreover, the question of how Rac1 and RhoA differ in the mechanisms that cause their inactivation was addressed.

In detail, this concerned following objectives:

- Characterization of the CNF1-induced inactivation of Rac1 and RhoA by effector pull-downs and actin rearrangements should be performed
- To analyze the role of proteasomal degradation in the process of inactivation
- Interaction partners of deamidated Rac1 should be identified
- The cellular localization of CNF1-deamidated Rac1 should be determined
- To evaluate the nuclear interaction partners of deamidated Rac1
- To compare CNF1 to CNFY towards RhoA activation
- To analyze the involvement of Cdc42 and RhoGDI concerning the inactivation of RhoA
- The role of the isoprenylated C-terminus of RhoA should be determined and the membrane-attachment of deamidated RhoA
- To investigate if membrane-binding correlates with the activation state of RhoA
- It should be tested if RhoA inactivation by CNF1 is present in different cell lines
- The biophysiological role of RhoA upon stimulation of CNF1 and CNFY in apoptotic human androgen-dependent prostate cancer cells LNCaP should be investigated

2 MATERIALS AND METHODS

2.1 Materials

2.1.1 Companies

All chemicals and materials were purchased from:

Abcam plc (Cambridge, UK)
Agilent Technologies Deutschland GmbH (Böblingen, Ger)
Apara Bioscience GmbH (Denzlingen, Ger)
BD Bioscience (Heidelbeg, Ger)
Biochrom AG (Berlin, Ger)
Biozol Diagnostica Vertrieb GmbH (Eching, Ger)
Cell signaling Technology (Frankfurt, Ger)
Fermentas GmbH (St. Leon-Rot, Ger)
GE Healthcare (München, Ger)
Invitrogen (Karlsruhe, Ger)
Karl Roth (Karlsruhe, Ger)
Millipore (Schwalbach, Ger)
NEB, New England Biolabs (Frankfurt, Ger)
PAN biotech (Aidenbach, Ger)
Peqlab (Erlangen, Ger)
Qiagen (Hilden, Ger)
Roche (Mannheim, Ger)
Santa Cruz Biotechnology (Heidelberg, Ger)
Sigma-Aldrich (München, Ger)
Stratagene GmbH (Heidelberg, Ger)
Tocris Biosciences (Bristol, UK)
Uptima Interchim (Sankt Augustin-Buisdorf, Ger)
Promega GmbH (Mannheim, Ger)
Thrombin (Sigma)
PfuUltra II HS DNA polymerase (Agilent Tech.)
T4 Ligase (NEB)
Restriction enzymes (Fermentas)

2.1.2 Inhibitors

MG132, Z-Leu-Leu-Leu-al #C2211 (Sigma)
Y-27632 dihydrochloride #1254 (Biozol)
H-1152 dihydrochloride #2414 (Tocris)
Cycloheximide #C7698 (Sigma)
Complete EASYpack, EDTA-free Protease Inhibitor Cocktail Tablets #5056489001 (Roche)

2.1.3 Kits

QIAGEN® Plasmid Midi and Maxi Kit (Qiagen)
Roti®-Prep Plasmid-Kit (Roth)
Zero Blunt II TOPO PCR Cloning Kit with One-Shot Top10 Chemically Competent
QIAquick® gel extraction kit (Qiagen)
BCA Assay protein Quantification Kit (Uptima)
Dual-Luciferase® reporter assay system (Promega)

2.1.4 Other materials

dNTPs, Nucleotides for PCR (Peqlab)
peqGOLD® Protein Marker III (Prestained) (Peqlab)
GeneRuler™ 1 kb DNA Ladder, (Fermentas)
10x PfuUltra II Reaction Buffer (Stratagene)
PEI, Polyethyleneimine (Sigma)
Glutathione Sepharose 4B (GE Healthcare)
Benzamidine Sepharose 6B (GE Healthcare)
Coomassie Brilliant Blue G-250 (Sigma)
Alexa fluorofores (Invitrogen)
ProLong® Gold antifade reagent with DAPI (Invitrogen)

2.1.5 Culture media and supplements

DMEM #FG0435 (Biochrom)
RPMI 1640 #FG1215 (Biochrom)
FCS, Fetal bovine serum (Biochrom)
BCS, Bovine calf serum (Biochrom)
NEA, Non-essential amino acids (100x) #K0293 (Biochrom)
Na-pyruvate #L0473 (Biochrom),
P/S, Penicillin/Streptomycin (100x) #A2213 (Biochrom)
TE, Trypsin/EDTA (100x) #P10-024100 (PAN biotech)
LB-broth (Luria/Miller) #X968.2 (Roth)
Agar-Agar #5210.2 (Roth)
ITS Liquid Media Supplement (100×) (Sigma)
OptiMEM (Invitrogen)

2.1.6 Cell lines

HeLa	Human Cervix cancer cells
HEK293	Human embryonic kidney cells
LNCaP	Human androgen-dependent prostate cancer cell line
CHO-1	Chinese hamster ovary cells
Caco-2	Human epithelial colorectal adenocarcinoma cells
C4-2	Human androgen-independent prostate cancer cell line
Vero cells	African green monkey kidney epithelial cells
MSC	Mouse mesangium cells (RhoGDI+/+ and RhoGDI-/-)
Swiss 3T3	Swiss mouse embryonic fibroblasts
MEF	Mouse embryonic fibroblasts

2.1.7 Antibodies for Western blotting and Immunoprecipitation

antibody	type	application	provider
Actin	mouse, monoclonal	1/30,000	MP Biomedicals
Cdc42 (17-299)	mouse, monoclonal	1/1000	Upstate
FLAG	rabbit, polyclonal	1/1000	Sigma
Karyopherin α2 (610485)	mouse, monoclonal	1/5000	BD Bioscience
Nuclear matrix protein p84	mouse, monoclonal	1/5000	Abcam
PARP1 (9542)	rabbit, polyclonal	1/1000	Cell signaling
Rac1 (23A8)	mouse, monoclonal	1/5000	Upstate
RhoA (26C4)	mouse, monoclonal	1/500	Santa Cruz
RhoGDIα (A-20)	rabbit, polyclonal	1/200	Santa Cruz
α-GAPDH (clone 6C5)	mouse, monoclonal	1/10,000	Millipore
α-tubulin (T9026)	mouse, monoclonal	1/20,000	Sigma

Table 1: Antibody list

2.1.9 Primers and vectors

Primers were purchased from Apara Bioscience.

Primer	Reading direction	Sequence
RhoAG14V	sense	5'-gattgttggtgatgtagcctgtggaaag-3'
	antisense	3'-ctttccacaggctacatcaccaacaatc-5'
3XFlag	sense	5'-gatccatggactacaaagaccacgacggcgactacaa agaccacgacatcgactacaaagacgacgacgacaaaa-3'
	antisense	5'-gatcttttgtcgtcgtctttgtagtcgatgtcgt ggtctttgtagtcgccgtcgtggtctttgtcgtccatg-3'

pCR-Blunt II – TOPO vector, pGEX-2T vector, pEGFP vector, pcDNA3.1. His© C vector

2.1.10 Buffers and solutions

buffer	ingredients
Agarose gel	1% (w/v) agarose in TAE buffer; heated to 90°C
Blocking solution (WB)	5% (w/v) milk powder in TBS-T
Blotting buffer	25 mM Tris; 192 mM glycine; 20% (v/v) methanol
Bradford reagent	0.035% Serva Blue G, 25% (v/v) ethanol, 50% (v/v) H_3PO_4
Brij-lysis buffer	20 mM Tris, 150 mM NaCl, 1 mM EDTA, 1 mM $MgCl_2$, 1 mM Na_3VO_4, 10 mM NaF, 10% (v/v) glycerol, 1% (v/v) Brij 97; adjusted to pH 7.4
Coomassie solution	0.25% (w/v) Coomassie Brilliant Blue R250, 50% (v/v) methanol, 10% (v/v) acetic acid
DNA sample buffer	0.25% (m/v) bromophenol blue, 40 % (m/v) saccharose
ECL 1	500 µl 250 mM Luminol in dimethyl sulfoxide (DMSO), 220 µl 90 mM p-coumaric acid in DMSO, 5 ml 1 M Tris/HCl (pH 8.5), H_2O ad 50 ml
ECL 2	31 µl 8.8 M H_2O_2, 5 ml 1 M Tris/HCl (pH 8.5), ad. 50 mL H_2O
Fixation solution	3.7% formaldehyde, 0.1% Triton-X 100 in PBS
GST-fish buffer	50 mM Tris, 100 mM NaCl, 2 mM $MgCl_2$, 10% (v/v) glycerol, 1% (v/v) NP40; adjusted to pH 7.4
High salt buffer	20 mM Hepes, 240 mM NaCl, 10 mM KCl, 1 mM EDTA, 20% (v/v) glycerol, 0.2% (v/v) NP40; adjusted to pH 7.9
Hypotonic buffer	20 mM Hepes, 10 mM KCl, 10% (v/v) glycerol, 0.2% (v/v) NP40; adjusted to pH 7.9

buffer	ingredients
Laemmli buffer	10 mM Tris/HCl, 20 mM DTT, 10% (w/v) SDS, 10% (w/v) sucrose, 10% (v/v) glycerol, 0.002% (w/v) bromophenol blue
Mammalian-lysis buffer	50 mM Tris, 150 mM NaCl, 5 mM $MgCl_2$, 1 mM EDTA; adjusted to pH 7.4
Phosphate buffered saline (PBS)	140 mM NaCl, 10 mM Na_2HPO_4, 2.7 mM KCl, 1.8 mM KH_2PO_4; adjusted to pH 7.4
Protein sample buffer	10 mM Tris/HCl, 20 mM DTT, 10 % (m/v) SDS, 10 % (w/v) sucrose, 10 % (v/v) glycerol, 0.002 % (m/v) bromophenol blue
Rhotekin lysis buffer	50 mM Tris, 150 mM NaCl, 5 mM $MgCl_2$, 10% glycerol, 0.5% triton-X100; adjusted to pH 7.5 Add fresh: 0.1 mM PMSF, 1 µg/ml aprotinin, 1 µg/ml leupeptin, 1 mM DTT
RIPA-lysis buffer	150 mM NaCl, 0.5% (w/v) Sodium desoxycholat, 1% (v/v) triton x-100, 5 mM EDTA, 10 mM Sodium phosphate, 10 mM NaF, 1 mM Na_3VO_4, 50 mM Hepes; adjusted to pH 7.4
SDS polyacrylamide running gel	152 mM Tris-HCl pH 6.8, 0.15% (w/v) SDS, 0.3% (w/v) APS, 0.15% (v/v) TEMED, 12.5% (w/v) acrylamide (1 M urea for urea SDS-PAGE)
SDS polyacrylamide stacking gel	152 mM Tris-HCl pH 6.8, 0.2% (w/v) SDS, 0.6% (w/v), APS, 0.3% (v/v) TEMED, 5% (w/v) acrylamide (1 M urea for urea SDS-PAGE)
SDS-running buffer	2 M glycine, 250 mM Tris, 35 mM SDS
SOB medium	0.5% (w/v) yeast extract, 2% (w/v) bactotryptone, 10 mM NaCl, 2.5 mM KCl, 10 mM $MgCl_2$; adjusted to pH 7.0
TAE buffer	40 mM Tris acetate; 1 mM ethylenediamine tetraacetic acid (EDTA); adjusted to pH 8,0
Tris buffered saline tween (TBS-T)	40 mM Tris, 1 mM EDTA, 0.05% Tween 20; adjusted to pH 8.0

Table 2: Recipes of buffers and solutions.

2.2 Methods

2.2.1 Polymerase chain reaction

The polymerase chain reaction (PCR) is a technique to amplify DNA sequences from a template such as plasmid- or genomic DNA. The reaction runs in a three step cycle of denaturation, annealing and elongation. First, the double stranded DNA is denatured to single strands. Then, the binding of sense and antisense primers occurs. In the third step, the heat-stable DNA polymerase anneals to the primers and extents the DNA complement. Specific conditions used are outlined in Table 3.

Reagent	**Final concentration**	**Volume**
Template	2 ng/µl	100 ng
Primer sense (10 µM)	0.4 µM	2 µl
Primer antisense (10 µM)	0.4 µM	2 µl
dNTP (10 mM)	1 mM	5 µl
Pfu Ultra II buffer (10x)	1x	5 µl
Pfu Ultra II polymerase	1U	1 µl
H_2O		up to 50 µl

Table 3: PCR pipette composition.

All steps of the PCR reaction are temperature sensitive and occur at 95 °C (denaturation), 55 °C (annealing) and 72 °C (elongation). Isolation of the amplified sequence is accomplished through DNA separation by agarose gel-electrophoresis and subsequent extraction.

2.2.3 Site-directed mutagenesis

By QuickChange® site-directed mutagenesis, point mutations, deletions, insertions of single or multiple amino acids can be introduced through primers constructed for this purpose. Sense and antisense primers bind complementary at the same site. In contrast to the PCR method described above, the whole plasmid is amplified with its respective mutation. The template plasmid, which was produced in *E. coli* is methylated and, therefore, recognized and digested by DpnI enzyme. In contrast, the amplified plasmid lacks this methylation and is protected from cleavage. After transformation into *E. coli*, growing clones contain the mutated construct which can then be isolated and sequenced.

2.2.4 Primer design

Good primer design is essential for successful reactions. Primers are reverse complements of target DNA bordering the amplified sequence. All primers used, vary in a length of 20-30 bp and an annealing temperature of 50 – 70 °C. They usually contain restriction enzyme recognition sequences for cloning, mutations and/or deletions, insertions for site-directed mutagenesis. Restriction enzyme sites are incorporated at the 5'-end, while e.g. point mutations are located in the center. Secondary structures, e.g. hairpin structures should be avoided. All primers used are outlined in section 2.1.8.

2.2.5 DNA purification

Plasmid DNA was purified from *E. coli* cells using Roti®-Prep Plasmid Kit for small scale preparations (Mini prep). The QIAGEN kit was used for large scale DNA preparations (Midi/Maxi prep). Plasmid DNA was purified according to the manufacturer's protocol. For Mini prep, 5 ml overnight culture was used, 30 ml for Midi and 250 ml overnight culture for Maxi preps. The DNA was eluted either in elution buffer (kit) or HPLC-H_2O. Concentrations were measured using the NanoDrop photometer.

2.2.7 Agarose gel electrophoresis and gel extraction

Agarose gel electrophoresis is a method used to separate DNA by its size. Negative charged DNA is forced to migrate through pores of a polymerized agarose matrix in response to an electric current. Small fragments run faster to the anode than large fragments. Here, a standard 1% agarose gel, TAE electrophoresis buffer and 1 µg/ml of the fluorescent dye ethidium bromide were used. Purification of DNA fragments were performed via QIAquick Gel Extraction Kit following the manufacturer's protocol.

2.2.8 Restriction enzyme digestion

Plasmid DNA, amplified sequences for cloning and control digestions, were subjected to restriction enzyme digestion. Enzymes and buffers (Fermentas) were applied following the manufacturer's protocol under respective digestion conditions.

2.2.9 Ligation

Ligation of digested DNA fragments with linearized vectors was performed with T4 DNA ligase. Ratios of insert to vector were calculated via the following equation:

$$[ng]insert = \frac{[ng]plasmid \times 3[bp]insert}{[bp]plasmid}$$

The ligation reaction (Table 4) was performed at 16 °C overnight and the plasmids transformed into *E. coli*.

Ingredients	**volume**
Plasmid DNA	100 ng
Insert DNA	as calculated
10x T4 ligase buffer	2 µl
T4 DNA ligase	1 µl
10 mM ATP	2 µl
H_2O	up to 20 µl

Table 4: Ligase pipette composition.

2.2.10 Transformation of bacteria by heat shock

Heat shock is a classical transformation method where DNA uptake into chemical competent cells is induced. After DNA (100 ng) was added to 100 µl competent cells, the mixture was incubated on ice for 30 min. Heat shock at 42 °C for 90 sec forces cell permeability and DNA uptake through the cell membrane. After 5 min incubation on ice, 250 µl pre-warmed SOC or LB medium was added. Prior to plating on LB-agar plates, cells recover during 1 h incubation at 37 °C with agitation.

2.2.11 Preparation of glycerol stocks

Each bacterial clone with its specific DNA construct was kept as a glycerol stock. Transformed clones were cultured and the DNA was purified by Mini prep. After DNA sequencing, the correct transformed bacterial clone was prepared for conservation at -80 °C: the bacteria overnight culture was diluted with sterile glycerol to a final concentration of 35% (v/v) and frozen in 1 ml Cryotubes at -80 °C.

2.2.12 Expression and purification of GST-constructs in *E. coli*

Proteins were purified as N-terminal GST-fusion constructs using the pGEX2T vector. The overnight culture (50-100 ml LB+amp) was inoculated with the respective glycerol stock and grown at 37 °C overnight (200rpm agitation). The overnight culture was added to the main culture of 1 L LB medium (+amp) and grown to 0.3-0.8 OD_{600} at 37 °C. Protein expression was induced by IPTG in a range of 100 µM-1 mM for several h to overnight, depending on the construct. Cells were centrifuged (15 min, 600x*g*) and the pellet was resuspended in lysis buffer. Lysis of cells occurred on ice by sonication (3x 20 sec, cycle 50, power 50%). Cell debris was removed by centrifugation (30 min, 15,000x*g*). Isolation of the GST-construct was done by glutathione-affinity-chromatography. Prior to binding, glutathione-sepharose beads were equilibrated with lysis buffer. The supernatant was incubated with washed beads for 1 h at 4 °C under rotation. Washings were performed with lysis buffer (2 min, 4,000x*g*).

For pull-down studies, beads with coupled proteins were kept as aliquots at -80 °C until use. In order to remove the proteins from the beads, they were eluted with glutathione or the GST-tag was cleaved off by thrombin (10 min, RT). Afterwards thrombin was removed with 20 µl of benzamidine-sepharose beads per 100 µl eluate (10 min, RT). Proteins were kept as aliquots at -20 °C or -80 °C depending on protein stability.

2.2.13 Cell culture

Mammalian cells from human and mouse were cultured as sub-confluent monolayers under optimized conditions of 5% CO_2 at 37 °C with their respective medium. They were passaged every two days by detachment with Trypsin/EDTA after washing with PBS, then re-suspended in pre-warmed medium and transferred into new flasks.

2.2.14 Toxin treatment

Cells were grown in 10 cm or 15 cm dishes. Media was exchanged and 400 ng/ml CNF1 or CNFY was applied and cells incubated for different time-points at 5% CO_2 and 37 °C. The reaction was stopped by direct lysis of the cells or freezing at 20 °C.

2.2.15 Transfection of mammalian cells

HEK293 or HeLa cells were transiently transfected with the mammalian pcDNA3.1 His C or pEGFP vector containing different inserts by using the polyethylenimin (PEI) transfection system. For the transfection mixture, 15 µg plasmid DNA was mixed with 24 µl 20 mM PEI stock solution in 500 µl OptiMEM, incubated for 15 min at RT and added drop wise to the cell layer (10 cm dish). During the incubation period, PEI binds to the negatively charged DNA and forms small agglomerates. Via unspecific endocytosis these particles are taken up and cells start expressing the transfected protein. Here, 48 h post-transfection cells were used for further experiments.

2.2.16 Preparation of cell lysate

For preparation of cell lysates, approximately 70% confluent cells, treated or untreated, were washed with PBS, disrupted in lysis buffer (Brij-, GST-fish-, or mammalian-lysis buffer) supplemented with EASY pack protease inhibitor cocktail (PIC) and collected by scraping. Lysates were cleared by centrifugation (30 min, 15,000x*g*, 4 °C) and the supernatant was subjected to protein quantification.

2.2.17 Subcellular fractionation of nuclei and cytosol

For the cytosolic fraction, cells were lyzed with hypotonic buffer (10 min, 250 µl hypotonic buffer/ 10 cm dish, on ice). Due to osmotic pressure of the hypotonic buffer, the cells swell and burst. Then, they were scraped and centrifuged (2,000x*g*, 1 min, and 4 °C). The supernatant containing the cytosolic fraction was removed. The pellet was further fractionated by re-suspension in 100 µl high salt buffer and incubation under rotation (30 min, 4 °C). In the hypertonic environment, the nuclei contract and release the nuclear cytoplasm. The nuclear fraction was obtained in the supernatant by centrifugation (15 min, 15,000x*g*, 4 °C).

2.2.18 Membrane isolation

In order to separate membrane and cytosol, cells from a 10 cm dish (70-90% confluency) were frozen, thawed and collected in mammalian lysis buffer without any detergents. Complete lysis of cells occurred with sonication (2x 20 sec, cycle 50, power 50%). After clearance of cell debris by centrifugation (30 min, 15,000x*g*, 4 °C), the lysate was subjected to ultracentrifugation (1 h, 40,000x*g*, 4 °C). The supernatant contained the membrane-free cytosol. The membrane fraction was collected in the pellet and re-suspended in pre-heated (95 °C) sample buffer.

2.2.19 BCA protein quantification assay

The bicinchoninic acid (BCA) assay is a biochemical method to determine protein concentrations. Advantages of this method are the measurement of low protein amounts and its resistance to Triton X-100 (mostly present in buffers). The reaction takes place in mainly two steps: First, the peptide bonds in proteins reduce Cu^{2+} ions from the cupric sulfate to Cu^{1+} (which is proportional). Then, two molecules of bicinchoninic acid chelate with each Cu^{1+} ion and form a purple-colored complex with an absorbance at 562 nm. Here, the BCA assay protein quantification kit was applied following manufacturer's protocol. Briefly, protein samples were diluted 1:10 (H_2O) in a final volume of 10 µl in 96 well plates. After adding of 200 µl BCA reagent, the reaction was carried out for 30 min at 37 °C. Read out was performed with the Tecan® microplate reader at 562 nm and protein concentrations were calculated against a BSA standard curve.

2.2.20 Effector pull-down assay

Pull-downs (e.g. with full-length RhoGDI) were developed to investigate direct protein interaction *in vitro*. To precipitate active Rho GTPases, effector pull-downs are used with the respective binding domains, Rho binding domain (RBD) from Rhotekin (RT) or CRIB domain. The full-length interacting protein or only the binding domain purified from *E. coli* is linked to glutathione beads via its GST-tag as described above. These beads are capable to "pull-down" the protein of interest via its interacting site. For this, cells lyzed in GST-fish buffer containing protease inhibitor cocktail (PIC) were incubated with the specific pre-washed effector pull-down beads (1 h, 4 °C). After two washing steps with GST-fish buffer, the bound protein was eluted from the beads by sample buffer (5-10 min, 95 °C).

2.2.22 Immunoprecipitation (IP) and Co-IP

Immunoprecipitation (IP) is a technique to precipitate a specific endogenous protein of interest via antibody binding *in vivo*. When examining protein-protein interactions or protein complexes, the process is called Co-Immunoprecipitation (Co-IP). To perform the Co-IP, PBS washed HeLa or HEK293 cells were frozen, thawn on ice and collected in mammalian-lysis buffer (+PIC). Cell debris was removed by centrifugation (30 min, 15,000x*g*, 4 °C). After protein quantification, approximately 500 µg to 2 mg was used for IP or Co-IP. Antibody (1-2 µg) was added to the lysate and binding occurred overnight at 4 °C. 25 µl bed-volume washed Protein A Sepharose beads was added to the antibody-lysate mixture and incubated (2 h, 4 °C) under rotation. During this time, the antigen-antibody complex binds via its Fc-region to Protein A Sepharose. Then, beads were centrifuged (500x*g*, 2 min, 4 °C) and unbound proteins removed with lysis buffer by several washing steps. The protein-protein complexes were eluted in sample buffer and boiled (5 min, 95 °C).

2.2.23 SDS polyacrylamide gel electrophoresis

Sodium dodecyl sulfate polyacrylamide gel-electrophoresis (SDS-PAGE) allows the separation of proteins according to their molecular weight. Native structures are denatured with sodium dodecyl sulfate (SDS), an anionic detergent that applies a negative charge to each protein in proportion to its mass. Disulfide bonds are reduced by dithiothreitol (DTT). Here, the discontinuous electrophoresis system with a stacking- and a running gel was used. The samples were boiled in sample buffer at 95 °C for 5-10 min and loaded onto a 12.5% gel. The gel was run in SDS running-buffer at 25-40 mA. Then, the gel was either stained with Coomassie, or used for Western blotting. 1 M urea was added to stacking- and running gel to increase separation efficiency in order to visualize smaller differences in mobility (e.g. Rho-shift).

2.2.25 Western blotting

Western blotting is a method to immobilize proteins from gel on membranes for specific protein detection. Prior blotting, PVDF (polyvinylidenfluoride) membranes were activated with methanol. The gels were blotted in a Biorad wet-blot apparatus at 20 V for 30 min and the membranes blocked with 5% non-fat-dried milk in TBS-T for 1 h (RT). Blots were incubated with the specific first antibody in TBS-T 1 h (RT) or overnight (4 °C). After another washing step with TBS-T, the membrane was incubated with the species secondary antibody for 1 h (RT) which binds to the Fc-fragment of the primary antibody. After washing again with TBS-T, the membrane was exposed to ECL 1+2 (enhanced chemiluminesence). HRP (horseradish-peroxidase), coupled to the secondary antibody, oxidizes luminol which exhibits chemiluminescence. The emitted light was analyzed and visualized by Fujifilm LAS3000 photomultiplier.

2.2.26 Preparation of probes for mass spectrometry

Mass spectrometry (MS) is an analytical technique that measures mass-to-charge ratio of charged particles. The detected protein peptide may then lead to identification of proteins. Moreover, specific modifications of protein fragments can be identified. Samples were prepared via “in-gel-digestion” for MS (Rosenfeld, J. *et al.*, 1992). Briefly, proteins were denatured and disulfide bonds reduced with sample buffer (10 min, 95 °C). After cooling down to RT, 120 mM iodacetamide (IAA) was added and an alkylation reaction was performed in the dark for 20min. Hereby, the disulfide bonds of the proteins are irreversibly broken up and the optimal unfolding of the tertiary structure is obtained. Subsequently, the probes were subjected to SDS-PAGE. In-gel digestion was achieved through e.g. trypsin, elastase and/or thermolysine proteases. Prepared peptides were then subjected to liquid chromatography tandem mass spectrometry (LC-MS/MS) on an ion trap mass spectrometer (Agilent 6340, Agilent Technologies) equipped with an ETD source and coupled to an 1200 Agilent nanoflow-system via a HPLC-Chip cube ESI interface (Schlosser, A. ZBSA, Freiburg).

2.2.28 Dual-Luciferase® reporter assay

The Dual-Luciferase® reporter assay provides an efficient system of performing two-reporter assays: Renilla and Firefly luciferase. The pSRE (plasmid serum response element) is linked to Firefly (*Photinus pyralis*) luciferase. Binding of Serum Response Factor (SRF) to Serum Response Element (SRE) induces its expression, while RhoA activates SRF. Therefore, the reporter plasmid is frequently used as a read-out system for RhoA signaling. The pRLTK plasmid encodes for Renilla (*Renilla reniformis*) luciferase, which is expressed constitutively and serves as a control for the transfection rate. For this assay, HEK293 cells were seeded in a 96-well plate and transfected with pSRE and pRLTK. After 48 h, luciferase activities were determined with the Dual-Luciferase® reporter assay system (Promega, Heidelberg, Germany) in accordance with the manufacturer's instructions. The activity of the experimental reporter was normalized against the activity of the control vector.

2.2.29 Immunostaining and microscopy

Fluorescence microscopy is a very important technique to examine cellular structures. In order to visualize certain proteins or compounds, cells are immunostained prior analysis. Grown on sterile coverslips, cells were removed from cell culture and immobilized with fixation solution (10 min, RT). The containing formaldehyde was used to fix proteins and Triton X-100 for permeabilization. After blocking with 3% BSA (1 h, RT), cells were exposed to the first antibody (1 h, RT). The antibody was removed by 3-5 washes with PBS, following incubation with the secondary antibody coupled to Alexa fluorophores (1 h, RT, in the dark). Optional, the actin cytoskeleton was also stained with rhodamine-phalloidin. After extensive washings with PBS/HPLC-H_2O, coverslips were mounted on glass slides with ProLong® Gold DAPI solution and kept protected from light. Analysis of stained cells was performed with an inverted fluorescence microscope. Depending on the fluorophore (Alexa488/Alexa568/DAPI/rhodamine) the sample was exposed to the respective light spectrum. Microscopic pictures were evaluated with MetaMorph® software.

3 RESULTS

CNF1 belongs to the CNF toxin family (1, 2, 3, Y), which shares deamidase activity towards Rho GTPases, such as Rac1, RhoA and Cdc42. This modification results in the constitutive activation of Rho GTPases and, thus, enhancing Rho GTPase-dependent cellular activities. Since this activation was found to be permanent *in vitro*, it was assumed that this modification provokes also the sustained activation of Rho GTPases in intact cells (Schmidt, G. *et al.*, 1997; Flatau, G. *et al.*, 1997). However, evidence has been provided, that CNF1 activation of Rho GTPases is not a permanent but a transient effect. This study focuses on the characterization of CNF1-induced inactivation of deamidated Rac1 and RhoA, on the precise steps and on the interacting proteins involved in this process. In addition to it, in respect to the role of RhoA in metastasis and cancer development, the effect of CNFs in Rho-dependent apoptotic prostate cancer cells LNCaP were investigated.

3.1 Effects on Rho GTPases by CNF1 and CNFY

3.1.1 Activation of Rac1, RhoA and Cdc42 by CNF1 and CNFY

CNF1 is produced by uropathogenic *E. coli* strains and belongs to the group of Rho activating proteins. It is about 60% identical to CNFY from *Yersinia pseudotuberculosis* (Lockman, H. A. *et al.*, 2002). Although both toxins deamidate the same glutamine residue to cause constitutive activation of Rho GTPases their substrate specificity differ in cultured cells. In this first experiment, the substrate specificity of CNF1 and CNFY was examined in terms of RhoA, Rac1 and Cdc42. Notably, deamidation of RhoA by CNFs leads to slower migration of the protein in SDS-gel electrophoresis (Oswald, E. and de Rycke, J., 1990; Oswald, E. *et al.*, 1994). This change in electrophoretic mobility indicates the deamidation and activation status of RhoA, while this is not the case for Rac1 or Cdc42. Instead, precipitation of the activated forms by the method of bead-coupled effectors was used additionally since the GTPase binding domains of the effectors such as p21-activated kinase (PAK) for Rac1 or Cdc42 and Rhotekin (RT) for RhoA solely interact with

the GTP-loaded structure. HEK293 cells were intoxicated with CNF1 (2 h) and CNFY (4 h) or left untreated as control (ctr). After protein adjustment, the lysate was subjected to PAK and Rhotekin pull-down, respectively, following Western blotting.

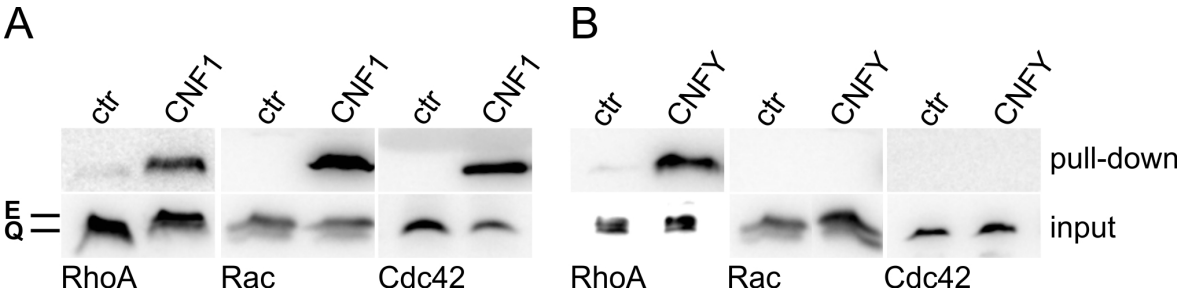


Figure 10: Effector pull-down assays for detection of active RhoA, Rac1 and Cdc42 after CNF1/Y intoxication. HEK293cells were intoxicated with CNF1 for 2 h (A) or CNFY for 4 h (B) in comparison to control (ctr). Upper panel: PAK pull-down for Rac1 and Cdc42, Rhotekin pull-down for RhoA, untreated control (ctr) compared to CNF1/Y intoxicated cells. Lower panel: Rho GTPase input from whole lysate. Rho shift: RhoAQ63 (**Q**) to RhoAE63 (**E**). Western blots are representative for at least six independent experiments.

As shown in Figure 10, incubation of cells for 2 h with CNF1 led to activation of RhoA, Rac1 and Cdc42 observed by Rhotekin and PAK pull-down compared to untreated cells. The activation of RhoA was also clearly confirmed by the Rho shift. CNFY exclusively induced a strong activation of RhoA detected by Rhotekin pull-down. These results confirm the prevalent view of CNF1 being an activator of Rho GTPases such as Rac1, RhoA and Cdc42 and CNFY specifically of RhoA.

3.1.3 Transient stress fiber and lamellipodia formation

General activation of Rho GTPases leads to typical morphological changes caused by rearrangements of the cellular actin cytoskeleton, such as lamellipodia for Rac1, filopodia for Cdc42 and stress fiber formation for RhoA. To demonstrate CNF1 and CNFY-induced constitutive activation of Rho GTPases by actin reorganization, toxins were applied to HeLa cells. After 2 h and 8 h CNF1/Y intoxication, cells were fixed, stained with rhodamine – phalloidin and the actin cytoskeleton was visualized by fluorescence microscopy.

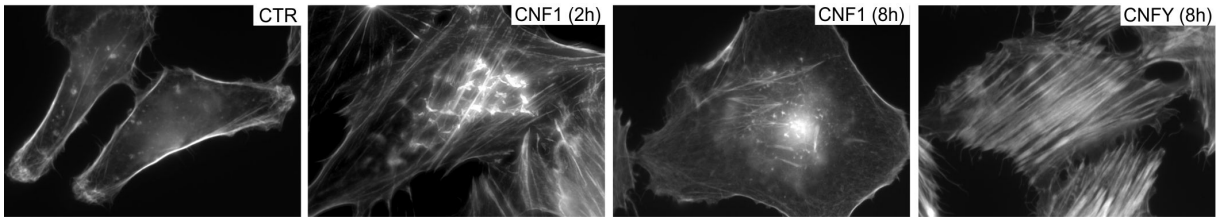


Figure 11: CNF1 effect on the actin cytoskeleton. Treated (CNF1 for 2 h and 8 h; CNFY for 8 h) and untreated HeLa cells (CTR) were subjected to actin staining after indicated time points. Fluorescence microscopic pictures were taken at 100x magnification. Microscopic pictures are representative for at least three independent experiments.

At 2 h-CNF1 intoxication extensive flattening of cells accompanied by highly dynamic membrane ruffle- and stress fiber formation was observed, indicating Rac1 and RhoA activity (Figure 11). Cdc42-dependent filopodia structures were less visible in HeLa cells. Intriguingly, these structures only occurred initially and completely disappeared with longer toxin exposure (8 h). In contrast, CNFY stimulated strong stress fiber formation that prolonged up to 8 h. The predominating RhoA-dependent phenotype confirmed that RhoA was activated by CNFY exclusively. Activation of the Rho GTPases detected in the pull-down experiments clearly depicted the morphological changes induced in HeLa cells at least for Rac1 and RhoA in the same timeframe of CNF1 intoxication (2 h). However, morphological changes with longer toxin exposure demonstrated that the CNF1-induced Rac1 and RhoA activation might be a transient effect, while with CNFY the RhoA phenotype remained stable.

3.2 Time-dependent inactivation of Rac1 after CNF1

To investigate the observed disappearance of Rac1-dependent structures, the course of Rac1 activation was monitored with increasing incubation times of CNF1. Therefore, HEK293 cells were treated with CNF1 and lyzed every 2 h up to 8 h. As a negative control, cells were treated with CNFY for 8 h, since it is specific for RhoA. Subsequently, after lysis and protein adjustment, the whole lysate was subjected to PAK pull-down and Western blotting.

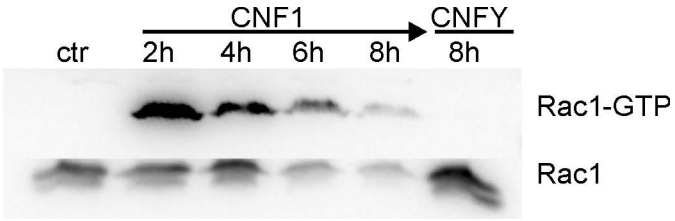


Figure 12: CNF1 induces transient Rac1-effector interaction. A] Upper panel: time-dependent CNF1 and CNFY intoxication and PAK1 pull-down of Rac1. Lower panel: input Rac1 of whole lysate. This Western blot is representative of at least three independent experiments.

As shown in Figure 12, Rac1 was activated by CNF1 after 2 h compared to untreated or CNFY-treated cells. However, when monitoring the amount of CNF1-activated Rac1 in the course of cell intoxication, it became evident that there was a strong reduction in its activity. Since the protein levels were adjusted prior the experiment, the decrease in the cellular content of Rac1 indicated its cellular instability, which was not observed in untreated or CNFY-treated cells. Furthermore, the time-dependent reduction of Rac1 protein levels seemed to correlate with the decrease of Rac1 activity. These results suggest that the transient activation of Rac1 might be a result from its cellular depletion.

3.2.2 CNF1 induces Rac1 degradation via the 26S proteasome

Determination of the degradative machinery responsible for Rac1 depletion was investigated by applying the cell-permeable proteasome inhibitor, MG132. MG132 blocks degradation of ubiquitin-conjugated proteins by interaction with the 26S proteasome (Han, Y. H. *et al.*, 2009). 30 µM MG132 was applied to HEK293 cells overnight prior toxin incubation (6 h). Subsequently, the cells were lyzed and protein levels adjusted. The cellular content of Rac1 was analyzed by immunoblotting.

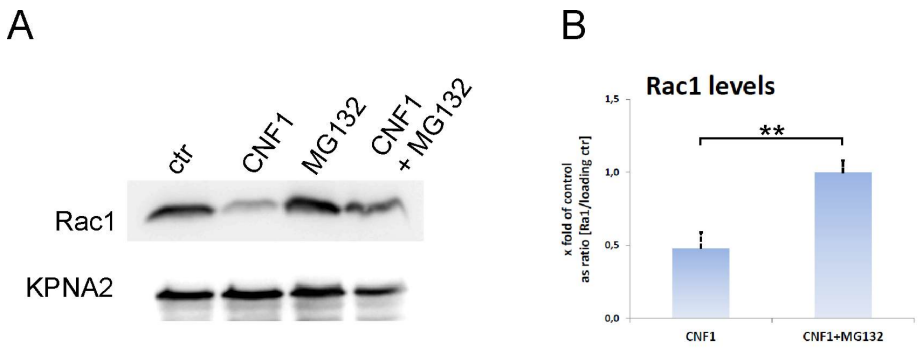


Figure 13: CNF1 induces Rac1 degradation by the 26S proteasome. A] CNF1 induced Rac1 degradation is inhibited by proteasomal inhibitor MG132. After overnight treatment with 30µM MG132, HEK293 cells were intoxicated with CNF1. Upper panel: Rac1 input. Lower panel: Karyopherin α2 (KPNA2) as loading control. B] Quantification of Rac1 levels after overnight treatment of HEK293 cells with 30 µM MG132 and CNF1 intoxication. Rac1 levels were calculated as x-fold of control (ctr) as a ratio of Rac1 to loading control. The mean standard deviation is generated from six independent experiments. (Significance after student's t-test, calculated p-value **<0.01, *<0.05)

In contrast to control cells, in which Rac1 appeared to be stable, protein levels were reduced in CNF1-treated cells. This effect was rescued by addition of MG132 prior CNF1 intoxication (Figure 13). These data confirmed that the CNF1-induced Rac1 depletion is achieved via the 26S proteasome machinery, which is in perfect agreement with published data (Pop, M. et al., 2004). However, the defined pathway by which CNF1-deamidated and activated Rac1 is directed to the 26S proteasome is still unclear and needs to be further elucidated.

3.2.3 Rac1 interaction with Karyopherin α2 after CNF1 deamidation

In the literature, it has been reported that degradation of proteins is observed in the cytosol and the nucleus (von, Mikecz A., 2006; Craiu, A. *et al.*, 1997). Furthermore, nuclear localization of Rac1 has been described (Michaelson, D. *et al.*, 2008). Recently, by using the method of the yeast two-hybrid screen, Karyopherin α2 (KPNA2) was identified as a new direct interaction partner of deamidated Rac1 (Q61E) (Sandrock, K., 2008). Karyopherin α proteins are nuclear shuttle proteins that interact with target proteins linking them to importin β to induce nuclear translocation. Consistent with this, one might speculate that Rac1 is translocated to the nucleus via the interaction to KPNA2 prior degradation. In co-operation with Sandrock, K., it was to be approved if deamidated Rac1 directly interacts with KPNA2 *in vivo*. This was analyzed with the method of Co-Immunoprecipitation (Co-IP) of the endogenous proteins after 5 h CNF1 intoxication of HEK293 cells with or without the proteasome inhibitor MG132 (30 µM). Co-IP was carried out with anti-KPNA2 antibody. Subsequently, bound proteins were subjected to Western blotting and immunoblotted with the anti-KPNA2 and anti-Rac1 antibodies.

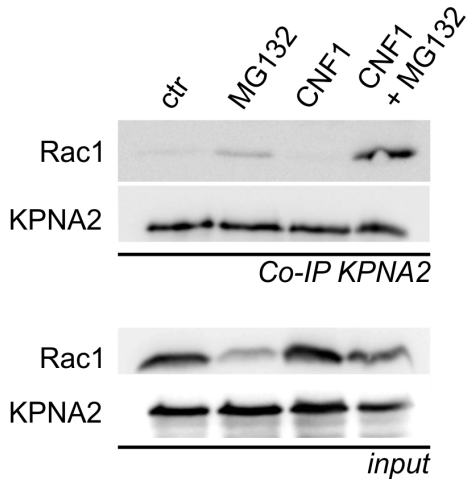


Figure 14: Deamidated Rac1 directly interacts with KPNA2. A] Co-IP of endogenous KPNA2 and Rac1 after CNF1 (5 h) and/or MG132 (30 µM) treatment was performed. Upper panels: Co-IP of the endogenous complex of Rac1 and KPNA2. Lower panels: Rac1 and KPNA2 detected in whole lysate (input). Shown are typical results of at least three different experiments.

In HEK293 cells, which were treated with CNF1 and MG132, Rac1 was unambiguously detectable in complex with KPNA2 by Co-IP (Figure 14). Inhibition of degradation by MG132 also led to a weak interaction in toxin-untreated cells. In contrast, Rac1 was not detectable in CNF1-treated cells without MG123, because CNF1-activated Rac1 was rapidly degraded.

3.2.4 CNF1 induces Rac1 translocation to the nucleus via its C-terminal polybasic region

To analyze nuclear accumulation of Rac1, cells were treated with CNF1 in the presence or absence of MG132 to block degradation. After lysis and protein adjustment, lysate was subjected to subcellular fractionation, PAK pull-down and Western blotting. Moreover, KPNA2 proteins are known to directly interact with the classical nuclear localization sequence (NLS). The C-terminal polybasic region (PBR) of Rac1 but not Rac2 and Rac3 comprises this structural motif. Interestingly, neither Rac2 nor Rac3 were found to interact with KPNA in yeast-two hybrid screen (Sandrock, K., 2008). Therefore, to elucidate the role of the NLS within the C-terminal PBR of Rac1 in terms of degradation and nucleocytoplasmic distribution, the subcellular localization of Rac1-PBR2 in comparison to wild-type Rac1 following stimulation by CNF1 was analyzed. The Rac1-PBR2 chimera represents the Rac1 protein containing the PBR of Rac2. Therefore, it does not contain the NLS motif (see Figure 3C) for the binding of KPNA2.

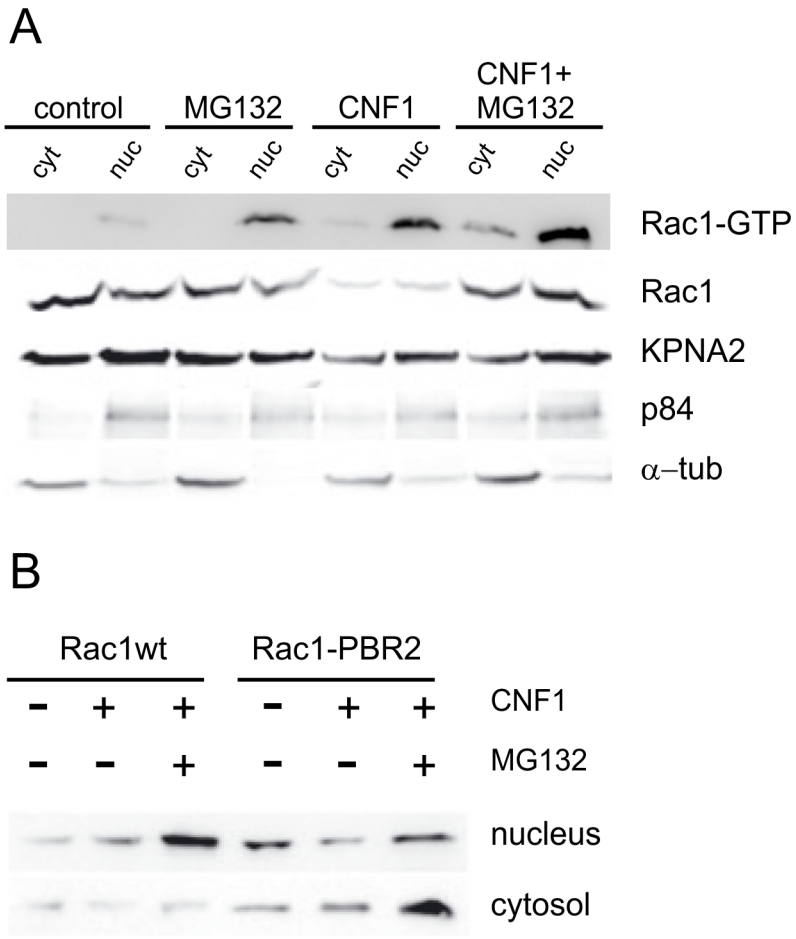


Figure 15: Activated Rac1 is translocated to the nucleus after CNF1 intoxication via its polybasic region (PBR). A] HEK293 cells were treated with 30 µM MG132 overnight prior CNF1 (6 h) intoxication. Cells were subjected to subcellular fractionation into the nuclear (nuc) and cytosolic (cyt) fractions. PAK pull-downs of each fraction were performed to determine the quantity of active Rac1 (Rac1-GTP) in comparison to total Rac1 (Rac1). Karyopherin α2 (KPNA2) was used as loading control. Subcellular fractionation was confirmed by the nuclear marker p84 (nuc) for the nucleus and the cytosolic fraction (cyt) by α-tubulin (α-tub). B] Cells were transfected with Rac1wt and Rac1-PBR2 chimera treated with or without 30 µM MG132 overnight before intoxication with CNF1 (4 h) and subsequent subcellular fractionation. At this time-point, degradation of Rac1 is only marginally detected. Shown are typical results of at least three different experiments.

As shown in Figure 15A, Rac1 is equally distributed in the cytosol and the nucleus in untreated cells. After CNF1 activation, Rac1 protein levels decreased in both fractions. It was observed that blockage by the 26S proteasome inhibitor, MG132, could rescue this effect. CNF1 deamidated and activated Rac1 predominantly accumulated in the nucleus even at basal levels of endogenous GTP-loaded Rac1 (see control in Figure 15A). Co-treatment of CNF1 and MG132 amplified the signal of active Rac1 in the cytosol but

predominantly in the nucleus. These results indicate that total Rac1 is equally distributed to the cytosol and the nucleus. Interestingly, CNF1- and endogenously activated Rac1 seemed to cause its translocation to the nucleus and depletion from the cytosol. As shown in Figure 15B, the presence of the proteasome inhibitor MG132 uncovered the different subcellular distribution of Rac1wt and the Rac1-PBR2 chimera after stimulation by CNF1. In contrast to Rac1wt, which showed increased accumulation in the nucleus after the addition of CNF1, Rac1-PBR2 was predominantly found in the cytosol. Thus, the PBR of Rac1 most likely represents the interaction site for KPNA2 to promote translocation into the nucleus.

Together, these results conclude that the CNF1-induced activation of Rac1 must be a prerequisite for its interaction with KPNA2 via the PBR of Rac1. Furthermore, this suggests that the Rac1-KPNA2 complex is translocated into the nucleus and Rac1 is directed to degradation by the 26S proteasome in the nucleus and/or the cytosol.

3.2.5 Rac1Q61E interacts with a variety of nuclear proteins

To get closer insight into signaling pathways related to nuclear Rac1, it was attempted to identify specific nuclear Rac1 effectors. The method of liquid chromatography tandem mass spectrometry (LC-MS/MS) is frequently used to identify proteins. Therefore, this method was used to identify interaction partners of Rac1 in the nucleus to reveal its nuclear functions. Prior LC-MS/MS, HEK293 cells were transfected with either the 3XFLAG-tagged constitutive active Q61E- or with the 3XFLAG-tagged T35A/Q61E double mutant. The latter construct represents an effector region mutant, which enters the nucleus but does not interact with effector proteins. This experiment allows differentiation between proteins interacting with active Rac1 in the effector region or at other sites. Prior LC-MS/MS, nuclear fractions were prepared from transfected cells, and Rac1 activity was analyzed by PAK pull-down and Western blotting against Rac1. In a second step, both Rac1 constructs were precipitated by anti-FLAG and probes were subsequently separated on SDS-PAGE following Coomassie staining.

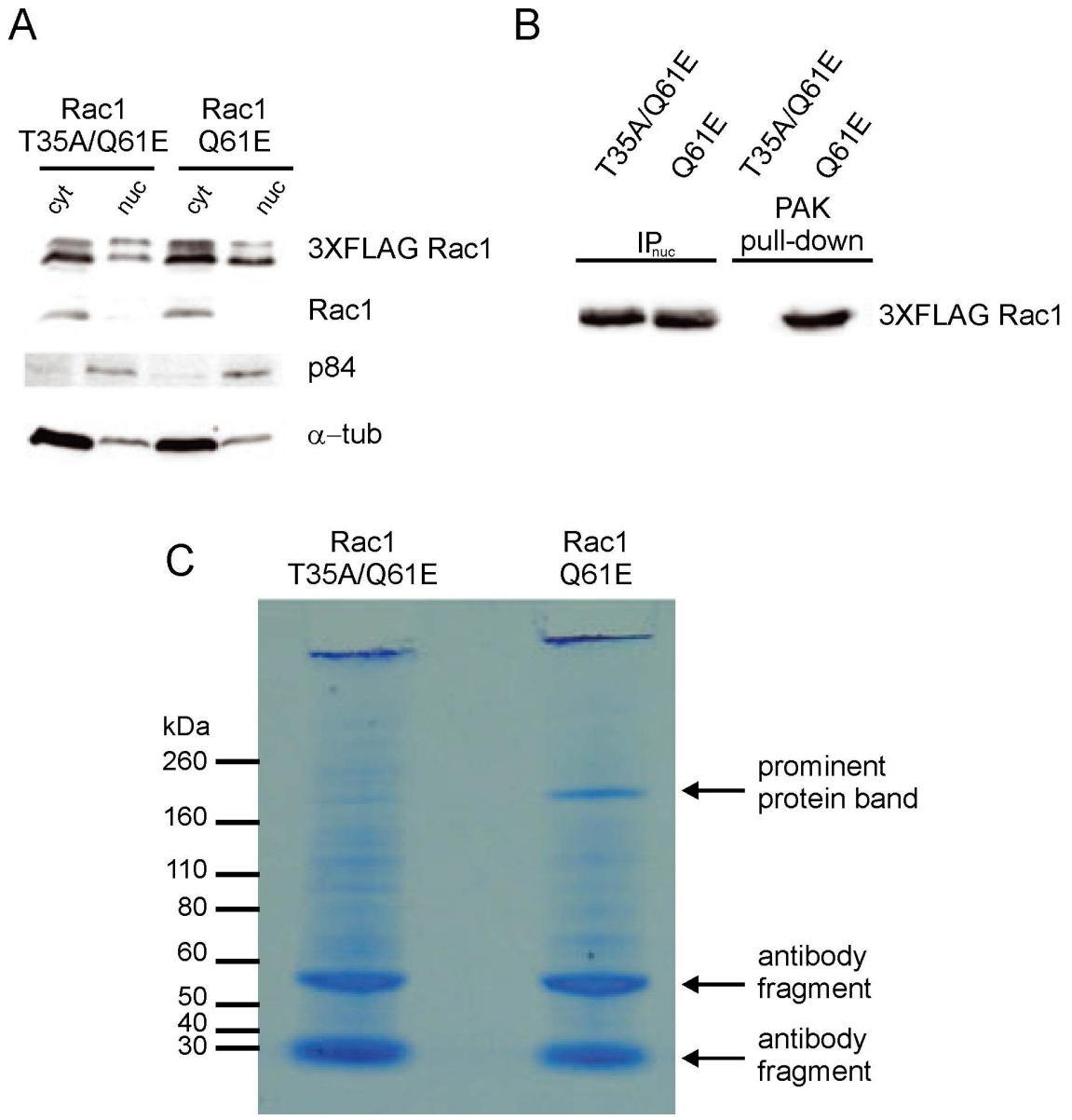


Figure 16: Identification of nuclear proteins interacting with active Rac1.
A] HEK293 cells were either transfected with the 3xFLAG-tagged Rac1Q61E mutant or with the 3XFLAG-tagged T35A/Q61E double mutant. After separation of the cytosolic and nuclear fractions, transfected and endogenous Rac1 was detected by a Rac1 antibody. Subcellular fractionation was confirmed by the nuclear marker p84 (nuc) for the nucleus and the cytosolic fraction (cyt) by α-tubulin (α-tub). B] Both constructs were immunoprecipitated from the nuclear fraction. Only the active Rac1Q61E mutant interacted with PAK. The PAK pull-down was performed with the cytosolic fraction. Data are representative of at least three independent experiments. C] Rac1 mutants were precipitated by anti-FLAG and applied on a SDS-Gel to identify interaction partners by LC-MS/MS analysis. Arrows indicate prominent bands.

As a precondition for LC-MS/MS, first transfection, effector interaction and Immunoprecipitation of the Rac1 mutants from the nuclear fraction needed to be confirmed. This could be verified in Figure 16A, where both 3XFLAG Rac1 constructs could be transfected and were also detected in the nuclear fraction. Moreover, only Rac1Q61E was precipitated by PAK (Figure 16B), which verified the capability of Rac1Q61E to interact with downstream effectors. In contrast, the double mutant Rac1T35A/Q61E was not able to interact with PAK. Both constructs could be immunoprecipitated by anti-FLAG antibody from the nuclear fraction. In Figure 16C, some distinct bands revealed a difference in the binding pattern of both constructs. Both complete lanes were subjected to LC-MS/MS analysis to identify the specific nuclear interaction partners.

As seen in Table 5, a series of proteins solely interacting with the Rac1Q61E mutant, but not with the T35A/Q61E double mutant could be identified (proteins marked with asterisk). Here, the nuclear shuttling proteins Karyopherin α2 (KPNA2) and importin ß were identified and confirmed the KPNA2 to importin ß pathway, which is an indicative of Rac1 nuclear translocation. Also, the fact that Rac1 is ubiquitinated could be confirmed by the presence of ubiquitin. Additionally, this experimental approach revealed a specific pattern of nuclear proteins solely interacting with active, nuclear Rac1. Thereby, this indicates that deamidated Rac1 might not only be directed to the nucleus for proteasomal degradation but most likely interacts with nuclear effectors to fulfill certain nuclear functions.

Nuclear interaction partners of Rac1	Molecular weight (Da)
Ras GTPase-activating-like protein IQGAP1*	189 134
Ras GTPase-activating-like protein IQGAP3*	184 432
Ras GTPase-activating-like protein IQGAP2*	180 500
DNA topoisomerases (e.g. isoform 3 of DNA topoisomerase 2-α)	178 600
Importin sub-unit β-1 (KPNB1)	97 108
Rho guanine-nucleotide exchange factor 6 (ARHGEF6)*	87 443
Isoform 1 of ARF GTPase-activating protein 1 (GIT1)*	84 289
ATP-dependent RNA helicases (e.g. ATP-dependent RNA helicase DDX3X)	73 198
Rho guanine-nucleotide exchange factor 7 (ARHGEF7)*	73 094
Heat shock 70-kDa protein	70 009
Lamin-B1	66 368
Nucleolar proteins (e.g. nucleolar protein 5A)	66 009
Importin subunit α-2 (KPNA2)	57 826
Elongation factor 1-α	50 109
60S Ribosomal proteins (e.g. 60S ribosomal protein L3)	46 080
Heterogenous nuclear ribonucleoproteins (e.g. heterogeneous nuclear ribonucleoprotein G)	42 306
Splicing factors (e.g. isoform 1 of splicing factor, arginine/serine-rich 7)	27 350
RhoGDI-α	23 193
Histones (e.g. histone H3)	15 421
Ubiquitin	8560

Table 5: List of Rac1 interacting proteins identified by LC-MS/MS. Proteins (marked by an asterisk) were identified only in the nuclear fractions of cells transfected with the Rac1Q61E mutant. The other proteins were detected in complex of the Q61E mutant as well as the T35A/Q61E double mutant.

3.3 Time-dependent inactivation of RhoA after CNF1

The dramatic disappearance of RhoA-dependent actin structures indicated that not only Rac1 but also RhoA signaling was disturbed, which might be a result of RhoA inactivation induced by CNF1. To analyze the course of RhoA activation, HEK293 cells were treated with CNF1 in a time-course of 2 h to 8 h and were compared to CNFY intoxication (4 h and 8 h). Subsequently, after lysis and protein adjustment, RhoA activation was analyzed by Rhotekin pull-down and Western blotting.

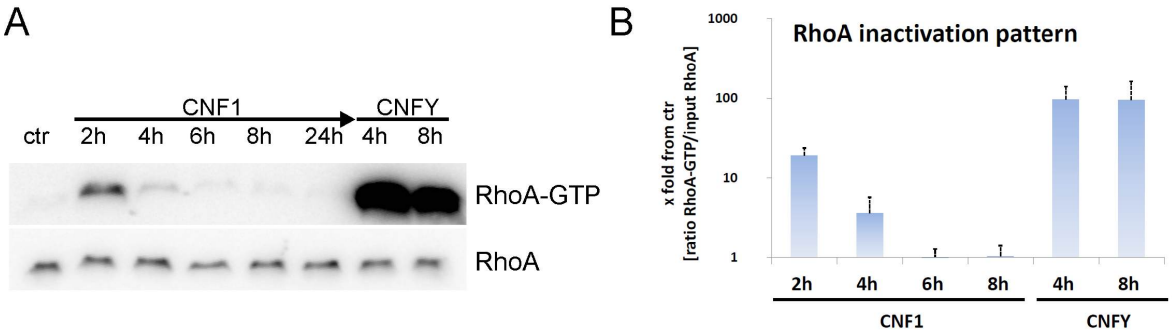


Figure 17: CNF1 induces transient RhoA-effector interaction. A] Upper panel: time-dependent CNF1 and CNFY intoxication and Rhotekin pull-down of RhoA. Lower panel: input RhoA of whole lysate. B] Quantifications of activated RhoA after CNF1/Y intoxication as x-fold from untreated probes (ratio Rhotekin pull-down of RhoA to input RhoA). Standard deviation of the mean is generated from at least three independent experiments.

Western blots and the respective quantifications in Figure 17 clarify that CNFY (4 h and 8 h) led to strong and sustained RhoA activation, while the CNF1-induced initial RhoA activation decreased in a time-dependent manner, dissipating significantly by 8 h-incubation. This effect was also observed in other RhoA effector pull-downs using Rho-binding domains from mDia or PKN (data not shown). Notably, CNF1-induced RhoA activation appeared to reach much less signal intensity at its peak within 2 h-intoxication compared to CNFY, which could indicate that the inactivation mechanism of RhoA is immediately present.

3.3.2 CNF1-deamidated RhoA is not degraded by the 26S proteasome

It was shown that deamidated Rac1 is directed to proteasomal degradation. Therefore, degradation of CNF1-deamidated RhoA could also explain the decreasing amount of the active pool. To analyze if CNF1 induces degradation of RhoA, HEK293 cells were pretreated with 30 µM MG132 overnight before CNF1 or CNFY was added to the cell media. After cell lysis and protein adjustment, lysates were subjected Western blotting. Additionally, CNF1 (and CNFY as a positive control) was added to cells pretreated with MG132 in a time-dependent manner to measure RhoA activity by Rhotekin pull-down following Western blotting against RhoA.

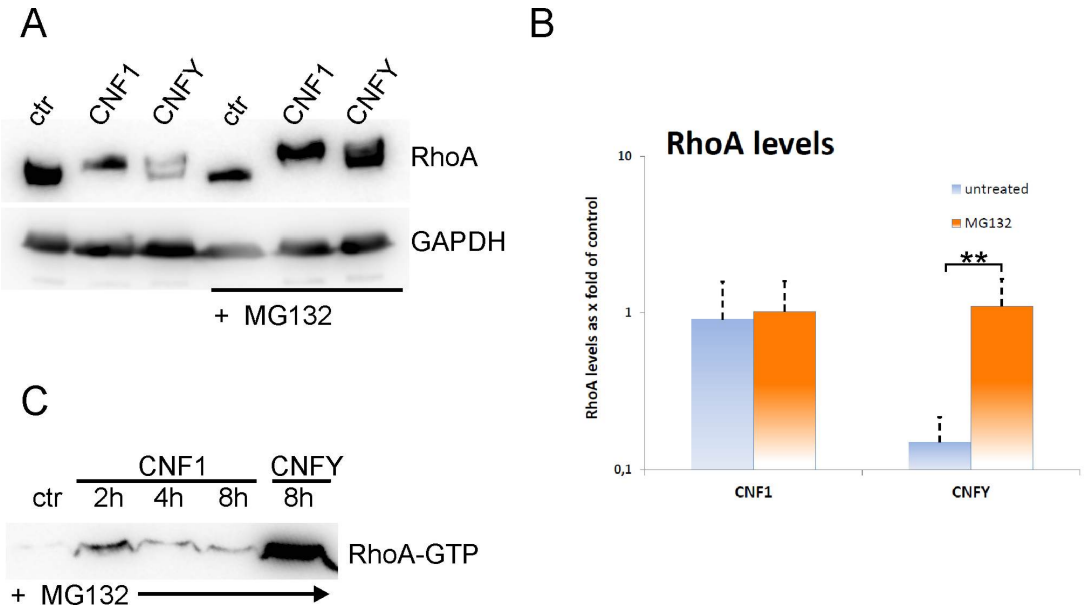


Figure 18: RhoA is degraded by CNFY but not CNF1. A] Cells were treated or untreated with 30 µM MG132 overnight prior CNF1 and CNFY intoxication. Upper panel: RhoA input from whole lysate as untreated control (ctr), CNF1 (6 h) and CNFY (6 h) intoxicated sample. Lower panel: the housekeeping protein GAPDH was used as a loading control. B] Quantification of RhoA levels are shown after CNF1/Y treatment with or without co-treatment of MG132. RhoA levels were calculated as x-fold of control. The mean standard deviation is calculated from three independent experiments. C] HEK cells were treated with 30µM MG132 overnight prior CNF1 and CNFY intoxication for indicated time-points and subsequent Rhotekin pull-down of RhoA. Results are representative of three independent experiments. (Significance after student's t-test, calculated p-value **<0.01, *<0.05)

Protein levels of RhoA did not significantly alter when CNF1 was added to the cells in comparison to the control (Figure 18A). Furthermore, the proteasome inhibitor MG132 did not lead to an increased RhoA signal in CNF1-treated probes, which was clearly illustrated by quantificational analysis. Interestingly, it was observed that CNFY induced a 0.8 fold decrease of RhoA levels, which was recovered by application of MG132 (Figure 18B). This led to the presumption that CNFY might stimulate RhoA degradation. However, RhoA was not degraded after CNF1. Moreover, when cells were analyzed for RhoA activation, MG132 had no effect on the activity pattern typically observed after CNF1 treatment (Figure 18C). Therefore, these data conclude that in contrast to Rac1, the inactivation of RhoA is not caused by proteasomal degradation.

3.3.3 Protein expression is not altered by CNF1

Even though degradation was ruled out, one could imagine that CNF1 could manipulate the expression of RhoA or the up-regulation of proteins that might be involved in this mechanism. To approach this possibility, the protein synthesis inhibitor cycloheximide was used in order to analyze, if CNF1-induced inactivation of RhoA takes place at the level of protein expression. Cycloheximide is produced by *Streptomyces griseus* and blocks translational elongation at the ribosome (Schneider-Poetsch, T. *et al.*, 2010). Therefore, HEK293 cells were treated with 100 nM cycloheximide for overnight and lyzed after certain time-points of CNF1 intoxication. Cell lysates were subjected to Rhotekin-pull-down following Western blotting against RhoA.

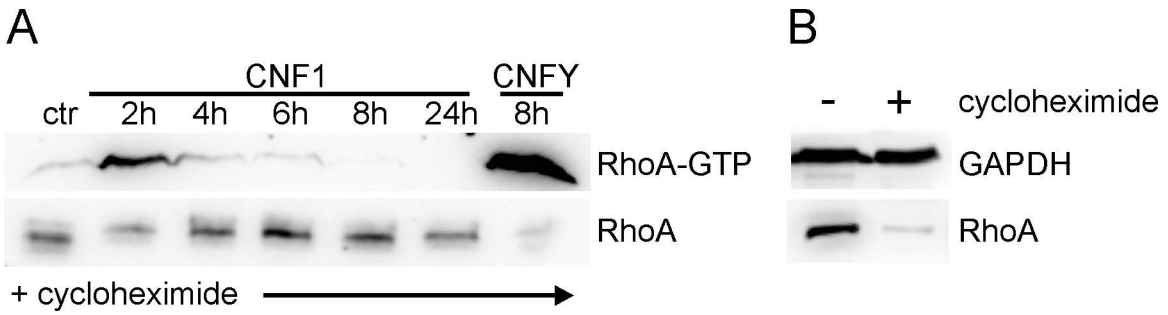


Figure 19: Protein synthesis inhibitor cycloheximide shows no influence on RhoA inactivation by CNF1. A] Time-dependent CNF1 and CNFY (400 ng/ml) intoxication and Rhotekin pull-down of RhoA after 24 h cycloheximide treatment (100 nM) (upper panel). Lower panel: Input RhoA of whole lysate run on Urea-PAGE to observe Rho-shift for deamidated RhoA. B] HEK293 cells were treated or untreated with 100 nM cycloheximide overnight. Upper panel: whole lysate was subjected to housekeeping protein GAPDH. Lower panel: total RhoA levels. Data represent at least three independent experiments.

As presented in Figure 19, the activity and stability of cycloheximide was confirmed since it blocked expression of RhoA, while the housekeeping protein GAPDH was less sensitive to cycloheximide and reflected equal loading amounts. However, cycloheximide treatment had no effect on the CNF1- and CNFY-induced activation pattern of RhoA. This suggests that general protein synthesis is not involved in the CNF1-induced mechanism to cause inactivation of RhoA.

3.3.4 Inactivation of RhoA by CNF1 is a dominant effect over CNFY-pre-activation

As illustrated previously, the activation of RhoA by CNFY was stronger than that of CNF1. This finding was in line with the observation that CNFY induced a stronger formation of stress fibers than CNF1. Furthermore, it becomes evident that the Rho shift does not necessarily reflect the activation status, since CNFY causes much slower deamidation of RhoA, not to mention that CNFY also stimulates RhoA degradation. All these observations suggest that the inactivation mechanism induced by CNF1 must proceed as a very strong and dominant effect, since RhoA was completely deamidated and the cellular content was not reduced in contrast to CNFY. Therefore, it was attempted to understand if the

mechanism promoted by CNF1 also dominates over CNFY pre-activated RhoA. In a second experiment, two questions were approached by applying the catalytically inactive mutant CNF1C866S (Schmidt, G. and Aktories, K., 1998): First it was to clarify if the inactivation effect is linked to deamidase activity of CNF1, and second, if receptor signaling might be involved in the inactivation of RhoA since CNF1 and CNFY take different routes into the cell.

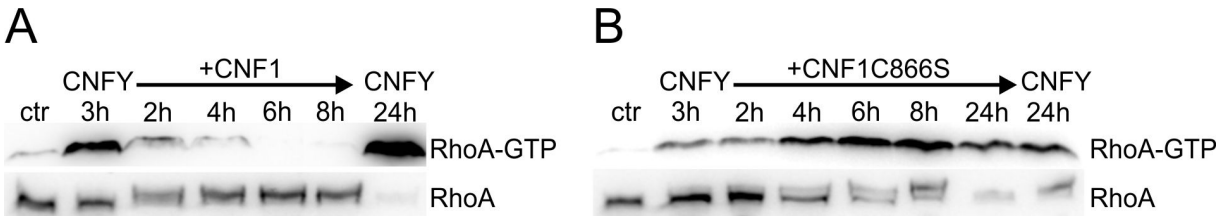


Figure 20: CNF1 enzymatic activity induces inactivation of CNFY-deamidated RhoA. Upper panel: time-course of RhoA-GTP precipitation by Rhotekin pull-down intoxicated with CNFY and co-treated with wild-type CNF1 (A) or the enzymatically inactive CNF1 mutant C866S (B). The lower panel displays total deamidation by the RhoA shift. This is a typical experiment, which was replicated three times with similar results.

Interestingly, toxin combination triggers the same RhoA activity pattern, observed when cells were treated with CNF1 (Figure 20A). This implies that the CNFY-induced deamidation and strong RhoA activation was incapable to prevent the subsequent decrease of RhoA activity by CNF1. However, inactivation of CNFY pre-activated RhoA was not detected when cells were co-treated with CNF1C866S (Figure 20B). These results prove that the underlying mechanism of CNF1 to cause inactivation of RhoA is certainly dominant over CNFY. Moreover, the catalytic domain of CNF1 is essential for this effect, while this experiment also excludes the possibility that receptor signaling of CNF1 might be involved.

3.3.6 CNF1 decreases CNFY-induced RhoA signaling in Dual-Luciferase® reporter assay

To test the consequence of the dominant CNF1-induced disruption of RhoA-effector binding the Dual-Luciferase® reporter assay was used. This read-out system determines RhoA activity downstream at the stage of gene transcription. Briefly, stimulation of RhoA activates the transcription factor Serum Response Factor (SRF), which binds to the Serum Response Element (SRE) in the promoter region of Firefly luciferase reporter gene. Thereby the Firefly luciferase is expressed and its activity is measured. Prior the experiment, HEK293 cells were transfected, intoxicated with CNF1/Y overnight and subsequently prepared to the assay as described in Materials and Methods.

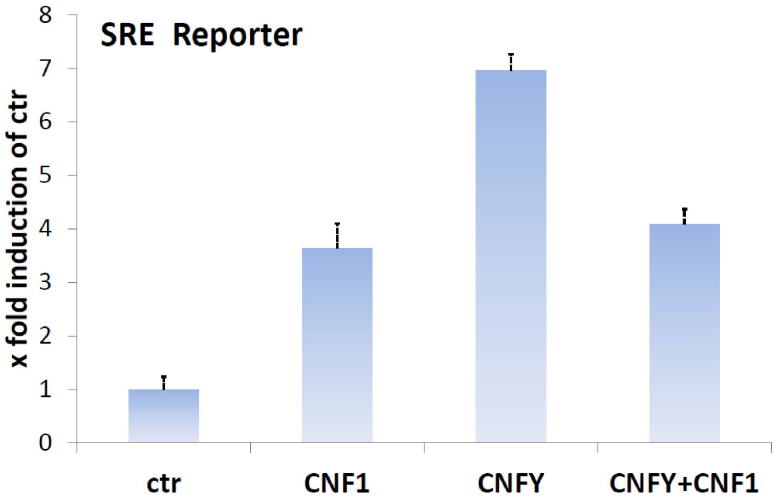


Figure 21: CNF1 decreases CNFY-induced SRE transcription. Co-transfected pSRE and pRLTK HEK293 cells were treated with CNF1/Y for 24 h and subjected to Dual-Luciferase® reporter assay. SRE reporter induction is displayed as Firefly- to Renilla luciferase ratio normalized to x-fold induction of control (ctr). Quantifications indicate the mean standard deviation of at least six independent experiments.

As shown in Figure 21, both toxins induced luciferase transcription, which confirms the activation of RhoA. Corresponding to prior results, also data from Dual luciferase assay affirmed that CNFY is the more potent activator of RhoA compared to CNF1. When cells were treated with CNFY in combination with CNF1, the SRE reporter signal dropped down to the level of CNF1 alone. The fact that CNF1 and the combination of both toxins produce a low luciferase signal rather than a signal at the level of the control is presumably due to the initial activation of RhoA. Nonetheless, this result is supportive to the hypothesis that CNF1 disruption of RhoA signaling is dominant over CNFY.

3.3.7 CNF1 induces inactivation of RhoAQ63E and RhoAG14V but not of RhoAQ63L

To substantiate the hypothesis that the time-dependent inactivation by CNF1 is a dominant effect over generally activated RhoA, other constitutive active RhoA mutants should be tested apart from CNFY pre-activation. CNF1 and CNFY cause deamidation of glutamine 63 in RhoA. Any substitution of this glutamine residue, such as RhoAQ63E and RhoAQ63L, inhibits the intrinsic as well as the GAP-stimulated GTPase activity of RhoA. Likewise, RhoAG14V represents another constitutive active mutant that is locked in its active form independent of glutamine 63 (Hoffmann, C. and Schmidt, G., 2004). Therefore, HEK293 cells were transiently transfected with RhoA wild-type (wt), RhoAQ63E, RhoAG14V and RhoAQ63L and intoxicated with CNF1/Y in a time-dependent manner. After cell lysis, RhoA-GTP was precipitated by Rhotekin pull-down and analyzed by Western blotting. Transfected RhoA constructs could be distinguished from endogenous RhoA by a higher molecular mass (30kDa) due to their N-terminal His-tag.

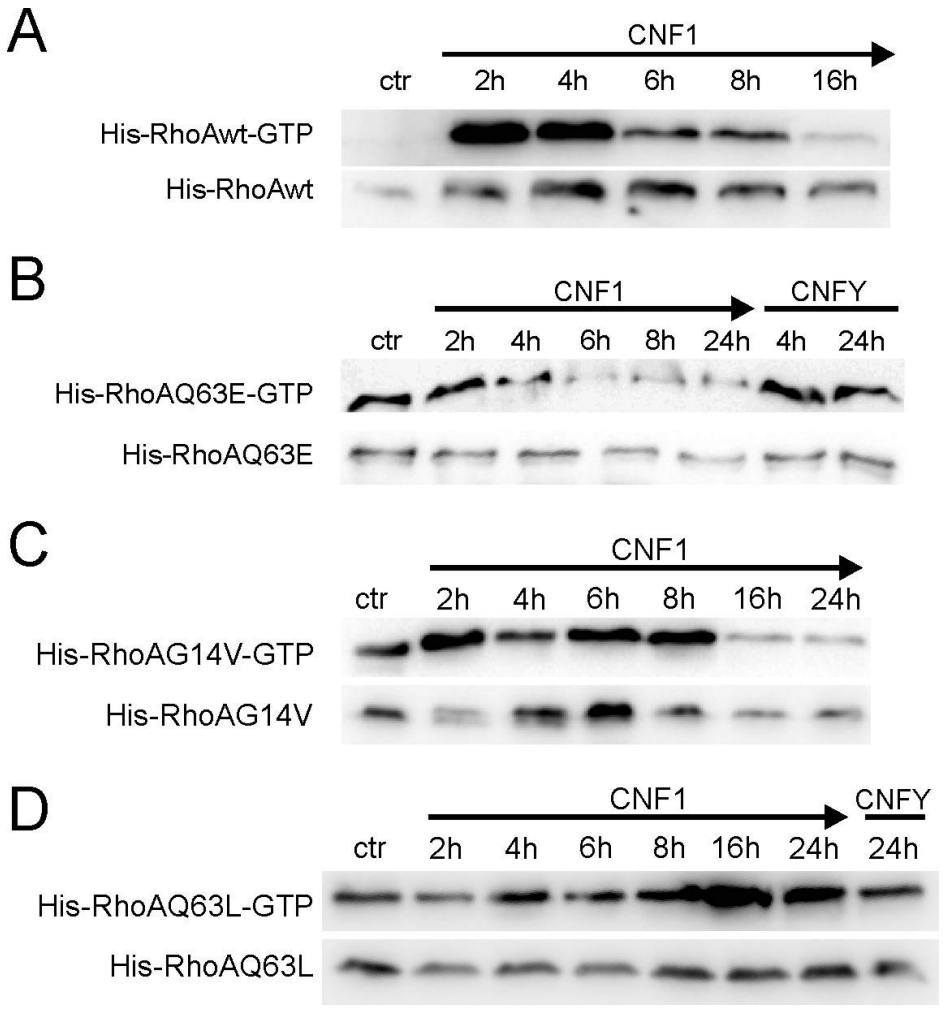


Figure 22: CNF1 inactivates constitutive active mutants RhoAQ63E and RhoAG14V but not RhoAQ63L. HEK293 cells were transfected with different RhoA mutants attached to a His-tag and intoxicated with CNF1/Y in a time-dependent manner. Upper panel: over-expressed active His-RhoAwt (A), His-RhoAQ63E (B) or RhoAG14V (C) was precipitated by Rhotekin pull-down after CNF1/Y treatment. Lower panel shows over-expressed total His-RhoAwt (A), His-RhoAQ63E (B), His-RhoAG14V (C) or His-RhoAQ63L (D) mutant. Data are representative of three independent experiments.

The Rho-shift of tagged construct such as the His-tag in pcDNA3.1 vector is less distinctive compared to the shift seen by endogenous RhoA since the migration is slower in SDS-PAGE. Therefore, deamidation and activation of RhoA is mainly confirmed by the increased precipitation through Rhotekin after toxin treatment. Thus, RhoA deamidation and activation by binding to Rhotekin could be confirmed in Figure 22A for the over-expressed His-tagged RhoAwt. As expected, His-RhoAwt was activated at 2 h and subsequently inactivated by CNF1. RhoAQ63E, RhoAG14V and RhoAQ63L mutants already

displayed RhoA activity within the control lane (ctr) confirming their constitutive activation (Figure 22B, C, D). In line with CNFY-modified and -activated RhoA, also RhoAQ63E and RhoAG14V constitutive active mutants were inactivated by CNF1 (Figure 22B), exhibiting a slower inactivation pattern compared to endogenous RhoA. In contrast, RhoAQ63L mutant was completely unaffected by the CNF1-induced inactivation. In conclusion, these data confirm that CNF1-induced inactivation is also dominant over generally activated RhoA. However, the resistance of RhoAQ63L to the CNF1 effect suggests that the region of glutamine 63 is of major importance. In contrast to RhoAQ63E, RhoQ63L has been shown to obtain a higher affinity to Rhotekin.

3.3.8 CNF1-induced RhoA regulation is independent of Cdc42 signaling

It has been shown that CNF1 and CNFY act equally effective *in vitro* targeting all GTPases RhoA, Rac1 and Cdc42, while *in vivo* the substrate specificity pattern differentiates. Furthermore, it was shown that both toxins promote the same signal intensity of Rho GTPase activation in lysate (Hoffmann, C. *et al.*, 2007). Since RhoA inactivation by CNF1 is restricted only to intact cells now emphasizes possible involved signaling pathways. The aspect that in contrast to CNFY, CNF1 also activates Rac1 and Cdc42 draws intensive attention to crosstalk mechanisms between these Rho GTPases. Recently, it was postulated that Cdc42 could be the candidate that might be involved in the inactivation of RhoA (Hoffmann, C., 2006). This conclusion was drawn from studies using the CNF1 loop 8 mutant (CNF1L8). This mutant showed decreased ability to activate Cdc42, and at the same time an enhanced RhoA activation.

To answer the question of Cdc42 involvement, HEK293 cells were transfected with constitutive active pEGFP-Cdc42Q61E, intoxicated with CNFY for 4 h and subjected to Rhotekin pull-down. Additionally, CNF1L8 was used to study the role of Cdc42. CNF1L8 inherits a mutation within the Rho GTPase binding pocket, where the loop8 region from CNF1 was exchanged by the respective amino acids from CNFY. It was postulated that this pocket is responsible for Rho GTPase specificity between CNF1 and CNFY. CNF1L8 was shown to exhibit no binding affinity to and activation of Cdc42 while it induced equally effective RhoA activation as seen after CNFY treatment. Therefore, it was postulated that

there is a correlation between decreased Cdc42 activation with increased RhoA activity and possible Cdc42 crosstalk (Hoffmann, C. and Schmidt, G., 2004). To test this, HEK293 cells were intoxicated with CNF1L8 or CNFY in a time-dependent manner, lysates were subjected to Rhotekin pull-down and Western blot analysis against RhoA.

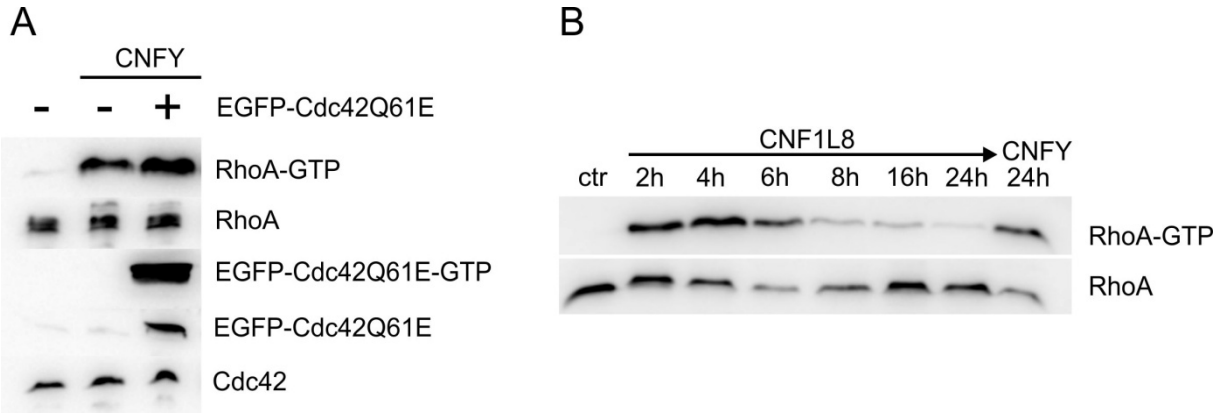


Figure 23: Cdc42 signaling is not involved in RhoA inactivation. A] HEK293 cells were transfected (+) with EGFP-tagged constitutive active Cdc42Q61E mutant or left untransfected (-). PAK pull-down confirmed activity of Cdc42Q61E. Cells were intoxicated with CNFY for 4 h and RhoA-GTP was precipitated by Rhotekin pull-down. RhoA and endogenous Cdc42 input confirmed equal loading amounts. B] Upper panel: Rhotekin pull-down of RhoA after CNF1L8 or CNFY intoxication at indicated time-points. Lower panel: RhoA input. Data are representative for three independent experiments.

Surprisingly, results presented in Figure 23 indicate that Cdc42 signaling is not involved in RhoA inactivation in contrast to previous data (Hoffmann, C. *et al.*, 2007). Indeed, CNF1L8 induced equally strong activation of RhoA as for CNFY, but the signal also decreased during the time-course of 24 h (Figure 23B). Moreover, RhoA activation by CNFY was not decreased when constitutive active Cdc42Q61E mutant was over-expressed (Figure 23A). Therefore, one can argue that the different substrate specificity of CNF1L8 may delay the effect of RhoA inactivation, but Cdc42 could be ruled out as the key determinant to cause the dominant inactivation of RhoA.

3.3.10 RhoGDIα is not involved in the CNF1-induced inactivation of RhoA

Most importantly, the activity cycle of Rho GTPases is regulated by RhoGDIs, which bind the GDP-bound form, sterically shielding the GTPase from the action of GEFs and GAPs. Consequently, RhoGDI regulates the activation cycle by blocking GDP to GTP exchange and by keeping the GTPases in the cytosol. It has also been postulated that RhoGDI is capable to bind the GTP-bound form of the Rho GTPase, serving as a chaperone to directly control interaction with effectors (DerMardirossian, C. and Bokoch, G. M., 2005). Interestingly, the interaction of Rho GTPases to RhoGDI has been target of some toxins. For example, C3 toxin produced by C*lostridium botulinum* enhances RhoA affinity to RhoGDI and thereby decreases RhoA-effector binding (Aktories, K. *et al.*, 2004). Therefore, an enhanced RhoA-RhoGDI complex formation could be a possible mechanism by which CNF1 could promote the inactivation of RhoA. In order to determine if RhoGDI has a general influence on Rho GTPase regulation, RhoGDI knockout (RhoGDI -/-) were compared to wild-type (RhoGDI +/+) mesangium cells (MSC) in terms of RhoA, Rac1 and Cdc42 basal activity. Therefore, lysate of both cell lines was subjected to PAK and Rhotekin pull-down, following Western blotting.

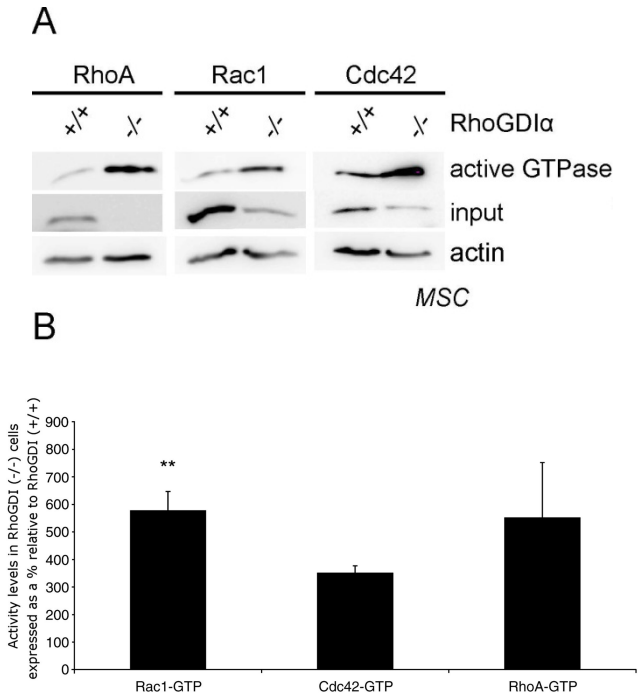


Figure 24: The absence of RhoGDI enhances basal Rho GTPase activity. A] RhoGDI +/+ and RhoGDI -/- mesangium cells (MSC) were compared for Rho GTPase activity by Rhotekin- and PAK pull-down for RhoA, Rac1 and Cdc42 activity (upper panel) compared to input (middle panel). Actin was used as loading control (lower panel). B] Quantification of Rho GTPase activities were normalized to actin expression levels. Results are given as normalized GTPase activity levels in RhoGDI -/- MSC as a percentage relative to that in RhoGDI +/+ MSC cells. Results shown, represent the standard deviation of at least three experiments. (significance after student's t-test: * $\rho < 0.05$, ** $\rho<0.01$) Depicted Results are representative of more than three independent experiments.

As depicted in Figure 24, RhoGDI knockout cells exhibited elevated levels of activated Cdc42 and Rac1, but most profoundly of RhoA. Simultaneously, it was observed that the protein levels were down-regulated (see *input* Figure 24A). This verified that RhoGDI acts as a crucial regulatory point for Rho GTPase activity by presumably keeping them in an inactive state and protecting them from degradation (Bielek, H. *et al.*, 2009). Therefore, these data provide hints that an enhanced RhoGDI interaction could be the cause of the CNF1-induced RhoA inactivation.

To analyze if RhoA-RhoGDI binding is influenced by CNF1 treatment, HEK293 cells were intoxicated with CNF1/Y, lyzed and subjected to GDI pull-down and Western blotting. Co-Immunoprecipitation (Co-IP) was performed to precipitate the endogenous RhoA-GDI complex in order to determine if CNF1 affects the binding affinity of the endogenous complex.

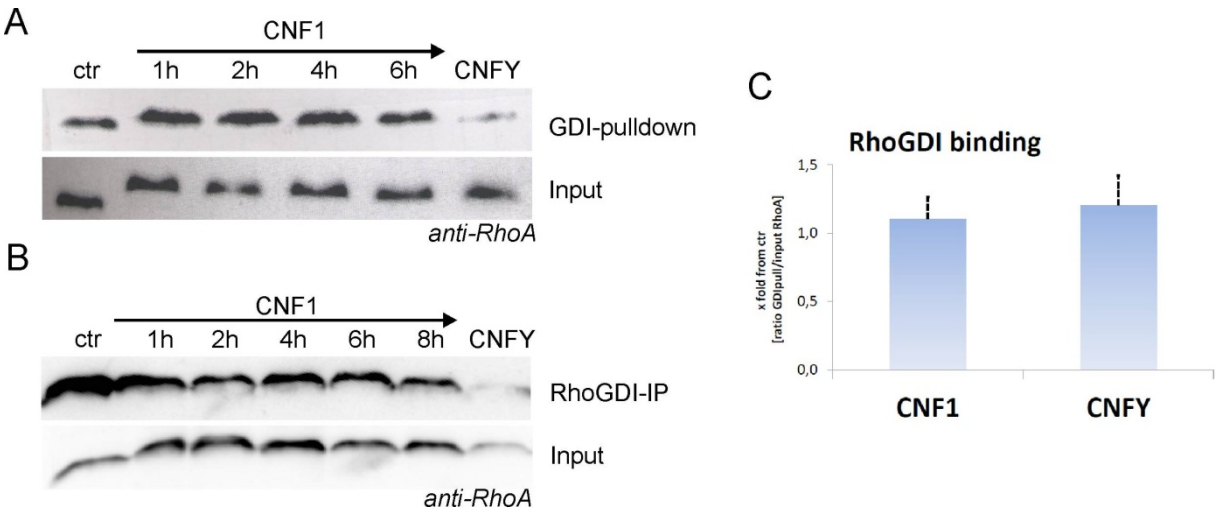


Figure 25: CNF1 does not affect RhoA binding to RhoGDI. Upper panels: RhoA-GDI interaction was observed by GDI pull-down (A) of HEK293 lysates intoxicated with CNF1/Y. The endogenous RhoA-GDI complex was observed by Co-IP precipitating with anti-RhoGDI antibody (B). Lower panels: Loading control of input RhoA. C] Quantification shows *in vitro* RhoA-GDI binding at 8 h CNF1/Y intoxication as x-fold from control (ratio RhoA-GDI pull-down/ input RhoA). Depicted Results with standard deviation of the mean are representative of more than three independent experiments.

Surprisingly, as displayed in Figure 25, the affinity of RhoA binding to RhoGDI by pull-down was unaffected in untreated and CNF1-treated cells. Also *in vivo* results by precipitation of the endogenous complex displayed likewise results. Interestingly, CNFY treatment showed decreased RhoGDI binding of RhoA by Western blotting of GDI pull-down and Co-IP (Figure 25A/B). However, when quantifying the amount of GDI-bound RhoA to RhoA input, it was observed, that RhoA binding to RhoGDI was not affected as depicted by quantificational analysis (see Figure 25C). The impression of low binding between RhoA and RhoGDI might be explained by the fact, that RhoA is degraded by CNFY as described previously and therefore less determined in complex with RhoGDI.

This concludes that neither CNF1 nor CNFY seem to influence the RhoA-RhoGDI-complex formation by noticeable disruption or enhanced interaction.

Although these studies revealed no difference in RhoA-RhoGDI binding, an indirect involvement of RhoGDI could still be possible. In order to analyze this, the effect of CNF1-induced inactivation of RhoA was tested in RhoGDI knockout cells. Therefore, RhoGDI -/- MSC cells were intoxicated with CNF1 (up to 10 h) and CNFY (4 h), lysates applied to Rhotekin pull-down and Western blotting to analyze the RhoA activation pattern.

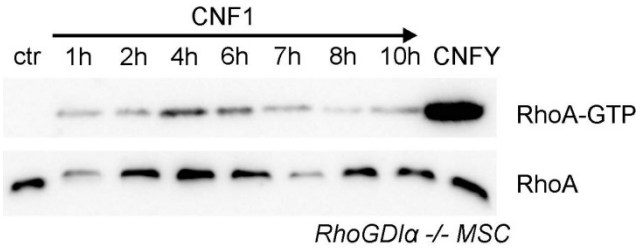


Figure 26: CNF1 effect is independent of RhoGDI. Active RhoA was precipitated by Rhotekin pull-down in RhoGDI -/- MSC cells. Lower panels: Loading control of RhoA input. The result is representative of more than three independent experiments.

As shown in Figure 26, even in the absence of RhoGDI the typical CNF1 and CNFY activation pattern was observed. Thus, these data suggest that CNF1-induced inactivation of RhoA is independent of RhoGDI.

3.3.12 Lack of Isoprenyl group blocks CNF1-induced RhoA regulation

Rho GTPases are post-translationally modified by isoprenylation. This hydrophobic group enables them to interact with RhoGDI and to attach to cellular. While Rac1 and Cdc42 are farnesylated, RhoA is geranylgeranylated at cysteine 190 (Roberts, P. J. *et al.*, 2008). To answer the question if isoprenylation is required for RhoA inactivation by CNF1, two methods were approached: inhibition of endogenous protein isoprenylation by lovastatin and mutational analysis of the C-terminal cysteine (C190). Lovastatin is an inhibitor of HMG-CoA reductase, an enzyme involved in the cholesterol synthesis pathway. By interfering with this pathway lovastatin blocks isoprenylation of proteins (Turner, S. J. *et al.*, 2008). Similarly, substitution of the C-terminal cysteine with a serine generates a mutant that is unprenylated.

Therefore, prior CNF1 and CNFY intoxication HEK293 cells were either treated with 10 µM lovastatin overnight or transfected with RhoAC190S. Lysates were subjected to Rhotekin pull-down to examine the activation pattern of RhoA.

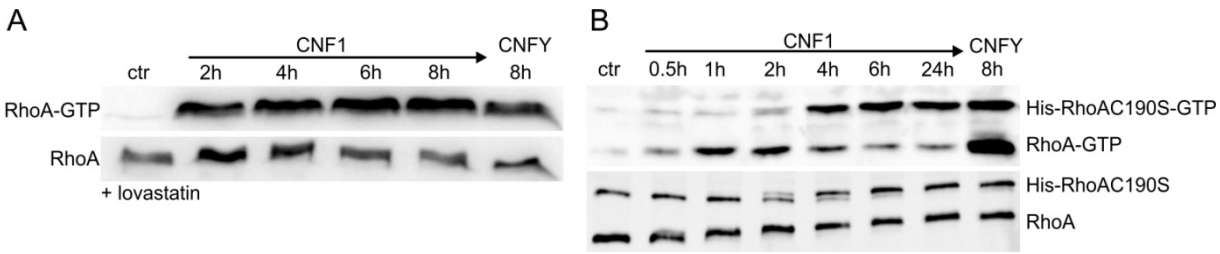


Figure 27: Isoprenylation of RhoA is essential for CNF1-induced inactivation. A] HEK293 cells were treated with 10 µM lovastatin overnight prior CNF1/Y intoxication. Upper panel show Rhotekin pull-down for active endogenous RhoA, lower panel presents the input of RhoA from whole lysate. B] His-RhoAC190S-transfected HEK293 cells were subjected to CNF1/Y intoxication. Upper panel shows Rhotekin pull-down of both endogenous and over-expressed RhoAC190S mutant. Lower panel: input of over-expressed and endogenous RhoA. Western blots represent data from three independent experiments.

As shown in Figure 27A, RhoA was activated by CNF1 at 2 h. Surprisingly, in the presence of lovastatin, RhoA remained active even after 8 h CNF1 exposure. Moreover, the discrepancy between CNF1 and CNFY of RhoA intensity was completely abolished. This suggests that lovastatin blocks the molecular mechanism that underlies the inactivation of RhoA. Similarly, the unprenylated RhoAC190S also seemed to resist the inactivation by CNF1 and showed comparably signal intensity to CNFY activation, in contrast to endogenous RhoA. These results implicate that RhoA proteins lacking the isoprenylated C-terminus are not susceptible towards the inactivation mechanism induced by CNF1. Thus, the isoprenylated C-terminus seems to play an essential role in the inactivation of RhoA.

3.3.13 RhoAS188E is not inactivated by CNF1 compared to RhoAS188A

Because prenylation is required for Rho proteins to interact with the membrane, it was attempted to further clarify the role of membrane binding. It has been published (Rolli-Derkinderen, M. *et al.*, 2005) that the phosphomimetic mutant RhoAS188E, preferably in its constitutive active form, resists ubiquitin/proteasome-mediated degradation by cytosolic sequestration through enhanced RhoGDI interaction. This mutant was shown not to be localized at the plasma membrane (although it is isoprenylated) and therefore will be used to study, whether membrane binding is a prerequisite for CNF1-mediated inactivation of RhoA. RhoAS188A serves as control since it is capable to insert into membranes but will exclude the possibility that the serine at position 188 itself is involved. To test this, the cytosolic, phosphomimetic RhoAS188E and membrane-binding RhoAS188A mutants were over-expressed in HEK293 cells, intoxicated with CNF1/Y in a time-course up to 24 h, subjected to Rhotekin pull-down and Western blotting.

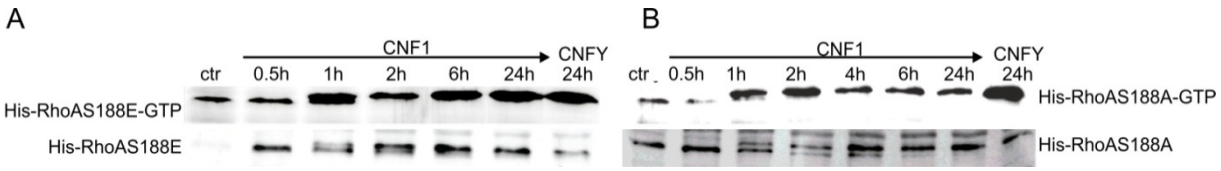


Figure 28: RhoAS188E is not regulated by CNF1 in contrast to RhoAS188A. HEK293 cells were transfected with His-RhoAS188E (A) and RhoAS188A (B) mutants, treated with CNF1/Y and subjected to Rhotekin pull-down (upper panels). Expression efficiency and deamidation by the RhoA shift is shown in the lower panels. Blots are representative for three independent experiments.

As depicted in Figure 28 RhoAS188A was susceptible to the inactivation mechanism induced by CNF1. In contrast, the cytosolic RhoAS188E resisted this effect and exhibited increasing activity with similar intensity to CNFY treatment. Therefore, these data suggest that the cytosolic localization of RhoAS188E seem to protect the protein from the CNF1-induced inactivation. These results provide further evidence that membrane localization is important for the underlying regulation of RhoA inactivation. Thus, membrane binding must be a prerequisite for the CNF1-induced inactivation of RhoA.

3.3.14 Membrane distribution correlates with the RhoA activity pattern

According to the general concept found in the literature that RhoGEFs and Rho effectors are anchored to membranes, one might assume that CNF-deamidated and -activated RhoA also correlates with membrane localization. To examine whether a relationship exists between membrane attachment and the CNF1-induced inactivation of RhoA, the presence of RhoA was assessed in membrane fractions after CNF1 and CNFY intoxication. For that reason, HEK293 cells were treated with CNF1 and CNFY for several hours. Cells were lyzed and whole lysates were subjected to membrane purification following Western blotting against RhoA.

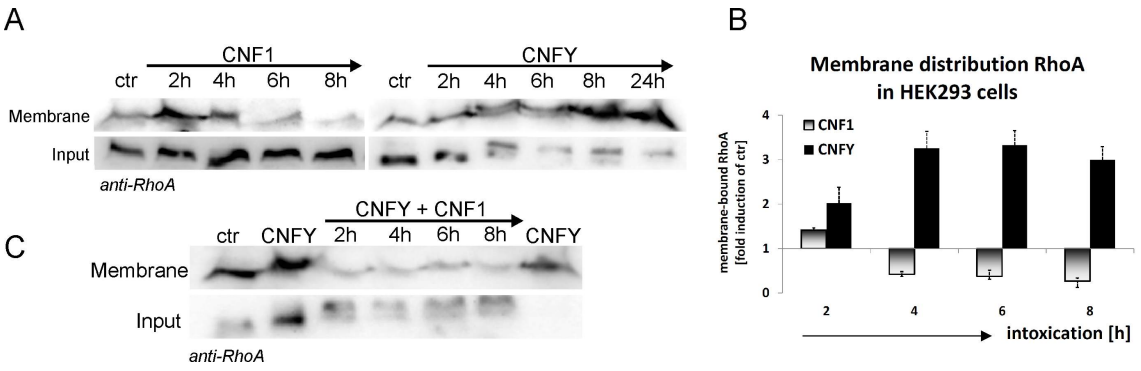


Figure 29: CNF1 inactivation pattern correlates with decreased membrane binding of RhoA in HEK293 cells. A] HEK293 cells were intoxicated with CNF1 (left) or CNFY (right) in a time-dependent manner. Cells were lyzed and membranes (upper panel) were isolated from whole lysate (lower panel) and subjected to Western blotting with anti-RhoA antibody. B] Quantifications of RhoA membrane distribution was calculated by membrane-bound to input RhoA ratio as x-fold increase to untreated control (ctr). Untreated controls were set to 1 and represent the baseline of the x-axis. Error bars represent the mean standard deviation of at least three independent experiments. C] HEK293 cells were co-treated with CNF1 and CNFY. Lysates (lower panel) were subjected to membrane fractionation (upper panel) and RhoA was detected by Western blotting.

As expected, CNFY-activated RhoA enriched and remained in the membrane fraction. Remarkably, although the CNF1- activated RhoA initially localized to membranes it was predominantly diminished from the membrane extract during longer toxin exposure (Figure 29). In fact, data obtained from toxin combination clarified that CNF1 seem to induce the dominant release of RhoA from membranes over CNFY stimulation. Quantifications of membrane-bound to total RhoA ratio visualize the antagonistic effects of CNF1 and CNFY. These observations are in agreement with the proposed role that active RhoA is membrane attached. Thus, these results strongly implicate that membrane release correlates with inactivation of RhoA induced by CNF1.

3.3.16 Cell line responsiveness to RhoA inactivation by CNF1

So far, the mechanism of RhoA inactivation by CNF1 was investigated in HEK293, HeLa and MSC cells and it was shown in the prostate cancer cell lines LNCaP and C4-2 (List, J. H., 2010). To test the responsiveness of CNF1 in other cell lines, a selection of cells was depicted and treated with CNF1 and/or CNFY within a timeframe of 2 - 24 h. After cell lysis and protein adjustment, lysates were subjected to Rhotekin pull-down and Western blotting to analyze the course of RhoA activation.

Cell lines	transient RhoA activity
C4-2	+
Caco-2	+
CHO-1	-
HEK293	+
HeLa	+
LNCaP	+
MEF	-
MSC	+
Swiss 3T3	+
Vero	+

Table 6: List of cell lines tested for transient RhoA activity by CNF1. Cells were treated with CNF1/Y in a time-dependent manner (up to 24h) and subjected to Rhotekin pull-down. Most cells exhibited transient RhoA activity (+), while CHO-1 and MEF cells displayed constant RhoA activation after CNF1 treatment (-). Each analysis was done for at least two independent experiments.

Vero and mesangium cells (MSC) are kidney epithelial cells derived from monkey (Vero) and mouse (MSC), Swiss 3T3 cells are fibroblast from mouse embryonic tissue while LNCaP and C4-2 cells derived from human prostate cancer. These cell lines are responsive to the effect of RhoA inactivation by CNF1 as listed in Table 6. A representative Western blot is depicted in Figure 30A for the MSC cell line. In contrast, mouse embryonic fibroblasts (MEFs) (Figure 30B) and Chinese hamster ovary cells (CHO-1) resisted this effect.

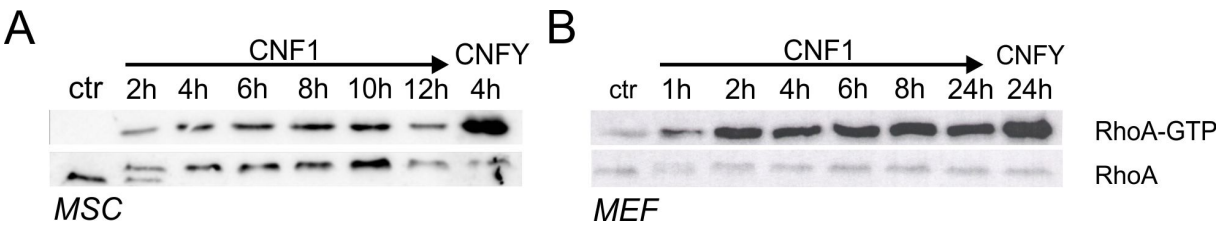


Figure 30: MSC and MEF cell lines show contrary RhoA activation patterns after CNF1/Y intoxication. Mesangium cells (MSC) (A) and mouse embryonic fibroblasts (MEFs) (B) represent each a cell line with transient (MSC) and constant (MEF) RhoA activation. Upper panels show Rhotekin pull-downs, lower panels represent input control of total RhoA and are representative for at least three independent experiments.

These results suggest that even though all cell lines were responsive to toxin uptake and deamidation of RhoA, the secondary effect of RhoA inactivation by CNF1 was not present in all cell lines. It is yet to clarify why certain cell lines are not responsive to the CNF1-induced inactivation of RhoA and presumably lack this regulatory pathway.

3.3.17 Membrane distribution of RhoA correlates with cell line specificity

CNF1 and CNFY induce different RhoA membrane distribution patterns in HEK293 cells, which seemed to correlate with the activation status of RhoA. Since the effect of inactivation of RhoA by CNF1 was found to be not redundant in every cell line it was of particular interest if cell line specificity correlates with different localization of RhoA. Thus, membrane distribution of RhoA was examined by using the responsive LNCaP- in comparison to the resistant MEF cells. Both cell lines were treated with CNF1/Y in a time-dependent manner for up to 8 h. Membranes were purified from lysates and separated on SDS gels following Western blotting.

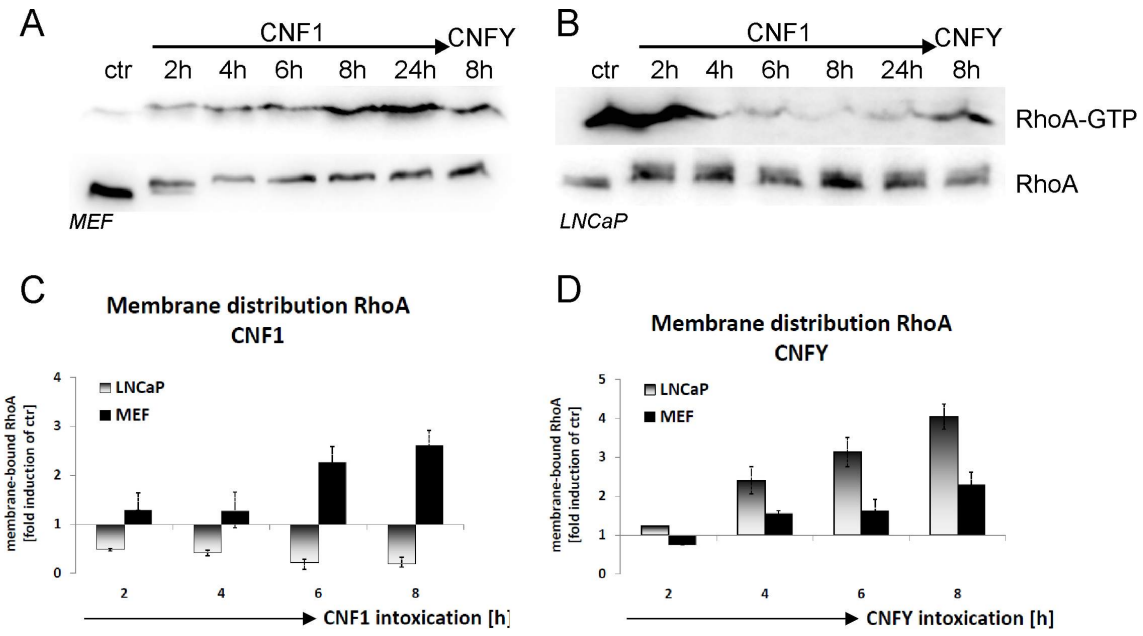


Figure 31: Membrane distribution of RhoA after CNF1 correlates with its activity pattern in LNCaP and MEF cells. LNCaP (A) and MEF cells (B) were subjected to membrane fractionation after CNF1/Y treatment and membrane-bound RhoA was detected (upper panels) in comparison to total RhoA in whole lysate (lower panels) by Western blotting. Quantifications of membrane-bound to total RhoA after CNF1 (C) or CNFY (D) intoxication was calculated as x-fold induction of untreated control (ctr) in LNCaP and MEF cells. Untreated controls were set to 1 and represent the baseline of the x-axis. Error bars represent mean standard deviation of at least three experiments.

As expected, the CNF1-induced membrane distribution pattern could be observed in LNCaP cells, where the amount of membrane-bound RhoA decreased in a time-dependent manner (Figure 31). This effect clearly demonstrates that the same mechanism of membrane release correlates with the inactivation of RhoA not only in HEK293 but also in LNCaP cells. Remarkably, this was not the case in MEF cells. CNF1 promoted an increase of membrane-bound RhoA but lacked the subsequent membrane release. Consistent with the difference in membrane binding between CNF1 and CNFY also data from these two cell lines support the hypothesis that membrane attachment and release of RhoA correlates with the CNF1 and CNFY-induced RhoA activity pattern. This leads to the presumption that membrane release is an essential part in the mechanism by which CNF1 induces the inactivation of RhoA. In conclusion, the findings support the notion that in CNF1-treated cells, the total amount of cellular RhoA is modified, but is not able to interact with localized effectors and therefore causes blockage of RhoA-dependent downstream signaling in contrast to CNFY. However, further studies are required to determine the detailed mechanism of how RhoA is released from the membrane and why RhoA is incapable to interact with effectors *per se* (e.g. in Rhotekin pull-down).

3.4 Biological relevance of RhoA inactivation by CNF1

So far, the effect of CNF1 on RhoA activation was analyzed in various assays concerning effector interaction, RhoGDI binding and membrane localization. Subsequently, the effect of CNF1-induced RhoA inactivation should be determined in complex signaling pathways, which are relevant to the RhoA dependent activity. Altered expression or regulation of RhoA can contribute to different cellular processes that could in particular affect cancer progression. By understanding their role in tumorigenesis, it will bring new possibilities to interfere with Rho regulation for anti-cancer therapy.

3.4.1 CNFY-induced RhoA signaling pathway leads to apoptosis in LNCaP cells

It was shown that the androgen-dependent prostate cancer cell line LNCaP undergoes apoptosis upon RhoA activation (Papadopoulou, N. *et al.*, 2008). Based on the presently available data, it was of great interest to investigate whether the activated RhoA pathway leads to apoptosis. To examine the physiological outcome on LNCaPs after RhoA activation, cells were treated with the strong RhoA activator CNFY with or without inhibitors of the Rho - Rho kinase (ROCK) pathway. Two inhibitors, Y-27632 and H-1152 block ROCK, while blebbistatin is an inhibitor of myosin II further downstream of Rho - ROCK signaling (Orlando, K. A. *et al.*, 2006). Prior CNFY intoxication (overnight) LNCaP cells were treated with 10 µM Y-27632, 1 µM H-1152 or 10 µM blebbistatin overnight. Apoptosis was determined by morphological changes observed by light microscopy and biochemically by poly (ADP-ribose) polymerase (PARP) cleavage after 48 h. Intoxication was confirmed by the RhoA shift and Rhotekin pull-down experiments.

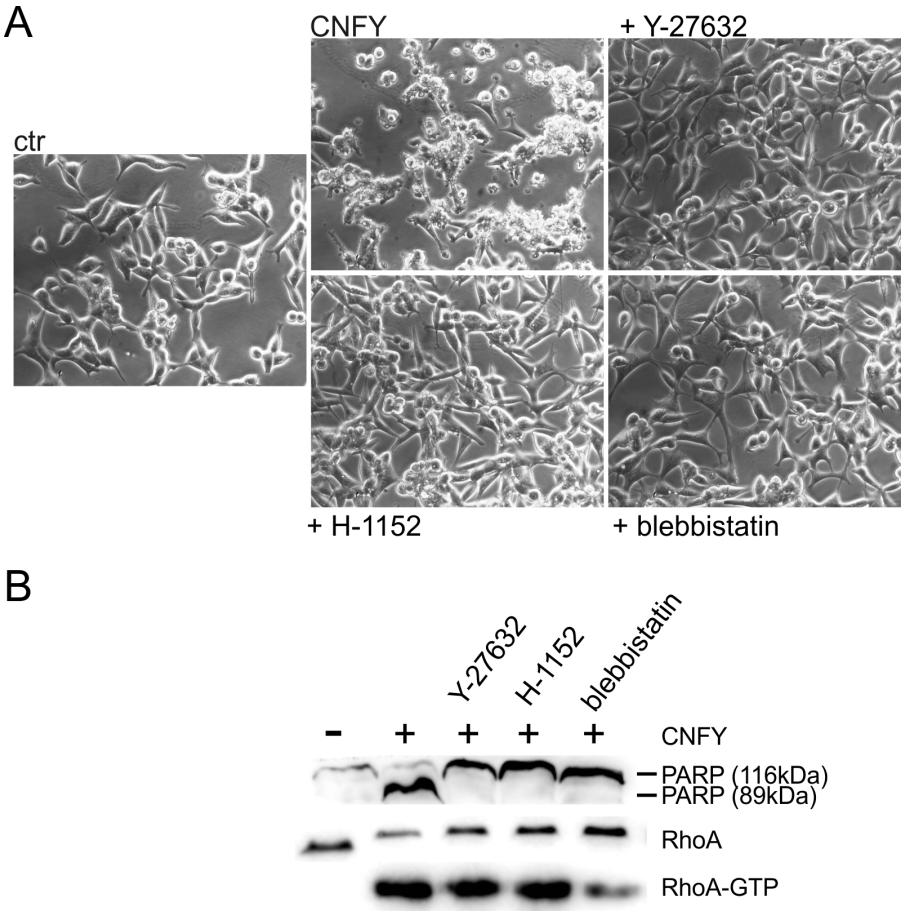


Figure 32: CNFY induced apoptosis in LNCaP that is blocked by inhibitors of the Rho-ROCK pathway. A] LNCaP cells were pre-treated with ROCK inhibitors H-1152 (1 µM) and Y-27632 (10 µM) or myosin II inhibitor blebbistatin (10 µM) overnight prior intoxication with CNFY or CNFY alone. Microscopic pictures were taken at 20x magnification by an inverted light microscope. B] LNCaP cells co-treated with CNFY +/- inhibitors were lyzed after 48 h, subjected to Rhotekin pull-down for GTP-RhoA (lower panel) in comparison to total RhoA (middle panel) and PARP-cleavage (upper panel). Data are representative for three independent experiments.

As expected, CNFY induced apoptotic blebbing in LNCaP cells after 24 h as shown in Figure 32A. Interestingly, this effect was blocked when cells were co-treated with ROCK inhibitors, Y-27632 and H-1152, or myosin II inhibitor blebbistatin. Figure 32B confirmed apoptosis by PARP cleavage, where full length PARP (116kDa) is cleaved into fragments of 89kDa and 27kDa (not shown) by caspase 3/7. CNFY intoxication and RhoA activation was approved by the RhoA shift and Rhotekin pull-down experiments. PARP cleavage was blocked when inhibitors of the Rho –ROCK pathway were present. These results provide evidence that CNFY induces RhoA activation and apoptosis in LNCaP cells via the Rho-ROCK pathway.

3.4.2 CNFY-dependent apoptosis in LNCaP cells is blocked by CNF1

CNFY and CNF1 have both been described as Rho-activating toxins. But the newly described dual functions of CNF1 suggest that the toxin exerts most apparently inactivating rather than activating functions towards RhoA. List, J., described previously that apoptosis can be induced by CNFY but not by CNF1, which correlates with the permanent activity of RhoA induced by CNFY (List, J. H., 2010). Here, it could be verified that LNCaP cells are susceptible to the CNF1-induced inactivation mechanism by Rhotekin pull-down. Therefore, it would be of great interest to analyze the physiological outcome of this effect in respect to apoptosis. The question is, whether the CNF1-induced inactivation of RhoA could block the CNFY-promoted apoptosis. Therefore, LNCaP cells were treated with CNF1 together with CNFY and analyzed for apoptotic blebbing. Further, LNCaP cells were intoxicated with CNFY in combination with CNF1 in a time-dependent manner for biochemical analysis of RhoA activation. Cells were lyzed, subjected to Rhotekin pull-down and subsequently separated on SDS-PAGE following Western blotting against RhoA.

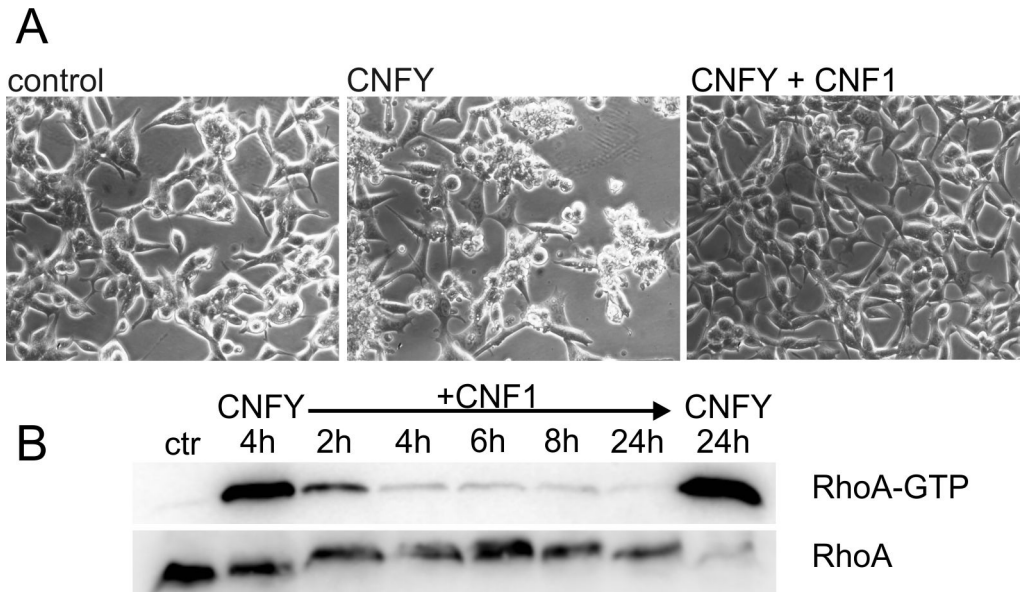


Figure 33: CNF1 blocks CNFY-stimulated and RhoA-dependent apoptosis in LNCaP cells.
A] LNCaP cells were untreated (control), treated with CNFY alone or co-treated with CNF1 for 24 h. Microscopic pictures were taken at 20x magnification by an inverted light microscope. B] LNCaP cells, co-treated with CNFY and CNF1, were lyzed and subjected to Rhotekin pull-down for GTP-RhoA (lower panel) in comparison to total RhoA (lower panel). Results shown are representative for at least three independent experiments.

As depicted in Figure 33A, CNF1 completely inhibited the CNFY-induced apoptosis when toxins were combined. Indeed, as displayed in Figure 33B, this effect correlated with the dominant impact of CNF1 to inactivate CNFY-deamidated RhoA. These results strongly imply that in terms of RhoA activation to trigger apoptosis in androgen-dependent prostate cancer LNCaP cells, CNF1 was shown to be dominant over CNFY pre-activated RhoA. In fact, CNF1 can be described as an inhibitor rather than an activator of Rho signaling. Therefore, one can speculate that in respect to chronic infections with *E. coli* producing CNF1 may have a pathophysiological relevance in LNCaP cells by protecting them from apoptosis and promote their survival. Moreover, the mechanism of RhoA inactivation would be the major force in this context.

4 DISCUSSION

Rho GTPases were first identified as regulators of the actin cytoskeleton, but in recent years a plethora of cell biological studies demonstrated that they are involved in many other cellular functions. Especially, their emerging role in tumor formation and malignant progression has raised great interest in understanding their function and regulation. The Cytotoxic Necrotizing Factor 1 (CNF1) from *E. coli* has been described as a toxin that activates Rho GTPases (Fiorentini, C. *et al.*, 1997). Therefore, CNF1 has been rendered as an attractive tool to study Rho GTPase function. However, recent findings reveal that the CNF1 activating effects are only transient (Hoffmann, C. *et al.*, 2007). This second effect of antagonistic regulation by CNF1 has been barely described. Therefore, the main objective of the present studies attempted to obtain new insights into the understanding of the molecular mechanisms by which CNF1 causes the inactivation of Rac1 and RhoA.

4.1 Activation of Rho GTPases Rac1 and RhoA by CNF1 is transient

CNF1 and the related CNFY from *Yersinia pseudotuberculosis* belong to the CNF toxin family, which share the same enzymatic activity by the deamidation of a specific glutamine residue in Rho GTPases (glutamine 61 in Rac1/Cdc42 and the equivalent glutamine 63 in RhoA) but differ in their substrate specificity. This glutamine residue is located in the switch II region of the Rho protein, a region that undergoes major conformational changes upon GTP or GDP binding, turning the Rho GTPase on or off. Thus, deamidation inhibits the intrinsic and GAP-stimulated GTP hydrolase activity. Therefore, CNF-deamidated Rho GTPases are expected to be active, because the turn-off mechanism of the GTPase is blocked. In fact, this could be verified by the method of effector pull-down assays with the Rho-binding domain of effectors that exclusively interact with the active GTP-bound form. Thereby, it could be shown that CNF1 induced activation of Rac1, RhoA, and Cdc42, while CNFY selectively activated RhoA. Concomitantly, the morphological features of stimulated Rac1-dependent lamellipodia

formation and RhoA-dependent stress fiber- correlated with this effect. Cdc42-promoted filopodia structures were only marginally detected in HeLa cells. This was found to be in line with previous studies (Fiorentini, C. *et al.*, 1997; Boquet, P., 2001; Hoffmann, C. *et al.*, 2004). Due to the posttranslational modification of Rho GTPases induced by CNFs, resulting in their permanent activation *in vitro*, it was assumed that this effect is also permanent *in vivo* (Schmidt, G. *et al.*, 1997). In fact, this was shown to be true for CNFY, which showed persistent stress fiber formation, indicating RhoA activation. However, it was observed that the Rac1 and RhoA-dependent morphological features decreased after 8 h of CNF1 intoxication. Therefore, these observations imply that, *in vivo*, the CNF1-induced activation of Rac1 and RhoA seems to be a transient rather than permanent effect, despite the fact that both Rho GTPases are covalently modified and, therefore, should be persistently activated.

4.2 Deamidated Rac1 is subjected to degradation

Consistent with the disappearance of lamellipodia structures, it was demonstrated that Rac1 interaction with downstream effector PAK1 decreased in a time-dependent manner. Interestingly, transience of Rac1 activity matched closely with the depletion of the total amount of Rac1 in CNF1-treated cells. This finding suggests that deamidated and therefore activated Rac1 could be negatively regulated by degradation. This hypothesis was supported by the application of MG132 prior CNF1, an inhibitor of the 26S proteasome, which increased the protein levels of Rac1 and rescued it from degradation. Therefore, this implicates that the inactivation of Rac1 is a consequence of its proteolytic degradation by the 26S proteasome. In fact, this finding is in perfect agreement with previously published data (Doye, A. *et al.*, 2002; Lerm, M. *et al.*, 2002). Ubiquitin-mediated degradation of Rac1 was shown to play a very essential role during the infection process since it enhances motility of CNF-treated cells and internalization of bacteria (Doye, A. *et al.*, 2002; Doye, A. *et al.*, 2006). This process was shown to require both activation and isoprenylation of Rac1, the canonical D-Box, effector binding and targeting to cellular membranes (Pop, M. *et al.*, 2004; Doye, A. *et al.*, 2002).

4.3 Deamidated Rac1 is translocated to the nucleus by C-terminal interaction with KPNA2

The defining steps and involved proteins by which deamidated Rac1 is directed to the 26S proteasome have barely been described. Surprisingly, it was hypothesized that degradation of Rac1 occurs in the nucleus. Recently, by using the method of the yeast two-hybrid screen, Karyopherin α2 (KPNA2) was identified as a direct interaction partner of deamidated Rac1. Together with Sandrock, K., this interaction was verified by precipitation of the KPNA2-Rac1 complex *in vivo*. Karyopherin α2 is a nuclear shuttle protein, which interacts directly with classical nuclear localization signal (NLS)-containing cargo proteins linking them to importin β to induce nuclear translocation. The polybasic region (PBR) of Rac1 contains a NLS sequence (K(K/R)X(K/R)) and a so-called canonical destruction box (D-box) (RXXL), which was shown to correlate with Rac1 ubiquitination and degradation by the 26S proteasome (Pop, M. et al., 2004). Rac2 and Rac3 lack the NLS motif and were not identified as interaction partners of KPNA2. Therefore, nuclear translocation of Rac1 by CNF1 could be affirmed by subcellular fractionation. Indeed, it could be shown that activated Rac1 enriched in the nucleus upon CNF1 activation. Furthermore, the construction of C-terminal chimeras between Rac1 and Rac2 unequivocally revealed that only the PBR with a functional NLS of Rac1 determines the translocation to the nucleus while Rac1-PBR2 was predominantly located in the cytosol. In this respect, the nuclear accumulation of deamidated Rac1 could be a prerequisite for its specific degradation by the 26S proteasome in the nucleus and/or the cytosol to terminate cytosolic functions. However, nuclear transport could also serve to promote certain nuclear functions of Rac1.

4.4 Interaction partners of nuclear Rac1

Rho proteins have been shown to localize in the cytosol, plasma membranes, the Golgi, multi-vesicular bodies and nuclei (Michaelson, D. *et al.*, 2001). Although Rac1 is thought to function mainly outside the nucleus, translocation to the nucleus might have several purposes. LC-MS/MS analysis served as method to identify interaction partners of activated Rac1Q61E in comparison to the double mutant T35A/Q61E from nuclear fractions. The double mutant was used as a negative control, which is capable to translocate to the nucleus via its deamidation, but incapable to bind to effectors. Several candidates were identified to interact with Rac1. One prominent protein band of about 190 kDa appeared in the lane of the precipitate from nuclear active Rac1, which was not visible in the lane of the activated effector mutant. The proteins were identified as IQGAPs which are actin-binding scaffold proteins and identified as effectors of Rho GTPases (Kuroda, S. *et al.*, 1996; Wang, S. *et al.*, 2007). Several laboratories have shown that the primary function of IQGAP proteins is to modulate cytoskeletal architecture (Fukata, M. *et al.*, 1997; Bashour, A. M. *et al.*, 1997). Most prominently, they co-localize with actin filaments in the cortical layer and the ruffling membrane. IQGAP1 has been shown to regulate cadherin- based cell adhesion downstream of Cdc42 and Rac1 (Fukata, M. *et al.*, 1999). Interestingly, nuclear accumulation has been observed for IQGAP2 (Yamashiro, S. *et al.*, 2003) but its function and possible regulation by Rac1 is completely unknown. IQGAPs have been shown to be required for actomyosin ring assembly and cytokinesis (Machesky, L. M., 1998). Since Rac1 has also been implicated in promoting cell division via cytosol-to-nucleus cycling (Michaelson, D. *et al.*, 2008) one might speculate a function of Rac1 with IQGAP2 in terms of cell division.

The list of identified proteins also contained KPNA2, ubiquitin and importin ß for both mutants. This further provides evidence for a model, where deamidated, ubiquitinated Rac1 translocates to the nucleus in complex with KPNA2 and importin ß. Rac1 could also serve as a transport cargo for certain proteins in the cytosol to immediately release them in the nucleus. Nuclear interaction partners that are in a complex of low stability might therefore not be detectable by MS/MS analysis. To mention some, it has been shown that small GTPases with a PBR can regulate the nuclear transport of SmgGDS, which is the only

known GEF containing similar structural elements as in KPNA2. The presence of a functional NLS in the PBR of Rac1 and a GTP-dependent signal has been shown to promote the nuclear entry of Rac1–SmgGDS complexes (Lanning, C. C. *et al.*, 2003). In fact, the structural similarities between SmgGDS and Karyopherin α proteins suggest that KPNA2 could interact with Rac1 in the same manner as Rac1 interacts with SmgGDS, thereby promoting nuclear translocation. Further evidence for a role of Rac1 in the nucleus arises from work with signal transducer and activator of transcription (STAT), e.g. STAT5 in association with MgcRacGAP (Kawashima, T. *et al.*, 2006). These transcription factors become phosphorylated upon cytokine stimulation and enter the nucleus to activate their target genes. It was shown that Rac1 and the GTPase-activating protein MgcRacGAP directly bind to p-STAT5A and that GTP-bound Rac1 and MgcRacGAP are required for the translocation of activated STAT to the nucleus, thus initiating transcriptional activity. Another candidate of a Rac1 effector in the nucleus is PAK1. PAK1 is well known to be involved in numerous functions such as cytoskeletal reorganization, motility and cell growth, but also in nuclear signaling pathways (Singh, R. R. *et al.*, 2005). Three functional NLS sequences were identified in the N-terminal region of PAK1 that are all important for its nuclear translocation. Nuclear PAK1 interacts with specific chromatin targets, thereby regulating gene transcription. This supports the hypothesis that the translocation of active Rac1 via KPNA2 is linked to nuclear functions prior degradation.

4.5 CNF1-deamidated RhoA is not degraded or differentially expressed

Similarly to Rac1, also the activation of RhoA in CNF1-treated cells was only transient as determined by RhoA-effector binding, while CNFY induced a much stronger and permanent RhoA signal. It has previously been reported by the group of Lemichez that the threshold of Rho GTPase activation by CNF1 is attenuated because of a concomitant decrease of their cellular protein levels (Boyer, L. *et al.*, 2006; Doye, A. *et al.*, 2002). Therefore, RhoA degradation similarly to Rac1 with subsequent new production of unmodified Rho protein could explain decrease of RhoA activity. However, this possibility was excluded by the fact that the content of RhoA remained constant and stayed stable in its deamidated form for over 24 h (Rho shift) as observed by immunoblotting. Moreover, the inactivation of RhoA by CNF1 was unaffected by the application of the proteasome inhibitor MG132 or protein synthesis inhibitor cycloheximide. Solely CNFY induced a slight decrease of RhoA levels, which was blocked by MG132, implicating degradation of RhoA. However, this mechanism seemed to have no, if only a marginal, impact on the strong RhoA-effector interaction induced by CNFY. Thus, by investigating the role of proteasomal degradation and protein expression the observed inactivation of RhoA promoted by CNF1 was independent of its turnover.

These results are most unexpected, since the model of proteasomal degradation is widely accepted as the most classical pathway by which signaling of active Rho GTPases is terminated. While this is true for CNF1-deamidated Rac1, it is exciting to speculate that inactivation of RhoA is caused by a complete different mechanism unknown so far.

4.6 CNF1-induced inactivation dominates over generally activated RhoA

Although CNF1 and CNFY catalyze the identical modification, the CNFY-induced activation of RhoA was much more pronounced, although deamidation proceeded less efficient in comparison to CNF1. The complete modification was achieved within 1 – 2 h after CNF1, while CNFY-intoxicated RhoA predominantly resided in its wild-type form, even after 4 h toxin incubation. Interestingly, the strong and long-lasting activation of RhoA induced by CNFY could be abrogated by addition of CNF1 to the cells. The same effect was observed in Dual-Luciferase® reporter assay with the Firefly luciferase coupled to Serum Response Element as a read-out system to measure RhoA downstream signaling. CNFY induced a stronger signal of Firefly luciferase expression in comparison to CNF1. Most prominently, when toxins were combined, the signal was limited to the level of CNF1 treatment alone. This result is supportive to the hypothesis that the CNF1-induced disruption of RhoA-signaling is dominant over CNFY. In contrast, RhoA activity was not affected by application of CNF1C866S. The substitution of cysteine 866 to a serine renders CNF1 catalytically inactive, while this mutant is still taken up into cells. Yet, this clarified that the deamidase activity of CNF1 is indispensable for the dominant inactivation of RhoA.

These results raised the question whether CNF1 is capable to inactivate each form of generally activated RhoA. To discriminate between different activated RhoA forms, active Rho mutants (RhoAQ63L, RhoAQ63E, RhoAG14V, RhoAwt) were recombinantly expressed in HEK293 cells. Interestingly, wild-type RhoA, RhoAG14V and RhoAQ63E appeared to be susceptible to the CNF1-promoted inactivation mechanism. Intriguingly, RhoAQ63L was not inactivated by CNF1 and remained active. It has been shown that RhoAQ63L exhibits a very strong interaction with certain effectors such as Rho kinase and Rhotekin (Zong, H. *et al.*, 1999). Thus, the data might indicate that CNF1 inhibits directly or indirectly the interaction of RhoAQ63E with Rhotekin (mDia, PKN, Rho kinase), however, is not able to block the strong interaction of RhoAQ63L with its effectors.

4.7 RhoA negative regulation is independent from Cdc42 or RhoGDI

In vivo, CNF1 and CNFY are distinguished by the extent and duration of RhoA activation. However, *in vitro* deamidation of RhoA leads to a permanent activation of the protein with the same signal intensity by both toxins (Hoffmann, C. *et al.*, 2007). This proves that it is not the deamidation *per se* which leads to inactivation of RhoA but rather the CNF1-effects of further signaling cascades present in intact cells that are not altered by CNFY.

4.7.1 Cdc42 is not involved in the CNF1-induced inactivation of RhoA

The most prominent difference between CNF1 and CNFY is their substrate specificity. As mentioned before, in contrast to CNFY, CNF1 also causes the activation of Rac1 and Cdc42. While CNF1-deamidated Rac1 is subjected to degradation, Cdc42 is permanently activated. Hoffmann, C. showed that the substrate specificity between CNF1 and CNFY depends on different loop regions in the substrate-binding pocket of the toxins. Interestingly, exchange of L8 from CNF1 by the respective region of CNFY, revealed an essential role of Cdc42 in regulating RhoA activity (CNF1L8). She could show that CNF1L8 was incapable to interact with Cdc42. At the same this was accompanied with an observable increase of RhoA activity. Thus, it was suggested that Cdc42 might be the key protein to cause a negative feedback loop on RhoA activity (Hoffmann, C. *et al.*, 2007). This presumption is supported by the fact that Rho proteins have been shown to cooperate or antagonize each other to control cellular functions (Burridge, K. and Doughman, R., 2006; Wang, G. and Beier, F., 2005; Burridge, K., 1999). These cross-regulations can be mediated via the proteins regulating the activation level of the Rho GTPases or through downstream signaling targets (Guilluy, C. *et al.*, 2011). However, the hypothesis of a CNF1-induced Cdc42 activation succeeding in RhoA inactivation was disproved in studies within this thesis. Although CNF1L8 caused a strong RhoA activation signal similar to CNFY, determined by effector interaction, deamidated RhoA was still subjected to inactivation in a time-dependent manner. Moreover, overexpression of constitutive active Cdc42 caused no fundamental difference on CNFY-activated RhoA as

compared to CNF1 co-treatment. Therefore, these experiments could rule out a possible role for Cdc42 in this mechanism.

4.7.2 RhoGDI is dispensable for the CNF1 effect

In the literature, various mechanisms regulating at different levels the networking between Rho GTPases have been described. This can be mediated via the proteins regulating the activation level of the Rho GTPases or through downstream signaling targets. Among these regulatory proteins, the Rho GDP-dissociation inhibitor (RhoGDI) has been reported to participate in this crosstalk. RhoGDIs function by extracting Rho family GTPases from membranes and solubilizing them in the cytosol. They inhibit nucleotide exchange and GTP hydrolyzing activities of Rho proteins by interacting with the switch regions and thereby restricting accessibility to GEFs and GAPs (DerMardirossian, C. and Bokoch, G. M., 2005). It was shown that C3-like ADP-ribosyltransferases (e.g. from *Clostridium botulinum*), which selectively modify RhoA (B and C), inhibits RhoA signaling by blockage of GEF-mediated nucleotide exchange and mainly by trapping the ADP-ribosylated RhoA in the inactive RhoA–RhoGDI complex (Vogelsgesang, M. *et al.*, 2007). Also modifications, such as phosphorylations e.g. at S188 of RhoA or S96 of RhoGDI mediate binding and inactivation of the GTPase (Dovas, A. and Couchman, J. R., 2005; DerMardirossian, C. and Bokoch, G. M., 2005). Therefore, it was suggested that RhoGDI might be involved in CNF1-induced inactivation of RhoA. Additionally, this hypothesis was encouraged by the fact that Rac1 and Cdc42, which also compete with RhoA for GDI-binding, are released from this complex after CNF1 activation. This, consequently, would lead to an increased RhoGDI pool, which is free to bind to RhoA. In fact, it could be shown here that basal Rho GTPase activity was clearly increased in RhoGDI knockout cells, strongly suggesting a role of RhoGDI in the CNF1-induced inactivation mechanism (Bielek, H. *et al.*, 2009). However, when investigating the course of RhoA binding to RhoGDI after the addition of CNF1 (and CNFY) to cells with increasing incubation times, it became evident that the interaction of RhoA with RhoGDI was unaffected by CNF1 and CNFY. The methods used comprised the determination of the RhoA amount bound to RhoGDI-coupled beads and precipitation of the endogenous

RhoA-RhoGDI complex. Moreover, it was also shown that the CNF1 effect was present in cells lacking RhoGDI. Therefore, these results implicate that RhoGDI is dispensable for the negative regulation of RhoA. In conclusion, all these findings suggest that classical pathways to negatively regulate Rho GTPase signaling including proteasomal degradation and RhoGDI entrapment play no favorable role in CNF1-induced RhoA inactivation.

4.8 The isoprenylation and membrane binding of RhoA is essential for the CNF1-promoted inactivation mechanism

It is known that Rho family GTPases undergo posttranslational isoprenylation at the C-terminus, which is considered to be essential for their downstream signaling (Samuel, F. and Hynds, D. L., 2010; Turner, S. J. *et al.*, 2008). This is signaled by the carboxyl-terminal CaaX motif, which promotes the isoprenylation of Rho proteins (farnesylation and/or geranylgeranylation). The hydrophobic feature enables the proteins to attach to different membranous compartments. At the plasma membrane Rho GTPases interact with membrane-bound GEFs, which catalyze the exchange from GDP to GTP. Upon the GTP-bound state they are capable to interact with downstream effectors to perform their various functions (Roberts, P. J. *et al.*, 2008; Turner, S. J. *et al.*, 2008). Therefore, this consequently links to the question whether the lipid modification plays an important role in the CNF1-induced inactivation of RhoA. To answer this question, general inhibitors of the cholesterol/isoprenoid biosynthetic pathway were used (e.g. lovastatin). Statins block 3-Hydroxy-3-Methylglutaryl Coenzyme A (HMG-CoA) reductase and thereby inhibit the biosynthesis pathway for both isoprenoids and cholesterol (Tobert, J. A., 2003). Thus, by preventing isoprene synthesis, statins interfere with Rho regulation, localization and signaling (Kusama, T. *et al.*, 2003). It was shown that lovastatin leads to disruption of the actin cytoskeleton and rounding of cells while CNF1 rescues this effect (Koch, G. *et al.*, 1997).

Remarkably, in lovastatin-pretreated CNF1-intoxciated cells RhoA was permanently activated. Most strikingly, it even diminished the difference of CNF1 and CNFY activation intensity of RhoA. The same was true for RhoAC190S, a mutant that lacks the CaaX Box

and is therefore not isoprenylated. This strongly suggests that carboxy-terminal isoprenylation is essential for the CNF1-induced RhoA inactivation. Therefore, importance of the prenyl-group most obviously must correlate with membrane attachment. Thus, membrane binding is a prerequisite for the negative regulatory mechanism was tested with RhoAS188E and RhoAS188A by interaction with the effector Rhotekin. The phosphomimetic mutant RhoAS188E has been shown to be cytosolic due to increased binding affinity to RhoGDI, while RhoAS188A is capable to bind to membranes (Rolli-Derkinderen, M. *et al.*, 2005). Interestingly, Rhotekin pull-down studies revealed that RhoAS188A was susceptible for CNF1 activation and inactivation, while the RhoAS188E could be activated by CNF1, but withstood the inactivation effect and showed constant activation. This concludes that both constructs are substrates of CNF1. However, RhoAS188E is not accessible for the CNF1 effect, possibly due to its cytosolic localization. Most excitingly, this result is in perfect agreement with the prevalent hypothesis that the molecular mechanism of inactivation only affects membrane-bound RhoA. Now the question is, what is the subsequent mechanism that occurs with membrane-bound, deamidated RhoA resulting in its inactivation?

4.9 CNF1 induces transient membrane binding of RhoA

The capacity of Rho GTPases to cycle on and off membranes is thought to be integral to their biological activity (Cox, A. D. and Der, C. J., 1992). Moreover, upon activation, Rho proteins have been shown to translocate from cytosol to membranes after receptor-mediated activation (Doye, A. *et al.*, 2006). When analyzing the amount of RhoA in the membrane fraction, it revealed that initially CNF1 as well as CNFY induce membrane recruitment of RhoA. This finding was not surprising since it is generally accepted that activated GTPases localize to cellular membranes (Symons, M. and Settleman, J., 2000). Interestingly, CNF1-deamidated RhoA was re-localized from the membrane to the cytosol in a time-dependent manner, whereas CNFY-activated RhoA remained membrane-bound. This matched perfectly with the activation and inactivation pattern of RhoA by CNF1 and CNFY seen in Rhotekin pull-downs. Moreover, toxin combination resulted in the CNF1-induced membrane release and confirmed the dominance of the inactivation mechanism, as observed by the activation pattern of RhoA. In fact, this is in line with recent data from our group (Hoffmann, C., 2006) where it was shown that CNFY leads to a redistribution of cellular RhoA from the cytosol to the membrane fraction whereas this was not observed with CNF1 at a fixed time-point.

It is also important to note that the effect of RhoA regulation was reproducible in nearly all cell lines tested (HEK293, HeLa, Swiss3T3, Caco-2, LNCaP, C4-2 and Vero cells). Only a few cell lines (e.g. MEFs) lacked this effect, where RhoA was permanently activated in Rhotekin pull-downs by CNF1 with no obvious difference to CNFY. Intriguingly, the CNF1-induced decrease of membrane-bound RhoA was only observed in cell lines that were responsive to the CNF1 effect. In contrast, MEF cells responded equally to CNF1 and CNFY. Here, both toxins induced permanent RhoA activation and membrane attachment. In conclusion, these data support the idea that initial membrane translocation is fundamental to further localized signaling mechanisms, which subsequently promote negative regulation of RhoA. Obviously, the subsequent disruption of RhoA-effector binding is accompanied by membrane detachment.

The correlation of Rho GTPase inactivation and membrane release has been described in the literature, where RhoA is sequestered in the cytosol e.g. bound to RhoGDI resulting in

the blockage of interaction with GAPs, GEFs and most importantly effectors (Dovas, A. and Couchman, J. R., 2005; Vogelsgesang, M. *et al.*, 2007; DerMardirossian, C. and Bokoch, G. M., 2005). However, the novel aspect in the mechanism observed in this thesis, is the fact that membrane release is completely independent of RhoGDI. Furthermore, membrane release alone would explain the blockage of localized effector interaction in intact cells. But blockage of effector interaction seen in bead-coupled pull-downs cannot be explained. Thus, one might ask if membrane release is the result of inactivation or vice versa. Nevertheless, these results have revealed new insights into the regulation of deamidated RhoA that might belong to a general new mechanism of cellular regulation.

4.10 Model of RhoA and Rac1 inactivation by CNF1

Collectively, the activation and inactivation mechanisms of Rac1 and RhoA after CNF1 deamidation were proposed in Figure 34: At first, the activation process occurs by CNF1-induced deamidation of glutamine 61/63 to glutamate and membrane recruitment of Rac1 and RhoA. Deamidation of this glutamine blocks the intrinsic and GAP-stimulated GTP hydrolysis. Therefore, both membrane-bound Rho GTPases constantly promote signal transduction to e.g. downstream effectors such as PAK1 (Rac1) and ROCK (RhoA), which consequently lead to the formation of lamellipodia and stress fibers, respectively. Secondly, the CNF1-induced subsequent inactivation mechanism of Rac1 and RhoA are achieved by different mechanisms. In terms of Rac1 (Figure 33A), the nuclear transport receptor KPNA2 (together with importin ß) binds to the NLS region of GTP-Rac1Q61E. The complex is transported through the nuclear pore complex. In the nucleus, active Rac1 interacts with e.g. IQGAP or others to regulate processes such as cell division. Other potential candidates are the transcription factors STAT3 and STAT5 or MgcRacGAP that may participate in this translocation process to perform transcriptional activity. Moreover, nuclear translocation of Rac1 potentially terminates its cytosolic functions. However, inactivation of Rac1 is finally achieved by ubiquitin-mediated proteasomal degradation in the nucleus and/or in the cytosol. In contrast to Rac1, deamidated RhoA is not degraded (Figure 33B). As a mandatory step of inactivation, modified RhoA is associated with the membrane. At the membrane RhoA is exposed to yet, undefined, modulation, which alters its biophysical properties resulting in its translocation to the cytosol. Cytosolic RhoA is still deamidated but localized effector interaction at the membrane is blocked. However, the precise mechanisms, which cause changes in the membrane-cytosol interactions of RhoA remain to be elucidated.

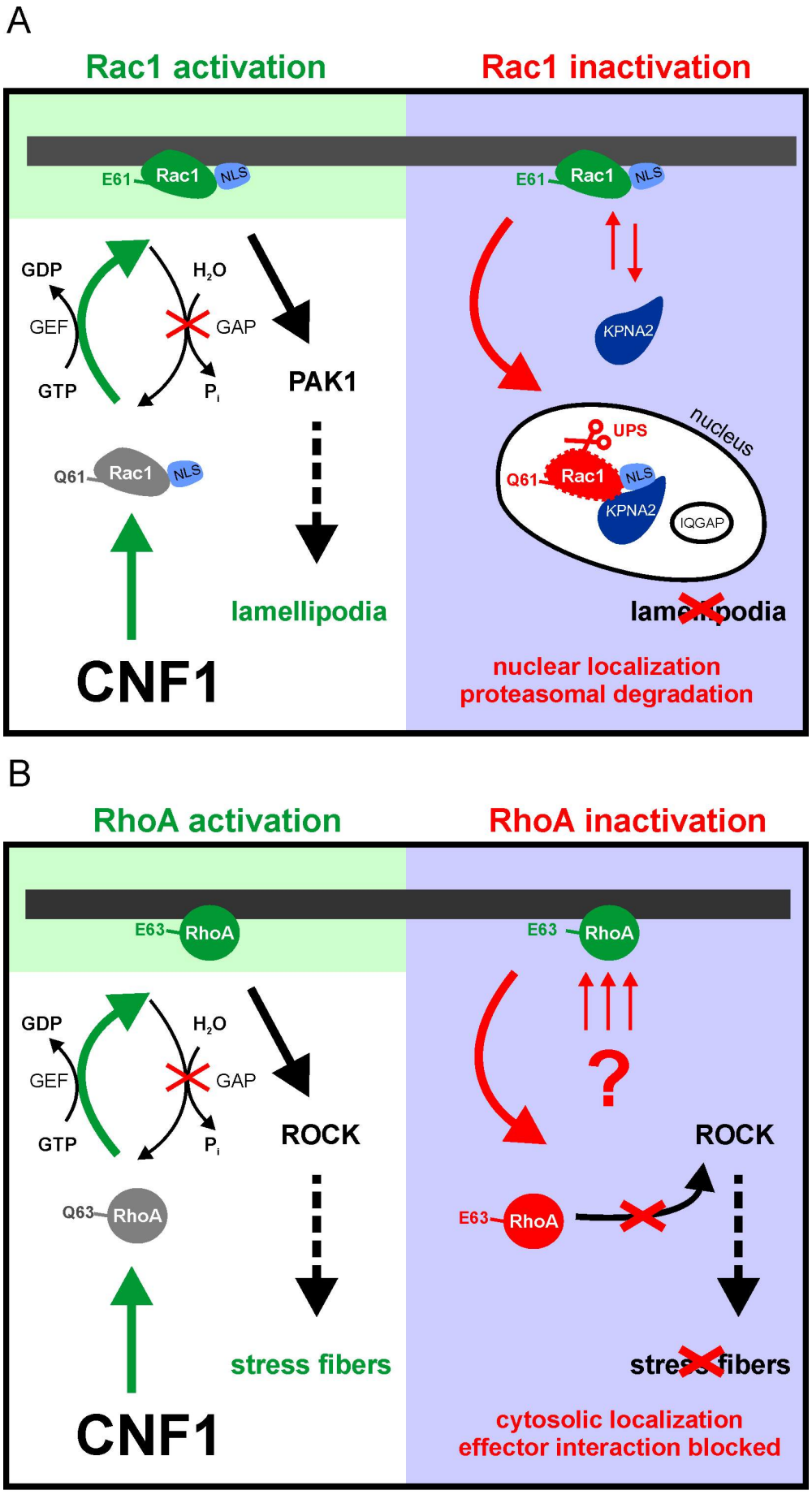

A
Rac1 activation
Rac1 inactivation
E61
Rac1
NLS
GDP
H2O
GEF
GAP
GTP
Pi
PAK1
Q61
KPNA2
nucleus
UPS
IQGAP
lamellipodia
CNF1
nuclear localization
proteasomal degradation
B
RhoA activation
RhoA inactivation
E63
RhoA
ROCK
Q63
?
stress fibers
cytosolic localization
effector interaction blocked

Figure 34: Model: CNF1-deamidated Rac1 and RhoA are inactivated by different mechanisms. After deamidation by CNF1, Rac1 (A) and RhoA (B) are translocated to the membrane where they interact with GEFs that promote GDP to GTP exchange. Since deamidation blocks the intrinsic and GAP-stimulated GTP hydrolysis, membrane-associated Rac1 and RhoA interact with their respective downstream effectors to promote lamellipodia and stress fiber formation. A] Membrane-bound Rac1 interacts with KPNA2 via its NLS. The complex is translocated to the nucleus to terminate its cytosolic but to promote nuclear functions. Subsequently, nuclear Rac1 is depleted by the UPS. B] Inactivation of RhoA is achieved by the decrease of membrane binding. C-terminal association to the membrane is a prerequisite for the subsequent signaling mechanisms, which cause RhoA translocation to the cytosol. The defined mechanism is yet unknown, but it is an obvious fact that the cytosolic accumulation correlates and possibly facilitates with the inhibition of RhoA signaling. Abbreviations: KPNA2, Karyopherin α2; NLS, nuclear localization sequence; UPS, ubiquitin proteasome system.

4.11 Physiological effects of CNFY and CNF1 in LNCaP cancer cells

Although RhoA, Rac1 and Cdc42 mainly regulate the actin cytoskeleton organization (Hall, A., 1998), it is known that these proteins also govern many other cellular processes such as cell cycle progression (Falzano, L. *et al.*, 2006), differentiation (Travaglione, S. *et al.*, 2005), cell-adhesion (Lacerda, H. M. *et al.*, 1997), transcription (Boyer, L. *et al.*, 2004), migration (Raftopoulou, M. and Hall, A., 2004) and apoptosis (Wang, G. and Beier, F., 2005). Especially in tumor cells, Rho GTPases contribute to different steps of cancer progression (Vega, F. M. and Ridley, A. J., 2008; Karlsson, R. *et al.*, 2009). Therefore, influence of Rho GTPase signaling renders CNFs as attractive putative “drugs” in different therapeutic purposes like prostate cancer. Recently, it has been shown that activation of RhoA is required for induction of apoptosis in phorbolester (PMA) treated prostate cancer cells LNCaP (Xiao, L. *et al.*, 2009). Moreover, it has been shown that Rho-dependent protein kinase (ROCK)-induced activation of myosin is involved in dissociation-mediated apoptosis of human embryonic stem cells (Ohgushi, M. *et al.*, 2010). Therefore, it was analyzed whether the activation of the RhoA-ROCK pathway is also required for blebbing and/or apoptosis induction of LNCaP cells. RhoA was stimulated by CNFY while the ROCK inhibitor Y-27632 and the myosin inhibitor Blebbistatin were used to determine the downstream pathway. Hallmarks of apoptosis were determined by apoptotic blebbing and poly (ADP-ribose) polymerase (PARP) cleavage. As expected, CNFY induced

morphological changes of the actin cytoskeleton that provoked an induction of apoptosis of LNCaP cells after 24 h. Interestingly, inhibition of ROCK as well as inhibition of myosin was sufficient to block CNFY-induced blebbing and PARP cleavage while RhoA activation by CNFY was unaffected. These data show that actomyosin activation is necessary for CNFY induced apoptosis of LNCaP cells. In fact, this is in agreement with other studies, where it was postulated that actin dynamics are crucial for apoptotic signaling (Gourlay, C. W. and Ayscough, K. R., 2005; Franklin-Tong, V. E. and Gourlay, C. W., 2008). For prostate cancer cells, Papadopoulou *et al.* described an early actin rearrangement as a central player for the late induction of apoptosis via Rho/ROCK signaling after membrane androgen receptor stimulation (Papadopoulou, N. *et al.*, 2008). Similarly, it was shown that sustained RhoA activation, followed by an activation of ROCK, cytoskeleton rearrangement, activation of JNK as well as up-regulation of the cell cycle inhibitor p21Cip1 resulted in apoptosis of the cells (Xiao, L. *et al.*, 2009).

CNF1 producing uropathogenic *E. coli* are mainly associated with urinary tract infections (UTIs). In the 5637 bladder cell line it was shown that CNF1 is able to cause apoptosis (Mills, M. *et al.*, 2000), while infection of CNF1-positive *E. coli* caused inflammation and tissue damage in rat prostates (Rippere-Lampe, K. E. *et al.*, 2001). In this thesis it could be shown that CNF1-induced inactivation of RhoA was present in LNCaP cells, as analyzed by Rhotekin pull-down experiments. Thus, the question rose, whether CNF1 is also capable to block CNFY-induced apoptosis in LNCaP cells. Interestingly, the CNF1 dominating effect over CNFY-deamidated RhoA was present in these cells. Moreover, even though both toxins initially activated RhoA, CNF1 inhibited the CNFY-promoted apoptosis presumably by inactivating RhoA. These findings are supportive to data from List (List, J. H., 2010). The pro-survival effects of CNF1 have already been reported from studies with HEp-2 epidermoid cancer cells, where CNF1 led to an up-regulation of the anti-apoptotic proteins Bcl-2 and Bcl-xl to promote cell survival (Fiorentini, C. *et al.*, 1998).

In view of all these studies, CNFY may be considered as a candidate for the treatment of advanced prostate cancer while CNF1 inhibits this effect. The bacterial toxins, *Pseudomonas* Exotoxin A from *Pseudomonas aeruginos*a and *Diphtheria* toxin from *Corynebacterium diphtheriae*, are prominent examples for the construction of immune-toxins, where the cytotoxic domains of the toxins were coupled to tumor-specific

antibodies for the targeted treatment of different cancers (Potala, S. *et al.*, 2008; Wolf, P. and Elsasser-Beile, U., 2009). The use of CNFY-based immunotoxins directed against androgen-dependent prostate tumor cells could therefore represent a future alternative for a hormone deprivation therapy without selective pressure leading to hormone-independent cancer. CNF1, on the other hand, could rather be used in cancer cells that contain over-activated RhoA and Rac1, such as testicular, gastric and breast cancer (Parri, M. and Chiarugi, P., 2010).

5 OUTLOOK

The results obtained in this thesis reveal deeper insights into effects induced by CNF1 towards Rac1 and RhoA. Further studies are required to clarify more detailed questions that concern the nuclear functions of Rac1 prior degradation. Especially the interaction and function of nuclear Rac1 effectors such as the detected IQGAPs but also other possible candidates such as STATs and PAK1 should be determined. Further, the aspect of degradation needs to be clarified in more detail concerning the subcellular localization of Rac1 targeted to the 26S proteasome. Here, it would be interesting to know if deamidated Rac1 is ubiquitinated in the nucleus or the cytosol.

In terms of RhoA, the defined molecular mechanism that underlies the translocation of RhoA to the cytosol needs to be clarified. Ongoing work in our group aims at identifying possible modifications of RhoA that are responsible for the blockage of effector binding e.g. by LC-MS/MS or by stable isotope labeling by amino acids in cell culture (SILAC). Another aspect to determine is whether CNF1 itself is a probable candidate to cause a second reaction on RhoA, e.g. C-terminal proteasomal cleavage similar to *Yersinia* outer protein T (YopT) (Schmidt, G., 2011). It would be quite feasible to imagine that CNF1 could also act as a protease. In fact, the catalytic center of the cysteine protease YopT contains the same Cys-His dyad as CNF1. It would be highly interesting to identify a putative aspartate for the classical CHD triade in proteases by mutational analysis. The CNF1C866S mutant was shown to be functionally dead to activate and/or inactivate RhoA. Therefore, one could imagine that CNF1 contains a catalytical center with two functions. Capotosti *et al.* reported about a glucosyltransferase (O-linked ß-N-acetylglucosamine transferase, OGT) with two enzymatic activities: O-GlcNAcylation and proteolytic cleavage of its substrate, the human epigenetic cell-cycle regulator HCF-1 (Capotosti, F. *et al.*, 2011). The catalytical triade of CNF1 consist of the residues Cys 866, His 881 and a stabilizing Val 833 (Schmidt, G. *et al.*, 1998). It should be tested whether a classical CHD triade with an aspartate as the third member exists in CNF1 (Buetow, L. *et al.*, 2001).

It is also possible that a second modification at the site of effector interaction rather than the C-terminus could cause the inactivation of RhoA. However as mentioned before, in cell lysate, CNF1-deamidated RhoA is not subjected to the negative regulation as seen in

intact cells. This shows that intact cells are required for the process of inactivation and makes the identification of a second modification more difficult. To over-come this problem, RhoA must precipitated from CNF1-treated cells with GDI coupled-beads since the deamidated, inactivated form also binds to GDI and should therefore also contain the putative secondary modification. Negative interference with Rho signaling by direct modifications such as glycosylation, ribosylation and adenylylation is quite well described for other bacterial toxins (Aktories, K., 2011). The family of large clostridial glucosylating cytotoxins (CGTs), e.g. toxin A/B from *Clostridium difficile*, modifies Rho GTPases by glycosylation of a crucial threonine residue (Thr37 in RhoA) to block binding to regulators of the GTPase cycle: GEFs, GDIs, GAPs but most importantly Rho effectors (Aktories, K. and Just, I., 2005). C3 from *Clostridium botulinum* enhances RhoA binding affinity to RhoGDI-like proteins promoted by ADP-ribosylation (Aktories, K. *et al.*, 1990). *Vibrio parahaemolyticus* effector VopS induces adenylylation by attachment of an AMP moiety derived from ATP to Thr37 in RhoA to cause functional inactivation similar to the CGTs (Yarbrough, M. L. *et al.*, 2009). Therefore, it is quite feasible that a second endogenous modification causes the inactivation of deamidated RhoA and should therefore be the focus for future studies.

6 SUMMARY

The Cytotoxic Necrotizing Factor family (CNF1, 2, 3, Y) modifies small GTPases of the Rho family by deamidation of a crucial glutamine (Gln63 in RhoA, Gln61 in Rac1/Cdc42), which leads to the constitutive activation of Rho proteins. However, the initial activation of Rac1 and RhoA by CNF1 is followed by inactivation mechanisms. It could be shown that CNF1-deamidated and constitutively activated Rac1 interacts with KPNA2 via its C-terminal NLS and is subsequently translocated to the nucleus. There, Rac1 interacts probably with various nuclear effectors such as IQGAPs. It was shown that the inactivation of Rac1 is achieved by Rac1 depletion by the 26S ubiquitin-proteasome-system. In contrast, RhoA inactivation is independent of degradation or protein turnover. While CNFY induces the persistent activation of RhoA, CNF1 promotes further signaling mechanisms that cause a robust and dominant effect over RhoA wild-type or CNFY pre-activated RhoA, RhoAQ63E and RhoAG14V constitutive active mutants. In contrast, it was observed that RhoAQ63L was not susceptible to this effect, which might be based on the high affinity of this mutant to its effectors. The dominance of the CNF1 action is not achieved by receptor-mediated signaling during uptake of the toxin, Cdc42 crosstalk or enhanced interaction of RhoA with RhoGDI. However, it was found that membrane interaction of RhoA is essential for the regulatory effect of CNF1.

CNF1- initially active or CNFY- deamidated RhoA is recruited to the plasma membrane where effector binding must occur. It could be shown that this membrane association is a prerequisite for the following process of inactivation by CNF1. Therefore, negative regulation of RhoA must proceed at the plasma membrane to cause translocation to the cytosol and blockage of Rho downstream signaling. This hypothesis was supported by studies with RhoAS188E, which was susceptible for activation but not inactivation of CNF1 probably due to its cytosolic localization, while the membrane binding RhoAS188A could be inactivated. Furthermore, the C-terminal lipid anchor plays an important role in CNF1-induced inactivation, because lack of the isoprenyl group by the action of an HMG-CoA-reductase inhibitor (lovastatin) or the RhoAC190S mutant blocks RhoA inactivation. Membrane release of RhoA is observed in HEK293 and LNCaP cell lines that are responsive to the CNF1 effect. In contrast, MEF cells are not responsive to this effect and

both toxins induce permanent RhoA activation and membrane binding with equal signal intensity. Therefore, the isoprenylated C-terminus and membrane distribution are found to be key determinants to regulate the CNF1-induced RhoA inactivation, which also accounts for the different cell line responsiveness to this effect. Studies analyzing the biological effect of CNF1 and CNFY in RhoA-dependent apoptotic LNCaP cells revealed that CNFY-induced apoptosis occurred via the RhoA-ROCK pathway. In contrast, it could be shown that CNF1 inhibited the CNFY effect and rescued LNCaPs from apoptosis.

All together, the findings show that beside the well-known activating effect of CNF1, this toxin is capable of inactivation of Rho GTPases either by indirectly-inducing degradation (Rac1) or by a membrane-dependent mechanism (RhoA).

7 REFERENCE LIST

1. **Aepfelbacher, M., R. Zumbihl, and J. Heesemann**. 2005. Modulation of Rho GTPases and the actin cytoskeleton by YopT of Yersinia. Curr.Top.Microbiol.Immunol. **291**:167-175.

2. **Aili, M., E. L. Isaksson, B. Hallberg, H. Wolf-Watz, and R. Rosqvist**. 2006. Functional analysis of the YopE GTPase-activating protein (GAP) activity of Yersinia pseudotuberculosis. Cell Microbiol. **8**:1020-1033.

3. **Aktories, K.** 2011. Bacterial protein toxins that modify host regulatory GTPases. Nat.Rev.Microbiol. **9**:487-498.

4. **Aktories, K., U. Braun, B. Habermann, and S. Rösener**. 1990. Botulinum ADP-ribosyltransferase C3, p. 97-115. *In*: J. Moss and M. Vaughan (eds.), ADP-ribosylating Toxins and G Proteins. American Society for Microbiology, Washington.

5. **Aktories, K. and I. Just**. 2005. Clostridial Rho-inhibiting protein toxins. Curr.Top.Microbiol.Immunol. **291**:113-145.

6. **Aktories, K., A. E. Lang, C. Schwan, and H. G. Mannherz**. 2011. Actin as target for modification by bacterial protein toxins. FEBS J.

7. **Aktories, K., C. Wilde, and M. Vogelsgesang**. 2004. Rho-modifying C3-like ADP-ribosyltransferases. Rev.Physiol Biochem.Pharmacol. **152**:1-22.

8. **Alberts, A. S., H. Qin, H. S. Carr, and J. A. Frost**. 2005. PAK1 negatively regulates the activity of the Rho exchange factor NET1. J.Biol.Chem. **280**:12152-12161.

9. **Andor, A., M. Essler, A. Roggenkamp, J. Heesemann, and M. Aepfelbacher**. 2001. YopE of Yersinia, a GAP for Rho-GTPases, selectively modulates Rac-dependent actin structures in endothelial cells. Cell Microbiol. **3**:301-310.

10. **Bashour, A. M., A. T. Fullerton, M. J. Hart, and G. S. Bloom**. 1997. IQGAP1, a Rac- and Cdc42-binding protein, directly binds and cross-links microfilaments. J.Cell Biol. **137**:1555-1566.

11. **Bielek, H., A. Anselmo, and C. DerMardirossian**. 2009. Morphological and proliferative abnormalities in renal mesangial cells lacking RhoGDI. Cell Signal. **21**:1974-1983.

12. **Boquet, P.** 2001. The cytotoxic necrotizing factor 1 (CNF1) from *Escherichia coli*. Toxicon **39**:1673-1680.

13. **Bourmeyster, N. and P. V. Vignais**. 1996. Phosphorylation of Rho GDI stabilizes the Rho A-Rho GDI complex in neutrophil cytosol. Biochem.Biophys.Res.Commun. **218**:54-60.

14. **Boyer, L., S. Travaglione, L. Falzano, N. C. Gauthier, M. R. Popoff, E. Lemichez, C. Fiorentini, and A. Fabbri**. 2004. Rac GTPase instructs nuclear factor-kappaB activation by conveying the SCF complex and IkBalpha to the ruffling membranes. Mol.Biol.Cell **15**:1124-1133.

15. **Boyer, L., L. Turchi, B. Desnues, A. Doye, G. Ponzio, J. L. Mege, M. Yamashita, Y. E. Zhang, J. Bertoglio, G. Flatau, P. Boquet, and E. Lemichez**. 2006. CNF1-induced ubiquitylation and proteasome destruction of activated RhoA is impaired in Smurf1-/- cells. Mol.Biol.Cell **17**:2489-2497.

16. **Buetow, L., G. Flatau, K. Chiu, P. Boquet, and P. Ghosh**. 2001. Structure of the Rho-activating domain of *Escherichia coli* cytotoxic necrotizing factor 1. Nature Struct.Biol. **8**:584-588.

17. **Burridge, K.** 1999. Crosstalk between Rac and Rho. Science **283**:2028-2029.

18. **Burridge, K. and R. Doughman**. 2006. Front and back by Rho and Rac. Nat.Cell Biol. **8**:781-782.

19. **Bustelo, X. R., V. Sauzeau, and I. M. Berenjeno**. 2007. GTP-binding proteins of the Rho/Rac family: regulation, effectors and functions in vivo. Bioessays **29**:356-370.

20. **Capotosti, F., S. Guernier, F. Lammers, P. Waridel, Y. Cai, J. Jin, J. W. Conaway, R. C. Conaway, and W. Herr**. 2011. O-GlcNAc transferase catalyzes site-specific proteolysis of HCF-1. Cell **144**:376-388.

21. **Caprioli, A., V. Falbo, L. G. Roda, F. M. Ruggeri, and C. Zona**. 1983. Partial purification and characterization of an *escherichia coli* toxic factor that induces morphological cell alterations. Infect.Immun. **39**:1300-1306.

22. **Chook, Y. M. and G. Blobel**. 2001. Karyopherins and nuclear import. Curr.Opin.Struct.Biol. **11**:703-715.

23. **Chung, J. W., S. J. Hong, K. J. Kim, D. Goti, M. F. Stins, S. Shin, V. L. Dawson, T. M. Dawson, and K. S. Kim**. 2003. 37 kDa laminin receptor precusor modulates cytotoxic necrotizing factor 1-mediated RhoA activation and bacterial uptake. J.Biol.Chem. **278**:16857-16862.

24. **Contamin, S., A. Galmiche, A. Doye, G. Flatau, A. Benmerah, and P. Boquet**. 2000. The p21 Rho-activating toxin cytotoxic necrotizing factor 1 is endocytosed by a clathrin-independent mechanism and enters the cytosol by an acidic-dependent membrane translocation step. Mol.Biol.Cell **11**:1775-1787.

25. **Cox, A. D. and C. J. Der**. 1992. Protein prenylation: more than just glue? Curr.Opin.Cell Biol. **4**:1008-1016.

26. **Craiu, A., M. Gaczynska, T. Akopian, C. F. Gramm, G. Fenteany, A. L. Goldberg, and K. L. Rock**. 1997. Lactacystin and clasto-lactacystin beta-lactone modify multiple proteasome beta-subunits and inhibit intracellular protein degradation and major histocompatibility complex class I antigen presentation. J.Biol.Chem. **272**:13437-13445.

27. **Denko, N., R. Langland, M. Barton, and M. A. Lieberman**. 1997. Uncoupling of S-phase and mitosis by recombinant cytotoxic necrotizing factor 2 (CNF2). Exp.Cell Res. **234**:132-138.

28. **DerMardirossian, C. and G. M. Bokoch**. 2005. GDIs: central regulatory molecules in Rho GTPase activation. Trends Cell Biol. **15**:356-363.

29. **DerMardirossian, C., A. Schnelzer, and G. Bokoch**. 2004. Phosphorylation of RhoGDI by PAK1 mediates dissociation of Rac GTPase. Mol.Cell **15**:117-127.

30. **Dominguez, R. and K. C. Holmes**. 2011. Actin structure and function. Annu.Rev.Biophys. **40**:169-186.

31. **Dovas, A., Y. Choi, A. Yoneda, H. A. Multhaupt, S. H. Kwon, D. Kang, E. S. Oh, and J. R. Couchman**. 2010. Serine 34 phosphorylation of rho guanine dissociation inhibitor (RhoGDIalpha) links signaling from conventional protein kinase C to RhoGTPase in cell adhesion. J.Biol.Chem. **285**:23296-23308.

32. **Dovas, A. and J. R. Couchman**. 2005. RhoGDI: multiple functions in the regulation of Rho family GTPase activities. Biochem.J. **390**:1-9.

33. **Downward, J.** 2003. Targeting RAS signalling pathways in cancer therapy. Nat.Rev.Cancer **3**:11-22.

34. **Doye, A., L. Boyer, A. Mettouchi, and E. Lemichez**. 2006. Ubiquitin-mediated proteasomal degradation of Rho proteins by the CNF1 toxin. Methods Enzymol. **406**:447-456.

35. **Doye, A., A. Mettouchi, G. Bossis, R. Clément, C. Buisson-Touati, G. Flatau, L. Gagnoux, M. Piechaczyk, P. Boquet, and E. Lemichez**. 2002. CNF1 exploits the ubiquitin-proteasome machinery to restrict Rho GTPase activation for bacterial host cell invasion. Cell **111**:553-564.

36. **Ellenbroek, S. I. and J. G. Collard**. 2007. Rho GTPases: functions and association with cancer. Clin.Exp.Metastasis **24**:657-672.

37. **Falzano, L., P. Filippini, S. Travaglione, A. G. Miraglia, A. Fabbri, and C. Fiorentini**. 2006. Escherichia coli cytotoxic necrotizing factor 1 blocks cell cycle G2/M transition in uroepithelial cells. Infect.Immun. **74**:3765-3772.

38. **Fiorentini, C., A. Fabbri, G. Flatau, G. Donelli, P. Matarrese, E. Lemichez, L. Falzano, and P. Boquet**. 1997. *Escherichia coli* cytotoxic necrotizing factor 1 (CNF1), a toxin that activates the Rho GTPase. J.Biol.Chem. **272**:19532-19537.

39. **Fiorentini, C., P. Matarrese, E. Straface, L. Falzano, G. Donelli, P. Boquet, and W. Malorni**. 1998. Rho-dependent cell spreading activated by E. coli cytotoxic necrotizing factor 1 hinders apoptosis in epithelial cells. Cell Death & Differentiation **5**:921-929.

40. **Flatau, G., E. Lemichez, M. Gauthier, P. Chardin, S. Paris, C. Fiorentini, and P. Boquet**. 1997. Toxin-induced activation of the G protein p21 Rho by deamidation of glutamine. Nature **387**:729-733.

41. **Franklin-Tong, V. E. and C. W. Gourlay**. 2008. A role for actin in regulating apoptosis/programmed cell death: evidence spanning yeast, plants and animals. Biochem.J. **413**:389-404.

42. **Friebel, A. and W. D. Hardt**. 2000. Purification and biochemical activity of Salmonella exchange factor SopE. Methods Enzymol. **325**:82-91.

43. **Fueller, F. and G. Schmidt**. 2008. The polybasic region of Rho GTPases defines the cleavage by Yersinia enterocolitica outer protein T (YopT). Protein Sci. **17**:1456-1462.

44. **Fukata, M., S. Kuroda, K. Fuji, T. Nakamura, I. Shoji, Y. Matsuura, K. Okawa, A. Iwamatsu, A. Kikuchi, and K. Kaibuchi**. 1997. Regulation of cross-linking of actin filament by IQGAP1, a target for Cdc42. J.Biol.Chem. **272**:29579-29583.

45. **Fukata, M., S. Kuroda, M. Nakagawa, A. Kawajiri, N. Itoh, I. Shoji, Y. Matsuura, S. Yonehara, H. Fujisawa, A. Kikuchi, and K. Kaibuchi**. 1999. Cdc42 and Rac1 regulate the interaction of IQGAP1 with beta-catenin. J.Biol.Chem. **274**:26044-26050.

46. **Genth, H., R. Gerhard, A. Maeda, M. Amano, K. Kaibuchi, K. Aktories, and I. Just**. 2003. Entrapment of Rho ADP-ribosylated by Clostridium botulinum C3 exoenzyme in the Rho-guanine nucleotide dissociation inhibitor-1 complex. J.Biol.Chem. **278**:28523-28527.

47. **Gourlay, C. W. and K. R. Ayscough**. 2005. A role for actin in aging and apoptosis. Biochem.Soc.Trans. **33**:1260-1264.

48. **Guilluy, C., R. Garcia-Mata, and K. Burridge**. 2011. Rho protein crosstalk: another social network? Trends Cell Biol.

49. **Hall, A.** 1998. Rho GTPases and the actin cytoskeleton. Science **279**:509-514.

50. **Han, Y. H., H. J. Moon, B. R. You, and W. H. Park**. 2009. The effect of MG132, a proteasome inhibitor on HeLa cells in relation to cell growth, reactive oxygen species and GSH. Oncol.Rep. **22**:215-221.

51. **Heasman, S. J. and A. J. Ridley**. 2008. Mammalian Rho GTPases: new insights into their functions from in vivo studies. Nat.Rev.Mol.Cell Biol. **9**:690-701.

52. **Hoffmann, C.** (2006). The Cytotoxic Necrotizing Factor CNFy of *Yersinia pseudotuberculosis*. (Dissertation).

53. **Hoffmann, C., K. Aktories, and G. Schmidt**. 2007. Change in substrate specificity of Cytotoxic Necrotizing Factor (CNF) unmasks proteasome-independent down-regulation of constitutively active RhoA. J.Biol.Chem. **282**:10826-10832.

54. **Hoffmann, C., M. Pop, J. Leemhuis, J. Schirmer, K. Aktories, and G. Schmidt**. 2004. The Yersinia pseudotuberculosis cytotoxic necrotizing factor (CNFY) selectively activates RhoA. J.Biol.Chem. **279**:16026-16032.

55. **Hoffmann, C. and G. Schmidt**. 2004. CNF and DNT. Rev.Physiol.Biochem.Pharmacol. **152**:49-63.

56. **Horoszewicz, J. S., S. S. Leong, E. Kawinski, J. P. Karr, H. Rosenthal, T. M. Chu, E. A. Mirand, and G. P. Murphy**. 1983. LNCaP model of human prostatic carcinoma. Cancer Res. **43**:1809-1818.

57. **Ihara, K., S. Muraguchi, M. Kato, T. Shimizu, M. Shirakawa, S. Kuroda, K. Kaibuchi, and T. Hakoshima**. 1998. Crystal structure of human RhoA in a dominantly active form complexed with a GTP analogue. J.Biol.Chem. **273**:9656-9666.

58. **Insall, R. H. and L. M. Machesky**. 2009. Actin dynamics at the leading edge: from simple machinery to complex networks. Dev.Cell **17**:310-322.

59. **Karlsson, R., E. D. Pedersen, Z. Wang, and C. Brakebusch**. 2009. Rho GTPase function in tumorigenesis. Biochim.Biophys.Acta.

60. **Kawashima, T., Y. C. Bao, Y. Nomura, Y. Moon, Y. Tonozuka, Y. Minoshima, T. Hatori, A. Tsuchiya, M. Kiyono, T. Nosaka, H. Nakajima, D. A. Williams, and T. Kitamura**. 2006. Rac1 and a GTPase-activating protein, MgcRacGAP, are required for nuclear translocation of STAT transcription factors. J.Cell Biol. **175**:937-946.

61. **Koch, G., C. Benz, G. Schmidt, C. Olenik, and K. Aktories**. 1997. Role of rho protein in lovastatin-induced breakdown of actin cytoskeleton. J.Pharmacol.Exp.Ther. **283**:901-909.

62. **Krugmann, S., I. Jordens, K. Gevaert, M. Driessens, J. Vandekerckhove, and A. Hall**. 2001. Cdc42 induces filopodia by promoting the formation of an IRSp53:Mena complex. Curr.Biol. **11**:1645-1655.

63. **Kuroda, S., M. Fukata, K. Kobayashi, M. Nakafuku, N. Nomura, A. Iwamatsu, and K. Kaibuchi**. 1996. Identification of IQGAP as a putative target for the small GTPases, Cdc42 and Rac1. J.Biol.Chem. **271**:23363-23367.

64. **Kusama, T., M. Mukai, M. Ayaki, F. Imamura, M. Tatsuta, Y. Matsumoto, H. Nakamura, and M. Inoue**. 2003. Inhibition of lysophosphatidic acid-induced RhoA activation and tumor cell invasion by 3-hydroxy-3-methylglutaryl-coenzyme A reductase inhibitors. Int.J.Oncol. **23**:1173-1178.

65. **Lacerda, H. M., G. D. Pullinger, A. J. Lax, and E. Rozengurt**. 1997. Cytotoxic necrotizing factor 1 from *Escherichia coli* and dermonecrotic toxin from *Bordetella bronchiseptica* induce $p21^{rho}$-dependent tyrosine phosphorylation of focal adhesion kinase and paxillin in swiss 3T3 cells. J.Biol.Chem. **272**:9587-9596.

66. **Lang, A. E., G. Schmidt, A. Schlosser, T. D. Hey, I. M. Larrinua, J. J. Sheets, H.-G. Mannherz, and K. Aktories**. 2010. *Photorhabdus luminescens* toxins ADP-ribosylate actin and RhoA to force actin clustering. Science **327**:1139-1142.

67. **Lange, A., R. E. Mills, C. J. Lange, M. Stewart, S. E. Devine, and A. H. Corbett**. 2007. Classical nuclear localization signals: definition, function, and interaction with importin alpha. J.Biol.Chem. **282**:5101-5105.

68. **Lanning, C. C., J. L. Daddona, R. Ruiz-Velasco, S. H. Shafer, and C. L. Williams**. 2004. The Rac1 C-terminal polybasic region regulates the nuclear localization and protein degradation of Rac1. J.Biol.Chem. **279**:44197-44210.

69. **Lanning, C. C., R. Ruiz-Velasco, and C. L. Williams**. 2003. Novel mechanism of the co-regulation of nuclear transport of SmgGDS and Rac1. J.Biol.Chem. **278**:12495-12506.

70. **Lappalainen, P. and D. G. Drubin**. 1997. Cofilin promotes rapid actin filament turnover *in vivo*. Nature **388**:78-82.

71. **Lerm, M., M. Pop, G. Fritz, K. Aktories, and G. Schmidt**. 2002. Proteasomal degradation of cytotoxic necrotizing factor 1-activated Rac. Infect.Immun. **70**:4053-4058.

72. **List, J. H.** (2010). Einfluss Rho-aktivierender Toxine auf Prostatakarzinom-Zelllinien. (Dissertation).

73. **Lockman, H. A., R. A. Gillespie, B. D. Baker, and E. Shakhnovich**. 2002. *Yersinia pseudotuberculosis* produces a cytotoxic necrotizing factor. Infect.Immun. **70**:2708-2714.

74. **Machesky, L. M.** 1998. Cytokinesis: IQGAPs find a function. Curr.Biol. **8**:R202-R205.

75. **Matozaki, T., H. Nakanishi, and Y. Takai**. 2000. Small G-protein networks their crosstalk and signal cascades. Cell.Signalling **12**:515-524.

76. **Maupin-Furlow, J.** 2012. Proteasomes and protein conjugation across domains of life. Nat.Rev.Microbiol. **10**:100-111.

77. **Mazur, A. J., D. Gremm, T. Dansranjavin, M. Litwin, B. M. Jockusch, A. Wegner, A. G. Weeds, and H. G. Mannherz**. 2010. Modulation of actin filament dynamics by actin-binding proteins residing in lamellipodia. Eur.J.Cell Biol. **89**:402-413.

78. **Michaelson, D., W. Abidi, D. Guardavaccaro, M. Zhou, I. Ahearn, M. Pagano, and M. R. Philips**. 2008. Rac1 accumulates in the nucleus during the G2 phase of the cell cycle and promotes cell division. J.Cell Biol. **181**:485-496.

79. **Michaelson, D., J. Silletti, G. Murphy, P. D'Eustachio, M. Rush, and M. R. Philips**. 2001. Differential localization of Rho GTPases in live cells: Regulation by hypervariable regions and RhoGDI binding. J.Cell Biol. **152**:111-126.

80. **Millard, T. H., S. J. Sharp, and L. M. Machesky**. 2004. Signalling to actin assembly via the WASP (Wiskott-Aldrich syndrome protein)-family proteins and the Arp2/3 complex. Biochem.J. **380**:1-17.

81. **Mills, M., K. C. Meysick, and A. D. O'Brien**. 2000. Cytotoxic necrotizing factor type 1 of uropathogenic *Escherichia coli* kills cultured human uroepithelial 5637 cells by an apoptotic mechanism. Infect.Immun. **68**:5869-5880.

82. **Ohgushi, M., M. Matsumura, M. Eiraku, K. Murakami, T. Aramaki, A. Nishiyama, K. Muguruma, T. Nakano, H. Suga, M. Ueno, T. Ishizaki, H. Suemori, S. Narumiya, H. Niwa, and Y. Sasai**. 2010. Molecular pathway and cell state responsible for dissociation-induced apoptosis in human pluripotent stem cells. Cell Stem Cell **7**:225-239.

83. **Orden, J. A., G. Dominguez-Bernal, S. Martinez-Pulgarin, M. Blanco, J. E. Blanco, A. Mora, J. Blanco, J. Blanco, and F. R. de la**. 2007. Necrotoxigenic Escherichia coli from sheep and goats produce a new type of cytotoxic necrotizing factor (CNF3) associated with the eae and ehxA genes. Int.Microbiol. **10**:47-55.

84. **Orlando, K. A., N. L. Stone, and R. N. Pittman**. 2006. Rho kinase regulates fragmentation and phagocytosis of apoptotic cells. Exp.Cell Res. **312**:5-15.

85. **Oswald, E. and J. de Rycke**. 1990. A single protein of 110 kDa is associated with the multinucleating and necrotizing activity coded by the Vir plasmid of *Escherichia coli*. FEMS Microbiol.Lett. **68**:279-284.

86. **Oswald, E., M. Sugai, A. Labigne, H. C. Wu, C. Fiorentini, P. Boquet, and A. D. O'Brien**. 1994. Cytotoxic necrotizing factor type 2 produced by virulent Escherichia coli modifies the small GTP-binding proteins Rho involved in assembly of actin stress fibers. Proc.Natl.Acad.Sci.U.S.A **91**:3814-3818.

87. **Papadopoulou, N., I. Charalampopoulos, K. Alevizopoulos, A. Gravanis, and C. Stournaras**. 2008. Rho/ROCK/actin signaling regulates membrane androgen receptor induced apoptosis in prostate cancer cells. Exp.Cell Res. **314**:3162-3174.

88. **Parri, M. and P. Chiarugi**. 2010. Rac and Rho GTPases in cancer cell motility control. Cell Commun.Signal. **8**:23.

89. **Pickart, C. M.** 1997. Targeting of substrates to the 26S proteasome. FASEB J. **11**:1055-1066.

90. **Pop, M., K. Aktories, and G. Schmidt**. 2004. Isotype-specific degradation of Rac activated by the cytotoxic necrotizing factor 1 (CNF1). J.Biol.Chem. **279**:35840-35848.

91. **Potala, S., S. K. Sahoo, and R. S. Verma**. 2008. Targeted therapy of cancer using diphtheria toxin-derived immunotoxins. Drug Discov.Today **13**:807-815.

92. **Raftopoulou, M. and A. Hall**. 2004. Cell migration: Rho GTPases lead the way. Dev.Biol. **265**:23-32.

93. **Ridley, A. J.** 2006. Rho GTPases and actin dynamics in membrane protrusions and vesicle trafficking. Trends Cell Biol. **16**:522-529.

94. **Ridley, A. J., H. F. Paterson, C. L. Johnston, D. Diekmann, and A. Hall**. 1992. The small GTP-binding protein rac regulates growth factor- induced membrane ruffling. Cell **70**:401-410.

95. **Rippere-Lampe, K. E., M. Lang, H. Ceri, M. Olson, H. A. Lockman, and A. D. O'Brien**. 2001. Cytotoxic necrotizing factor type 1-positive *Escherichia coli* causes increased inflammation and tissue damage to the prostate in a rat prostatitis model. Infect.Immun. **69**:6515-6519.

96. **Roberts, P. J., N. Mitin, P. J. Keller, E. J. Chenette, J. P. Madigan, R. O. Currin, A. D. Cox, O. Wilson, P. Kirschmeier, and C. J. Der**. 2008. Rho Family GTPase modification and dependence on CAAX motif-signaled posttranslational modification. J.Biol.Chem. **283**:25150-25163.

97. **Rolli-Derkinderen, M., V. Sauzeau, L. Boyer, E. Lemichez, C. Baron, D. Henrion, G. Loirand, and P. Pacaud**. 2005. Phosphorylation of serine 188 protects RhoA from ubiquitin/proteasome-mediated degradation in vascular smooth muscle cells. Circ.Res **96**:1152-1160.

98. **Rosenfeld, J., J. Capdevielle, J. C. Guillemot, and P. Ferrara**. 1992. In-gel digestion of proteins for internal sequence analysis after one- or two-dimensional gel electrophoresis. Anal.Biochem. **203**:173-179.

99. **Sahai, E. and C. J. Marshall**. 2002. RHO-GTPases and cancer. Nat.Rev.Cancer **2**:133-142.

100. **Samuel, F. and D. L. Hynds**. 2010. RHO GTPase signaling for axon extension: is prenylation important? Mol.Neurobiol. **42**:133-142.

101. **Sanders, L. C., F. Matsumara, G. M. Bokoch, and P. de Lanerolle**. 1999. Inhibition of myosin light chain kinase by p21-activated kinase. Science **283**:2083-2085.

102. **Sandrock, K.** (2008). **Identifizierung und Charakterisierung neuer Interaktionspartner von Rac-GTPasen**. (Dissertation).

103. **Schleberger, C., H. Hochmann, H. Barth, K. Aktories, and G. E. Schulz**. 2006. Structure and Action of the Binary C2 Toxin from Clostridium botulinum. J.Mol.Biol. **364**:705-715.

104. **Schmidt, G.** 2011. Yersinia enterocolitica outer protein T (YopT). Eur.J.Cell Biol. **90**:955-958.

105. **Schmidt, G. and K. Aktories**. 1998. Bacterial cytotoxins target Rho GTPases. Naturwissenschaften **85**:253-261.

106. **Schmidt, G., P. Sehr, M. Wilm, J. Selzer, M. Mann, and K. Aktories**. 1997. Gln63 of Rho is deamidated by *Escherichia coli* cytotoxic necrotizing factor 1. Nature **387**:725-729.

107. **Schmidt, G., J. Selzer, M. Lerm, and K. Aktories**. 1998. The Rho-deamidating cytotoxic-necrotizing factor CNF1 from *Escherichia coli* possesses transglutaminase activity - cysteine-866 and histidine-881 are essential for enzyme activity . J.Biol.Chem. **273**:13669-13674.

108. **Schneider-Poetsch, T., J. Ju, D. E. Eyler, Y. Dang, S. Bhat, W. C. Merrick, R. Green, B. Shen, and J. O. Liu**. 2010. Inhibition of eukaryotic translation elongation by cycloheximide and lactimidomycin. Nat.Chem.Biol. **6**:209-217.

109. **Singh, R. R., C. Song, Z. Yang, and R. Kumar**. 2005. Nuclear localization and chromatin targets of p21-activated kinase 1. J.Biol.Chem. **280**:18130-18137.

110. **Sorg, I., U.-M. Goehring, K. Aktories, and G. Schmidt**. 2001. Recombinant *Yersinia* YopT leads to uncoupling of RhoA-effector interaction. Infect.Immun. **69**:7535-7543.

111. **Spiering, D. and L. Hodgson**. 2011. Dynamics of the Rho-family small GTPases in actin regulation and motility. Cell Adh.Migr. **5**:170-180.

112. **Stoll, T., G. Markwirth, S. Reipschlager, and G. Schmidt**. 2009. A new member of a growing toxin family - *Escherichia coli* cytotoxic necrotizing factor 3 (CNF3). Toxicon **54**:745-753.

113. **Symons, M. and J. Settleman**. 2000. Rho family GTPases: more than just simple switches. Trends Cell Biol. **10**:415-419.

114. **Takai, Y., T. Sasaki, and T. Matozaki**. 2001. Small GTP-binding proteins. Physiol.Rev. **81**:153-208.

115. **Tobert, J. A.** 2003. Lovastatin and beyond: the history of the HMG-CoA reductase inhibitors. Nat.Rev.Drug Discov. **2**:517-526.

116. **Travaglione, S., G. Messina, A. Fabbri, L. Falzano, A. M. Giammarioli, M. Grossi, S. Rufini, and C. Fiorentini**. 2005. Cytotoxic necrotizing factor 1 hinders skeletal muscle differentiation *in vitro* by pertubing the activation/deactivation balance of Rho GTPases. Cell Death & Differentiation **12**:78-86.

117. **Turner, S. J., S. Zhuang, T. Zhang, G. R. Boss, and R. B. Pilz**. 2008. Effects of lovastatin on Rho isoform expression, activity, and association with guanine nucleotide dissociation inhibitors. Biochem.Pharmacol. **75**:405-413.

118. **van, T. M. and J. L. Bos**. 2004. Pull-down assays for guanoside 5'-triphosphate-bound Ras-like guanosine 5'-triphosphatases. Methods Mol.Biol. **250**:97-102.

119. **Vega, F. M. and A. J. Ridley**. 2008. Rho GTPases in cancer cell biology. FEBS Lett. **582**:2093-2101.

120. **Vetter, I. R. and A. Wittinghofer**. 2001. The guanine nucleotide-binding switch in three dimensions. Science **294**:1299-1304.

121. **Visvikis, O., M. P. Maddugoda, and E. Lemichez**. 2010. Direct modifications of Rho proteins: deconstructing GTPase regulation. Biol.Cell **102**:377-389.

122. **Vogelsgesang, M., A. Pautsch, and K. Aktories**. 2007. C3 exoenzymes, novel insights into structure and action of Rho-ADP-ribosylating toxins. Naunyn Schmiedebergs Arch.Pharmacol. **374**:347-360.

123. **von Pawel-Rammingen, U., M. V. Telepnev, G. Schmidt, K. Aktories, H. Wolf-Watz, and R. Rosqvist**. 2000. GAP activity of the *Yersinia* YopE cytotoxin specifically targets the Rho pathway: a mechanism for disruption of actin microfilament structure. Mol.Microbiol. **36**:737-748.

124. **von, M. A.** 2006. The nuclear ubiquitin-proteasome system. J.Cell Sci. **119**:1977-1984.

125. **Wang, G. and F. Beier**. 2005. Rac1/Cdc42 and RhoA GTPases antagonistically regulate chondrocyte proliferation, hypertrophy, and apoptosis. J.Bone Miner.Res. **20**:1022-1031.

126. **Wang, S., T. Watanabe, J. Noritake, M. Fukata, T. Yoshimura, N. Itoh, T. Harada, M. Nakagawa, Y. Matsuura, N. Arimura, and K. Kaibuchi**. 2007. IQGAP3, a novel effector of Rac1 and Cdc42, regulates neurite outgrowth. J.Cell Sci. **120**:567-577.

127. **Wolf, P. and U. Elsasser-Beile**. 2009. Pseudomonas exotoxin A: from virulence factor to anti-cancer agent. Int.J.Med.Microbiol. **299**:161-176.

128. **Xiao, L., M. Eto, and M. G. Kazanietz**. 2009. ROCK mediates phorbol ester-induced apoptosis in prostate cancer cells via p21Cip1 up-regulation and JNK. J.Biol.Chem. **284**:29365-29375.

129. **Yamashiro, S., T. Noguchi, and I. Mabuchi**. 2003. Localization of two IQGAPs in cultured cells and early embryos of Xenopus laevis. Cell Motil.Cytoskeleton **55**:36-50.

130. **Yarbrough, M. L., Y. Li, L. N. Kinch, N. V. Grishin, H. L. Ball, and K. Orth**. 2009. AMPylation of Rho GTPases by Vibrio VopS disrupts effector binding and downstream signaling. Science **323**:269-272.

131. **Zong, H., K. Kaibuchi, and L. A. Quilliam**. 2001. The insert region of RhoA is essential for Rho kinase activation and cellular transformation. Mol.Cell Biol. **21**:5287-5298.

132. **Zong, H., N. Raman, L. A. Mickelson-Young, S. J. Atkinson, and L. A. Quilliam**. 1999. Loop 6 of RhoA confers specificity for effector binding, stress fiber formation, and cellular transformation. J.Biol.Chem. **274**:4551-4560.

8 LIST OF ABBREVIATIONS

ADF	actin-depolymerizing factor
ADP	adenosine-5'-diphosphate
amp	ampicillin
APS	ammonium persulfate
Arp	actin related protein
Asn	asparagine
ATP	adenosine-5'-triphosphate
BCA	bicinchonic acid
BCH	BNIP-2 and Cdc42GAP homology
BCS	bovine calf serum
bp	base pair
BSA	bovine serum albumin
C3	*Clostridium botulinum* C3 exoenzyme
CaaX	C:cystein, a:aliphatic, X:any aminoacid
Cdc42	cell division control protein 42 homolog
CGT	*Clostridium* glucosylating toxin
CIP	calf intestine phosphatase
CNF	Cytotoxic Necrotizing Factor
Cys	cysteine
DAPI	4’,6-Diamidin-2-phenylindol
D-box	destruction box
DMSO	dimethylsulfoxide
DNA	deoxyribonucleic acid
DNT	dermonecrotic toxin
dNTP	deoxynucleoside triphosphate
DTT	dithiothreitol
ECL	enhanced chemiluminescence
EDTA	ethylendiaminetetraacetate
F-actin	filamentous actin
Fc	fragment, crystallizable
FCS	fetal calf serum
g	g-force
G-actin	globular actin
GAP	GTPase activating protein
GAPDH	glyceraldehyde 3-phosphate dehydrogenase
GDI	guanine nucleotide dissociation inhibitor

GDP	guanosine-5’-diphosphate
GEF	guanine nucleotide exchange factor
GFP	green fluorescence protein
Gln	glutamine
Glu	glutamate
GST	glutathione S-transferase
GTP	guanosine-5’-triphosphate
GTPase	GTP hydrolyzing protein
GTPγs	non- hydrolysable Guanosine-5’-triphosphate
h	hour/hours
His	histidine
HMG-CoA	3-hydroxy-3-methylglutaryl-coenzyme-A-reductase
HPLC	high-performance liquid chromatography
HRP	horseradish-peroxidase
IP	Immunoprecitpitation
IPTG	isopropyl-ß-D-thiogalactopyranosid
ITS	Insulin–Transferrin–Selenium
kb	kilo base pairs
kDa	kilo Dalton
LB	Luria Bertani
LC-MS/MS	tandem liquid mass spectrometry
LIMK	LIM domain kinase
M	molar
mDia	mammalian Diaphanous
MEF	mouse embryonic fibroblasts
min	minutes
MLC	Myosin light chain II
MLC-K	Myosin light chain kinase
MLC-P	Myosin light chain phosphatase
MS	mass spectrometry
MSC	mesangial cells
MW	molecular weight
NEA	non-essential aminoacids
NLS	nuclear localization sequence
P/S	penicillin/streptomycin
PAK	p21 activated kinase
PARP	poly(ADP-Ribose)-polymerase
PBR	polybasic region
PBS	phosphate buffered saline
PCR	polymerase chain reaction
PEI	polyethylenimine

PIC	protease inhibitor cocktail
PK	protein kinase
PMT	*Pasteurella multocida* Toxin
PVDF	polyvinylidenfluoride
Rac1	Ras-related C3 botulinum toxin substrate 1
Ras	rat Sarcoma
RBD	rho-binding domain
Rho	Ras homologous
ROCK	Rho-associated, coiled-coil containing protein kinase
RT	room temperature
SDS-PAGE	sodium dodecyl sulfate polyacrylamide gel electrophoresis
SILAC	stable isotope labeling by amino acids in cell culture
SopE	*Salmonella* outer protein E
SptP	*Salmonella* protein tyrosine phosphatase
SRE	serum response element
SRF	Serum Response Factor
T3S	type 3 secretion system
TBS	Tris buffered saline
TEMED	tetramethylethylendiamine
Thr	threonine
Tris	tris(hydroxymethyl)-aminomethane
UPS	ubiquitin-proteasome system
Val	valine
WASP	Wiskott–Aldrich syndrome protein
WAVE	WASP-family verprolin homologue
WT	wild-type
Yop	*Yersinia* outer protein

9 PUBLICATIONS

Publications

Bielek,H., Anselmo,A., and DerMardirossian,C. (2009). Morphological and proliferative abnormalities in renal mesangial cells lacking RhoGDI. Cell Signal. *21*, 1974-1983.

Sandrock,K., Bielek,H., Schradi,K., Schmidt,G., and Klugbauer,N. (2010). The nuclear import of the small GTPase Rac1 is mediated by the direct interaction with karyopherin alpha2. Traffic. *11*, 198-209.

Bielek,H. and Schmidt,G. (2012). 4: How to Analyze Bacterial Toxins Targeting Rho GTPases, Rho GTPases-Materials and Methods. Series: Methods in Molecular Biology. *827*, 59-75.

Presentations

Bielek, H. (2008) The role of RhoGDI in Rho GTPase signaling. PhD Schauinsland meeting. (Freiburg, Germany)

Bielek, H. and Schmidt, G. (2011) CNF1 toxin: A potent tool to limit RhoA over-activation. 77. Jahrestagung der Deutschen Gesellschaft für experimentelle und klinische Pharmakologie und Toxikologie e.V. (DGPT) (Frankfurt, Germany)

Poster

List, J.H., **Bielek, H.,** P. Wolf and Schmidt, G. (2010) Rho activating bacterial toxins are potent pharmacological tools. International Symposium "Signalling Meets Synthetic Biology". (Freiburg, Germany)

Schmidt, G., Lang, S., Guttenberg, G., **Bielek, H.** and Aktories, K. (2009). Modifikation von Rho-Proteinen durch bakterielle Toxine- Werkzeuge zur Hemmung von Metastasierung, Invasion und Tumorentwicklung. SFB Besichtigung, Biochemie. (Freiburg, Germany)

Bielek, H., Sandrock, K., Schmidt, G. and Klugbauer, N. (2009). The nuclear import of the small Rho GTPase Rac1 is mediated by the direct interaction with Karyopherin α2. 75. Jahrestagung der Deutschen Gesellschaft für experimentelle und klinische Pharmakologie und Toxikologie e.V. (DGPT). (Frankfurt, Germany)